

Verification, validation and evaluation of FireFOAM  
as a tool for performance based design



## KEYWORDS

OpenFOAM, FireFOAM, Validation, Verification, CFD

Denna rapport utgör ett slutligt arbetsmanuskript för det rubricerade projektet. Den officiella projektrapporten, till vilken referens bör ske återfinns på LTHs hemsida: ”Verification, validation and evaluation of FireFOAM as a tool for performance based design”

Report 3208

ISSN: 1402-3504

ISRN: LUTVDG/TVBB--3176--SE

[www.brand.lth.se](http://www.brand.lth.se)

Brandforsk rapport 2017:2





**Verification, validation and evaluation of FireFOAM as a  
tool for performance based design**

***Bjarne Husted  
Ying Zhen Li  
Chen Huang  
Johan Anderson  
Robert Svensson  
Haukur Ingason  
Marcus Runefors  
Jonathan Wahlqvist***

**Lund 2017**

Verification, validation and evaluation of FireFOAM as a tool for performance design

Bjarne Husted, LTH  
Ying Zhen Li, RISE Fire Research  
Chen Huang, RISE Fire Research  
Johan Anderson, RISE Fire Research  
Robert Svensson, RISE Fire Research  
Haukur Ingason, RISE Fire Research  
Marcus Runefors, LTH  
Jonathan Wahlqvist, LTH

**Report 3208**

**ISSN: 1402-3504**

**ISRN: LUTVDG/TVBB--3208--SE**

Number of pages: 85

Keywords: OpenFOAM, FireFOAM, Validation, Verification, CFD,

**Abstract:**

The open source CFD code FireFOAM has been verified and validated against analytical solution and real fire tests. The verification showed that FireFOAM solves the three modes of heat transfer appropriately. The validation against real fire tests yielded reasonable results. FireFOAM has not been validated for a large set of real fires, which is the case for FDS. Therefore, it is the responsibility of the user to perform the validation, before using the code.

One of the advantages of FireFOAM compared to the Fire Dynamic Simulator is that FireFOAM can use unstructured grid.

FireFOAM is parallelised and scales reasonable well, but is in general considerably slower in computation speed than the Fire Dynamic Simulator. Further, the software is poorly documented and has a steep learning curve. At present it is more a tool for researchers than for fire consultants.

© Copyright: Brandteknik, Lunds tekniska högskola, Lunds universitet, Lund 2017.

---

Brandteknik  
Lunds tekniska högskola  
Lunds universitet  
Box 118  
221 00 Lund  
brand@brand.lth.se

Department of Fire Safety Engineering  
Lund University  
P.O. Box 118  
SE-221 00 Lund, Sweden  
brand@brand.lth.se  
<http://www.brand.lth.se/english>

## Foreword

This is a joint Brandforsk project, number 2015-11-02, between RISE Research Institutes of Sweden department of Fire Research (former SP Brandteknik) and Lund University.

The goal is to evaluate the CFD code FireFOAM, and specifically to evaluate whether it can be used in the consulting industry as a tool for doing performance-based design.

## Acknowledgments

We would like to acknowledge BrandForsk for the financial support.

Parts of the computations were performed on resources provided by SNIC through LUNARC under Project SNIC 2017/1-34. Joachim Hein at LUNARC is acknowledged for assistance concerning technical and implementational aspects in making the code run on the Aurora cluster.

# Contents

Foreword .....	5
Acknowledgments .....	6
1. Introduction .....	9
Objective of this study.....	10
Project benefits for stakeholders .....	10
2. Presentation of program, history, models, (main features of the programs) .....	11
2.1 Open foam.....	11
2.2 Fire Foam.....	12
Turbulence and thermophysical models .....	12
Spray model.....	13
Combustion model .....	13
Radiation model .....	15
Pyrolysis model.....	16
2.3 Comparison of FireFOAM and FDS.....	16
3 How to work with the code (tutorial) .....	17
3.1 Compilation .....	17
Download and compile source code .....	17
Set environment variable .....	17
Compilations problems .....	17
3.2 Run.....	18
Single thread.....	18
Parallel.....	19
A group of computers or clusters.....	19
Single computer with multiple processors.....	19
Shell .....	19
Batch running of jobs .....	19
3.3 Postprocessing.....	20
Data visualization .....	20
Data acquisition.....	20
3.4 Tutorials.....	21
Geometry.....	21
Fire source .....	23
Boundary conditions .....	23

Running.....	24
Postprocessing.....	24
Parallel running of the case.....	26
Short summary .....	26
4 Verification of heat transfer in FireFOAM .....	27
4.1 Radiative heat transfer.....	27
4.2 Convective heat transfer .....	30
4.3 Conductive heat transfer.....	31
4.4 Short summary .....	32
5 Case studies – validation of FireFOAM.....	33
5.1 Small scale .....	33
5.1.2 Inclined tunnel.....	33
5.2 Large scale .....	44
5.2.1 Room fire .....	44
5.2.2 Fire hall .....	68
6. Discussion .....	79
6.1 Tutorial case with Steckler room.....	79
6.2 Verification of heat transfer .....	79
6.3 Inclined tunnel.....	79
6.4 Room fire case .....	79
6.5 Smoke filling and ventilation .....	80
7. Conclusion.....	81
7.1 Suggestion for future work.....	81
8 References .....	83

## 1. Introduction

FireFOAM is a new open-source software for fire simulation using Computational Fluid Dynamic (CFD) that is developed by FM Global. [1]. This tool has until now had limited use within the fire community in Sweden, but at the same time it has features which cannot be found in similar software. Among these features are the ability to model the suppression of fires by sprinklers [2, 3], detailed modelling of the radiation from soot [4, 5] and simulation of a ceiling jet under an inclined ceiling [6].

In order to gain trust and confidence in a CFD program, its need to be validated against experimental results as stated by several authors [7, 8]. Validation means that the same input data and boundary conditions, which were used in the experiments, are used in the simulation. Appropriate results from the simulation is then compared with the experimental results. That could for example be to compare the temperatures at different positions in the fire room or to compare the velocity in opening. A good example of this can be found in the validation guide of the Fire Dynamics Simulator (FDS) [9] where they have included more than 50 different experiments and compared with results from FDS.

Another validation study was done in Sweden in 2008 [10], where four different CFD programs were investigated. These tools were the most widely used at that time and it was CFX, FDS, SMAFS and SOFIE [10]. Today the dominating software is the Fire Dynamic Simulator (FDS), developed by NIST and partners in Europe (e.g. VTT in Finland) and the three other programs only have a limited number of users. The scenarios in the validation study were selected to represent scenarios that often occur in performance-based design. The main problems with validating CFD codes are the lack of well-documented experiments. Certainly, there are many experiments carried out to measure smoke spread, but in many cases, these cannot be used because of the lack of important input data. It is very rare that there is information about repeatability and reproducibility for large-scale fire experiments. Therefore, much effort was put in the project to study and assess the quality of internationally published experiments [10]. Following an extensive discussion, five scenarios were selected. All scenarios had a good input in terms of heat release rate and did not contain complicated phenomena such as flame spread, sprinkler activation or mechanical ventilation. The scenarios in the validation study consisted of a fire in a large room, a corridor, a tunnel, retail premises (shop) and a room-corridor-room setup [10]. The validation study showed some difference between the results of the computations, which both could be due to the different methodology, but also how the operator set up the input parameters [10]. It has also been shown in two recent publications about the retail shop experiments that even if the overall figures looked right, - detailed analysis of the temperatures close to the floor in the shop revealed differences between experiments and simulation when using FDS [11, 12].

Since the Swedish validation study, the development has progressed with regard to CFD codes and their application and capability. The capacity of available computing power has also increased rapidly. FireFOAM is especially developed for fire and fire modelling and is based on OpenFOAM (<http://www.openfoam.org>). OpenFOAM is a general CFD tool written in C ++. It uses the finite volume (FVM) on an unstructured grid, which in principle is very scalable as opposed to structured networks and can run on parallel computers. FireFOAM has not been extensively validated and no validation of FireFOAM has been done in a Swedish context. Therefore, this research project was initiated.

## Objective of this study

1. Obtain basic and advanced knowledge within FireFOAM's functionality and use. Expertise on FireFOAM is currently not available in Sweden, but primarily in the USA as the main developers are at FM Global in Boston. In order to being able to contribute to advances in research with FireFOAM is therefore required to get a deep knowledge of the program itself.
2. Validate FireFOAM against well-specified experimental scenarios. To ensure that the program is used correctly and then that the program is working satisfactory. Simulations must be compared with well-specified experimental scenarios. A well-conducted comparison will then provide a picture of the program's possible strengths, weaknesses, opportunities and limitations.
3. Report any weaknesses and provide suggestions for future research.

The work was divided into four work packages.

## Project benefits for stakeholders

1. Information about the capabilities and limitations of CFD codes is important. With a new and relatively untested CFD code like FireFOAM it is even more critical that the code is validated and evaluated before the user base becomes wider.
2. Although the Fire Dynamics Simulator (FDS) is an extremely versatile tool, it has its limitations, such as the absence of complex geometries, a simplified combustion model and one-dimensional heat transfer. FireFOAM can be an option for cases where these parameters are of significance or crucial.
3. Consultants could use FireFOAM in their work for tasks were FDS has limitations or lacks features. Currently most consultants use FDS. It may be advantageous to have another open source code, for example for third party audits.
4. Authorities get knowledge of software that can be used as an alternative to FDS in a third party audits. In some countries, there is already a requirement to use another software for third party control.
5. Because FireFOAM is being developed by FM Global, which is a major player in the insurance industry it can also be beneficial to the Swedish insurance industry. One reason why FM Global started the development of FireFOAM was that they felt that FDS did not meet all the requirements they had for a calculation tool.
6. If the experience of the basic principles and validation of FireFOAM is positive, the program can also be used in other research projects, which contains more complex scenarios, such as sprinkler tests performed at RISE and PRISME2 test with mechanically ventilated fires.
7. Through a collaboration between RISE (former SP) and LTH Brandteknik, there is a good base for getting a well-functioning Swedish user group in the future. We need to widen our competence in Sweden outside of FDS to maintain a strong international position.

## 2. Presentation of program, history, models, (main features of the programs)

### 2.1 Open foam

OpenFOAM (Open Field Operation and Manipulation) code is a general CFD software package for simulating thermo- and fluid-dynamics, chemical reactions, solid dynamics and electromagnetics, and it solves various partial differential equations using finite volume method on unstructured mesh. It has been attracting growing interests from both industries and academies since its release in 2004. OpenFOAM code has two main advantages: license free and open source. First, industrial companies are keen to adopt less expensive CFD software, since a commercial CFD program can easily cost tens of thousands of euros per license per year. Second, researchers are strongly interested in access to source codes in order to develop and implement new models and to easily exchange knowledge and experience with each other. Moreover, OpenFOAM has a very attractive feature; it is written in object-oriented language C++. Accordingly, solvers, written using the OpenFOAM classes, closely resemble the corresponding partial differential equations. For example, the following equation

$$\frac{\partial \rho \mathbf{U}}{\partial t} + \nabla \cdot \phi \mathbf{U} - \nabla \cdot \mu \nabla \mathbf{U} = -\nabla p$$

is directly represented by OpenFOAM code as follows

```
solve
(
    fvm::ddt(rho, U)
  + fvm::div(phi, U)
  - fvm::laplacian(mu, U)
  ==
  - fvc::grad(p)
);
```

One drawback of OpenFOAM and mainly due to the limited documentation, the learning curve of OpenFOAM is steeper as compared to a well-documented Open-source program, e.g. Fire Dynamic Simulator (FDS) [13].

The overall OpenFOAM structure is shown in Figure 1. The workflow of using OpenFOAM is similar to conventional CFD programs, and it is categorized as pre-processing, solving and post-processing. First, OpenFOAM has relatively flexible meshing capability. For instance, the simplest way of generation mesh using blockMesh utility in OpenFOAM is to define a box with 8 vertices, and then to specify how many divisions needed in  $x$ ,  $y$  and  $z$  directions. In addition, there is a utility snappyHaxMesh. It uses a background mesh to sculpture the domain surface. Then it can refine and adjust the mesh to fit to the geometry file, e.g. STL file, and add boundary layers at the requested patches. Moreover, it is possible to import the mesh generated by a third party meshing tool, e.g. ICEM CFD, using utilities, e.g. fluent3DMeshToFoam. After the computational mesh is ready, there are various kinds of solvers designed to solve specific computational continuum mechanics. OpenFOAM offers a set of libraries that are dynamically linked to the solvers, and the libraries serve as the source code of physical models. Detailed description about physical models relevant to fire research is discussed later in this report. Finally, post-processing of computed results especially for data visualization can be achieved using both an open source program ParaView, and commercial programs, e.g. EnSight, Fieldview and Tecplot. Moreover, there are utilities for data acquisition as well.

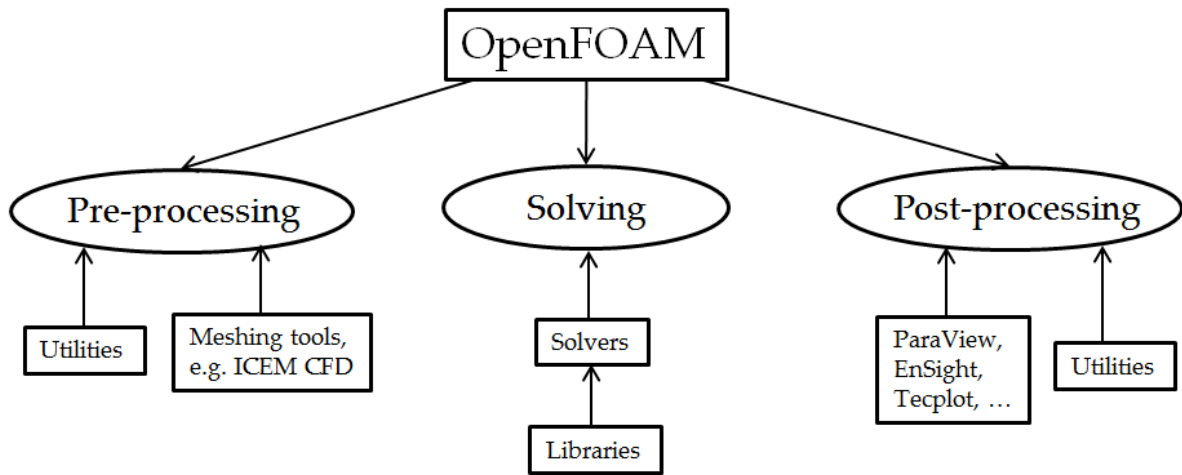


Figure 1. Overview of OpenFOAM structure

OpenFOAM is available mainly for Linux operating system. Currently, Open CFD releases both source code and pre-compiled binaries for certain versions of Ubuntu system, and users can freely download the source code from the internet [14]. Usually compilation of OpenFOAM requires certain version of gcc, which is a C++ compiler, installed on the computer. The users are required to be familiar with Linux operation system, being able to work in terminals using commands. Moreover, the installation of ParaView, which is an open source, data visualization application released together with OpenFOAM, requires certain packages in Linux operation system. Fortunately, there is distribution of ParaView for Microsoft Windows, which is relatively easy to install. To complicate things even further there are different provides of the OpenFOAM, The OpenFOAM Foundation at [openfoam.org](http://openfoam.org) and a version provided by the company ESI on [www.openfoam.com](http://www.openfoam.com).

## 2.2 Fire Foam

FireFOAM, an open source software package, has been mainly developed and maintained by FM Global based on the platform of OpenFOAM. Similar to FDS, FireFOAM is aimed at modelling problems relevant to thermo- and fluid-dynamics and multiphase flow. However, it is specialized in simulating heat and smoke transport in fires and it is a LES solver for incompressible flow. It is worth noting that there are mainly two versions of FireFOAM code. One is released as a solver for transient fire and diffusion flame simulation by Open CFD (an official release) [14]. The other is an extended version of the official release, and it is maintained by FM Global consisting of modified libraries, solvers and cases for fire research [15]. If no special statements are made, the following work is based on FireFOAM version released by FM Global on 24 Nov. 2014 with commit code 5f28904ffd.

The key sub-models linked to FireFOAM are shortly depicted in the following.

### Turbulence and thermophysical models

Since the general turbulence library is called by the FireFOAM solver, it is able to run simulations using both Large Eddy Simulation (LES) and Reynolds-Averaged Navies-Stokes (RANS) turbulence models. Unlike FDS, in which the flow is treated as incompressible, FireFOAM is a compressible flow solver. The ideal gas law is invoked as follows

$$P = \rho R_{spec} T$$

where,  $P$  is the gas pressure;  $T$  is the gas temperature;  $\rho$  is the gas density and  $R_{spec} = R^0/W$  is the specific gas constant in unit of J/(K·kg).

In FireFOAM solver, transport equation for sensible enthalpy  $h_s$  is solved, and the relation between sensible and total enthalpy  $h$  is as follows

$$h = h_s + \sum_k h_{f,k}^0 Y_k$$

where  $h_{f,k}^0$  and  $Y_k$  are the heat of formation and mass fraction, respectively, of species  $k$ .

By default, in FireFOAM, temperature and sensible enthalpy are connected by the widely used temperature dependent JANAF thermodynamic polynomial from NIST as follows

$$h_s = \frac{R^0}{W} \left( \sum_{k=1}^5 \frac{a_k}{k} T^k + a_6 \right)$$

### Spray model

The FireFOAM solver offers a possibility of simulating Lagrangian sprays, e.g. sprinkler sprays for fire suspension. Different physical phenomena are modelled, including liquid injection, liquid atomization, droplet breakup, droplet evaporation, turbulent dispersion, droplet-wall interaction and surface film. A detailed description about sub-models implemented in OpenFOAM Lagrangian library can be found in Ref [16].

### Combustion model

Most of the fires are considered as turbulent diffusion flames, in which fuel and oxidant are burning while they are mixing. The combustion rate is controlled by turbulent mixing time scale of fuel and oxidant, and the chemical reaction time scale is negligible as compared to turbulent time scale. Therefore, in the vast majority of fire applications, the Eddy Dissipation Model (EDM) is used.

Before discussing the EDM model, a short description about its earlier variant Eddy-Break-Up (EBU) model is described. The EBU model was originally introduced by Spalding [17] for simulating premixed turbulent combustion. This model is based on the fast-chemistry assumption, meaning that once the fuel and air are mixed, they are burned immediately. Accordingly, the mean chemical reaction rate

$$\bar{\omega}_f = -C_{EBU} \frac{\sqrt{\overline{Y_f'^2}}}{\tau_t}$$

is considered to be controlled by a characteristic turbulent time  $\tau_t$ , which is equal to

$$\tau_t = \frac{\tilde{k}}{\tilde{\varepsilon}}$$

within the framework of the standard  $k - \varepsilon$  model. Here,  $C_{EBU}$  is a model coefficient;  $\sqrt{\overline{Y_f'^2}}$  is the variance of the mixture fraction of the fuel; the  $\tilde{k}$  and  $\tilde{\varepsilon}$  are the Favre-averaged turbulent kinetic energy and its dissipation rate, respectively.

Later, Magnussen and Hjertager [18] introduced a similar model for both premixed and diffusion flames called the Eddy Dissipation Model (EDM) in which the  $\sqrt{\overline{Y_f'^2}}$  term is replaced by the mass fraction of the deficient species, i.e. fuel for a lean mixture and oxygen for a rich mixture,

$$\bar{\omega}_f = -C_{EDM} \frac{\min \left[ \tilde{Y}_f, \frac{\tilde{Y}_o}{s}, \frac{\tilde{Y}_p}{1+s} \right]}{\tau_t}$$

where  $C_{EDM}$  is a model coefficient;  $\tilde{Y}_f$ ,  $\tilde{Y}_o$  and  $\tilde{Y}_p$  are the Favre-averaged mass fractions of the fuel, oxidizer and products, respectively; and  $s$  is the stoichiometric mass ratio of oxidizer to fuel.

The EBU and EDC models have been used widely in turbulent combustion simulations because (i) it yields a plausible dependence of global burning rate on rms turbulent velocity fluctuations  $u'$  [19] and (ii) it can be easily implemented into CFD codes since the mean reaction rate depends on known quantities. Accordingly, this model is available in almost every commercial CFD code. However, researchers have often complained that it ignores the effect of mixture composition and therefore requires constant tuning. When simulating the influence of mixture stratification on the burning rate, the neglect of the mixture composition effects becomes unacceptable.

In both FireFOAM and FDS, the EDM model was implemented differently from the model described above. The difference stems from the modelling of reacting time scale  $\tau_t$ . In the FireFOAM package released by FM Global, EDM model is available, and the mean chemical reaction rate is implemented as follows,

$$\bar{\omega}_f = \bar{\rho} \frac{\min \left[ \tilde{Y}_f, \frac{\tilde{Y}_o}{s} \right]}{\Delta t C_{stiff}} \left( 1 - \exp(-C_{stiff} \Delta t r_t) \right)$$

where  $\bar{\rho}$  is the mean density;  $\Delta t$  is the integration time step;  $r_t$  is the reciprocal of characteristic turbulent timescale;  $C_{stiff}$  is a constant to switch on and off the exponential term in the parentheses in the above equation as follows,

$$\bar{\omega}_f = \bar{\rho} \frac{\min \left[ \tilde{Y}_f, \frac{\tilde{Y}_o}{s} \right]}{\Delta t} \left( 1 - \exp(-\Delta t r_t) \right), \quad \text{if } C_{stiff} = 1$$

$$\bar{\omega}_f = \bar{\rho} \frac{\min \left[ \tilde{Y}_f, \frac{\tilde{Y}_o}{s} \right]}{\Delta t}, \quad \text{if } C_{stiff} \rightarrow 0$$

The purpose of  $C_{stiff}$  is to switch on and off the transient term  $(1 - \exp(-\Delta t r_t))$  in calculating the mean reaction rate, and  $(1 - \exp(-\Delta t r_t))$  is bounded between 0 and 1. When  $C_{stiff} \rightarrow 0$ , the transient term disappears.

In the above equations,  $r_t$  is the reciprocal timescale of turbulence and it is defined as follows

$$r_t = \max(r_{tTurb}, r_{tDiff})$$

where,  $r_{tTurb}$  is the reciprocal of the turbulent mixing time scale, whereas  $r_{tDiff}$  is the reciprocal of diffusion timescale, and they are defined as follows

$$r_{tTurb} = C_{EDC} \frac{\tilde{\epsilon}}{\max(\tilde{k}, SMALL)}$$

$$r_{tDiff} = C_{diff} \frac{\alpha}{\rho \Delta^2}$$

where SMALL is a dimensional scalar [ $\text{m}^2/\text{s}^2$ ] with a value of  $1.0\text{e-}6$  in OpenFOAM;  $\alpha$  is the laminar thermal conductivity [ $\text{kg/m/s}$ ];  $\Delta$  is the LES filter width.

In FDS, the EDM model is implemented as follows [20, 21]

$$\overline{\omega_f} = \rho \frac{\min\left[\tilde{Y}_f, \frac{\tilde{Y}_o}{S}\right]}{\tau_{mix}}$$

where  $\tau_{mix}$  is a mixing time scale, and it depends on chemical time scale, diffusion time scale, subgrid scale advection, and bouyant accelaration as follows

$$\tau_{mix} = \max\left(\tau_{chem}, \min(\tau_d, \tau_u, \tau_g, \tau_{flame})\right)$$

$$\tau_d = \frac{\Delta^2}{D_F}$$

$$\tau_u = \frac{\Delta}{\sqrt{2k_{sgs}}}$$

$$\tau_g = \sqrt{\frac{2\Delta}{g}}$$

Besides EDM model used by the FireFOAM solver, there are many other combustion models available in OpenFOAM. For example, the Partially Stirred Reactor (PaSR) model developed by Golovichev et al. [22] at Chalmers for diffusion combustion is linked to reactingFoam solver. The Flame Speed Closure (FSC) for premixed flame mainly developed by Lipatnikov et al. [23] at Chalmers was implemented in OpenFOAM and applied for gasoline direct injection engine combustion.

### Radiation model

The radiation model linked to FireFOAM employs finite volume discrete ordinates model (fvDOM) to solve radiation heat transfer equation. The weighted sum of gray gas model is used to evaluate the absorption/emission coefficient.

When solving the sensible enthalpy equation  $h_s$  in FireFOAM, the radiation source term is included as follows [24]

$$\frac{\partial \overline{\rho h_s}}{\partial t} + \nabla \cdot (\overline{\rho \mathbf{u} h_s}) - \nabla \cdot (\overline{\rho \alpha_{eff} \nabla h_s}) = \frac{D\overline{p}}{Dt} + \overline{Q_c} + \overline{Q_R}$$

where  $\alpha_{eff}$  is the effective turbulence thermal diffusivity;  $\overline{Q_c}$  is the heat generated by combustion;  $\overline{Q_R}$  is the radiation source term, and it can be written as follows

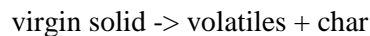
$$\overline{Q_R} = Ru() - Rp()T^4$$

Here  $Ru()$  is a source term component;  $Rp()$  is also a source term component for  $T^4$ , and  $Rp() = 4a\sigma$ .  $a$  is the Planck mean absorption coefficient, and  $\sigma = 5.67E - 8$  [ $W/m^2/K^4$ ] is the Stefan-Boltzmann constant.

In the case setup in \$FOAM\_CASE/constant/radiationProperties, users need to specify nPhi (an azimuthal angle in x-y plane) and nTheta (a polar angle from axis z to x-y plane). The total number of solid angle used in radiation calculation is  $4*nPhi*nTheta$ . maxIter is the number of iterations for radiation solver.

### Pyrolysis model

Pyrolysis covers a wide spectrum of complex and often poorly understood physical and chemical processes including heat conduction and in-depth radiation in solid material, heat convection in material (e.g. porous media), decomposition and oxidation reactions in forming flammable hydrocarbons, tar (liquid) char and ash, melting, bubble formation as an intermediate state of gasification, geometrical changes and so on. The current pyrolysis model in FireFOAM as well as that in FDS is considered to be relatively crude and semi-empirical. In FireFOAM, the pyrolysis modelling is based on the assumption of one-dimensional treatment, which is perpendicular to the exposed solid surface, of thermal degradation across a solid based on conservation statement for heat and mass [25]. The corresponding global reaction for pyrolysis is as follows



The pyrolysis reaction rate is based on Arrhenius-like degradation chemistry. It was complained that the model ignores the change of solid volume, the evaporation of free and bounded water, liquid phase melting and so on [26].

## 2.3 Comparison of FireFOAM and FDS

An alternative way to evaluate the features of FireFOAM is to compare the program with the widely used Fire Dynamic Simulator (FDS).

**Table 1. Comparison of FireFOAM and FDS features**

Feature	FireFOAM	FDS
Unstructured grid	yes	no
Automatic decomposition of domain for parallel run	yes	no
Sprinkler extinguishment model	yes	no
Shielding of Radiation of Droplets	no	yes
Flow of water of surfaces	yes	no
Calculation of fractional effective dosis (FED)	no	yes
Event based control (e.g. opening fire ventilation on smoke detector activation)	no	yes

The features compared in table 1 is not extensive, but shows that FDS includes more features used in general fire safety engineering compared to FireFOAM. FireFOAM focus is more on extinguishment and advanced grid generation.

## 3 How to work with the code (tutorial)

### 3.1 Compilation

FM Global together with many universities and research organizations has been contributing in developing and maintaining the FireFOAM code. The fireFOAM solver and its corresponding source code is included with standard release of OpenFOAM. However, FM Global releases a FireFOAM version including more submodels, e.g. combustion models via GitHub. Hence, this tutorial focuses on installing FireFOAM released by FM Global for general computer platform.

#### Download and compile source code

The FireFOAM source code and its platform OpenFOAM source code can be downloaded from the website of GitHub <sup>2,3</sup>. The FireFoam version which was used in this report is Version 1.0.9, updated on 24th Nov. 2014 with a commit number 5f28904ffd7e82a9a55cb3f67fafb32f8f889d58. A detailed description about downloading OpenFOAM from git repository and compiling OpenFOAM on a general linux computer is described on the Open CFD's homepage <sup>4</sup>[27]. In addition, a detailed description about downloading FireFoam and compiling it can be found here <sup>5</sup>.

#### Set environment variable

Add the following line to ~/.bashrc to create an alias:

```
alias OF22x='module load gcc/4.8.1 openmpi/1.6.3; export FOAM_INST_DIR=~/.OpenFOAM; . $FOAM_INST_DIR/OpenFOAM-2.2.x/etc/bashrc'
```

Next time when user have logged in in linux computer, just type OF22x, and then they can run OpenFOAM or FireFOAM binaries.

#### Compilations problems

In general, it can be a problem compiling FireFOAM if the correct version of the compilers are not installed. The is especially true if also the post processing tool Paraview program is going to be used. It requires specific version of the compiler for C++, linker and of the third party tools. The best way is to use a module system on the linux machine, which simplifies the installation of all the software packages. E.g. for the OpenFOAM-dev edition from May 2017, all the required modules can be loaded by module load goolf/1.7.20, module load Qt/4.8.6, module load CMake/3.5.2. Which gives the following all the 16 different kind of software listed in the text box, Figure 2.

If a compilations fails with strange and incomprehensive error messages a trick is do a clean installation and start over, - even if this seems to be very time consuming at first.

---

<sup>2</sup> <https://github.com/fireFoam-dev/fireFoam-2.2.x>

<sup>3</sup> <https://github.com/OpenFOAM/OpenFOAM-2.2.x>

<sup>4</sup> <http://www.openfoam.org/download/git.php>

<sup>5</sup> <https://github.com/fireFoam-dev/fireFoam-2.2.x/blob/master/INSTALL>

Currently Loaded Modules:

- |   |                    |
|---|--------------------|
| 1) GCC/4.8.4                                    | 9) libffi/3.1      |
| 2) numactl/2.0.10                               | 10) gettext/0.19.2 |
| 3) hwloc/1.10.1                                 | 11) zlib/1.2.8     |
| 4) OpenMPI/1.8.4                                | 12) libxml2/2.9.2  |
| 5) OpenBLAS/0.2.13-LAPACK-3.5.0                 | 13) GLib/2.40.0    |
| 6) FFTW/3.3.4                                   | 14) Qt/4.8.6       |
| 7) ScaLAPACK/2.0.2-OpenBLAS-0.2.13-LAPACK-3.5.0 | 15) ncurses/6.0    |
| 8) goolf/1.7.20                                 | 16) CMake/3.5.2    |

Figure 2 Software required to compile FireFOAM including ParaView on the Aurora cluster

## 3.2 Run

### Single thread

Each application is designed to be executed from a terminal command line, typically reading and writing a set of data files associated with a particular case. The data files for a case are stored in a directory named after the case as described in section 4.1; the directory name with full path is here given the generic name <caseDir>.

For any application, the form of the command line entry for any can be found by simply entering the application name at the command line with the -help option, e.g. typing

*blockMesh*

*blockMesh -help*

Usage: *blockMesh* [-region region name] [-case dir] [-blockTopology]  
[-help] [-doc] [-srcDoc]

Like any UNIX/Linux executable, applications can be run as a background process, i.e. one which does not have to be completed before the user can give the shell additional commands. If the user wished to run the *blockMesh* example as a background process and output the case progress to a log file, they could enter:

*blockMesh > log &*

If special geometries, e.g. baffles and panels, are constructed in the cases, extra command lines are required to execute after *blockMesh*. The commands for this execution can be found in folder called <mesh.sh>.

After the meshes are created, the program can be evoked by the following command:

*fireFoam*

## Parallel

The method of parallel computing used by OpenFOAM is known as domain decomposition, in which the geometry and associated fields are broken into parts and allocated to separate processors for solution.

Before conducting parallel simulations with FireFOAM, decomposition of the mesh needs to be done by the following command:

```
decomposePar
```

On completion, a set of subdirectories are created, one for each processor, in the case directory. The directories are named processor  $N$ , where  $N = 0, 1, \dots$ , represents a processor number. Each directory includes a time directory containing the decomposed field descriptions, and a constant/polyMesh directory containing the decomposed mesh description.

## A group of computers or clusters

For parallel simulations in clusters or a network with multiple computers, the program can be executed by the following line:

```
mpirun --hostfile machines -np 4 fireFoam -parallel > log &
```

For example, let us imagine that a user wishes to run openMPI from machine aaa on the following machines: aaa; bbb, which has 2 processors; and ccc. The <machines> would contain:

```
aaa  
bbb cpu=2  
ccc
```

## Single computer with multiple processors

For parallel simulations in one single computer with multiple processors, the command can be simplified into:

```
mpirun -np 4 fireFoam -parallel > log &
```

Note that by default the output files are stored in individual processor folders. At the stage of post-processing, they need to be combined into time folders with the command:

```
reconstructPar
```

## Shell

All the command lines can be written into a shell document. By default in FireFOAM the shell for execution of simulations is called “AllRun”. By simply clicking on it, all the commands will be executed sequentially.

## Batch running of jobs

On some larger clusters, the users are not allowed to run jobs directly from a terminal. Instead, the jobs are run using a job scheduler, which will put the job on a queue and run the job, when resources are available. FireFOAM can also be run in such a way, - for example using the Slurm Workload Manager.

## 3.3 Postprocessing

### Data visualization

There are several alternative programs, e.g. ParaView, FieldView, Tecplot, EnSight, for visualizing OpenFOAM results. In this report, we focus on ParaView since it is also an open source program connected to OpenFOAM official release, and we assume that you run simulation on SP cluster Calculon and post-process results to Windows PC.

First, it is possible to use ParaFoam to open OpenFOAM results directly, but it does not work well all the time. It is recommended to convert OpenFOAM results to ParaView readable data using OpenFOAM utility foamToVTK.

Second, download finished simulation to local Windows PC in a windows command prompt as follows

```
pscp -r chen@10.111.47.229:OpenFOAM/chen-2.2.x/run/inclindeTunnel22xGlassPromatect/
inclindeTunnel22xGlassPromatect
```

Third, open the case result using ParaView. The result is located in inclindeTunnel22xGlassPromatect/VTK/

A slice of the computational domain and velocity vector field are of interest to get. Users can click icon

slice  in the ParaView toolbox to create slices in the domain, and users can click icon Glyph  to create velocity vector fields. In order to save the images, users can use File -> save Screenshot to save the slices to e.g. a jpeg image file.

### Data acquisition

In certain cases, we need to know exact values at exact locations, e.g. temperatures at locations of thermocouples, in order to make comparison between simulation and measurements. Users can add the following keywords in the case/system/controlDict

```
probes1
{
    type probes; // Type of functionObject
    functionObjectLibs ("libsampling.so");
    probeLocations // Locations to be probed. runtime modifiable!
    (
        (9.15 0.25 0.15) //T1
        (6.90 0.25 0.15) //T2
    );
    // Fields to be probed. runTime modifiable!
    fields
    (
        T U p_rgh p O2
    );
}
```

It is possible to output heat release rate (HRR) against time by adding the following key words in the case/system/controlDict, doing a volume integration over all the cells.

```

HRR
{
    type        cellSource;
    functionObjectLibs ("libfieldFunctionObjects.so");
    enabled     true;
    outputControl  timeStep; //outputTime;
    outputInterval 1;
    log         false;
    valueOutput  false;
    source      all; //cellZone;
    sourceName  c0;
    operation   volIntegrate;
    fields
    (
        dQ
    );
}

```

Then users can use third party data processing program for making plots, e.g. excel or matlab.

### 3.4 Tutorials

Here we shall describe the process of set-up, simulation and post-processing of one FireFOAM case. The Steckler room fire case is selected here as an example.

#### Geometry

The blockMesh utility is used for mesh generation. The mesh is generated from a dictionary file named blockMeshDict located in the constant/polyMesh. In the file, information on vertices, blocks (volumes) and boundary surfaces are defined. The blockMeshDict file is listed here with explanation beside:

```

convertToMeters 0.01; // cm used in the file

vertices
(
    (-200 0 -200) // number 0
    ( 400 0 -200) // number 1
    ( 400 300 -200) // number 2
    (-200 300 -200) // number 3
    (-200 0 200) // number 4
    ( 400 0 200) // number 5
    ( 400 300 200) // number 6
    (-200 300 200) // number 7
);

blocks
(
    hex (0 1 2 3 4 5 6 7) (30 15 20) simpleGrading (1 1 1)
); //30,15,20 grid points in x, y, z axis respectively.

edges

```

```

(
);

Boundary // boundary conditions
(
  Top
  {
    type patch;
    faces
    (
      (3 7 6 2)
    );
  }
  sides
  {
    type patch;
    faces
    (
      (4 7 6 5) // sideRight
      (0 3 2 1) // sideLeft
      (6 2 1 5) // sideFront
      (0 4 7 3) // sideBack
    );
  }
  base
  {
    type wall;
    faces
    (
      (4 0 1 5)
    );
  }
);

mergePatchPairs
(
);

```

Simple grading is applied to obtain an evenly distributed structured mesh. The number of grid points in each direction can be set in the blocks parenthesis in blockMeshDict. In this case, they are 30,15,20 grid points in x, y, z direction respectively.

A large domain embedding the room with dimensions of 6m(L)×4m(W)×3m(H) is created, see Figure 3. The room has a geometry of 2.8m(L)×2.8m(W)×2.18m(H). The door is 1 m high and 1 m wide. The room in this case is created within the domain using virtual planes, or “thermal baffle” in OpenFOAM, and specifically one dimensional (1D) thermal baffle with the createBaffles utility, see the file “mesh.sh”. The geometry of the walls is defined by the topoSet utility. There is large space outside of door of the room.

Note that the 1D thermal baffle model simulates steady state thermal conduction through the thin baffle. In Steckler et al’s tests, the fire tests in the rooms with thin fiber insulation boards as walls lasted for 30 minutes in order to reach a quasi-steady state for research purposes. This fireFoam simulation with 1D thermal baffle could be reasonable. However, in reality, all fires are transient and the walls are mostly not thermally thin. In other words, the 1D thermal baffle is mostly unrealistic.

Therefore this method is not recommended to be used to simulate the heat loss through the wall surfaces in such a room fire. In a word, this case is only a tutorial case but not a practical case.

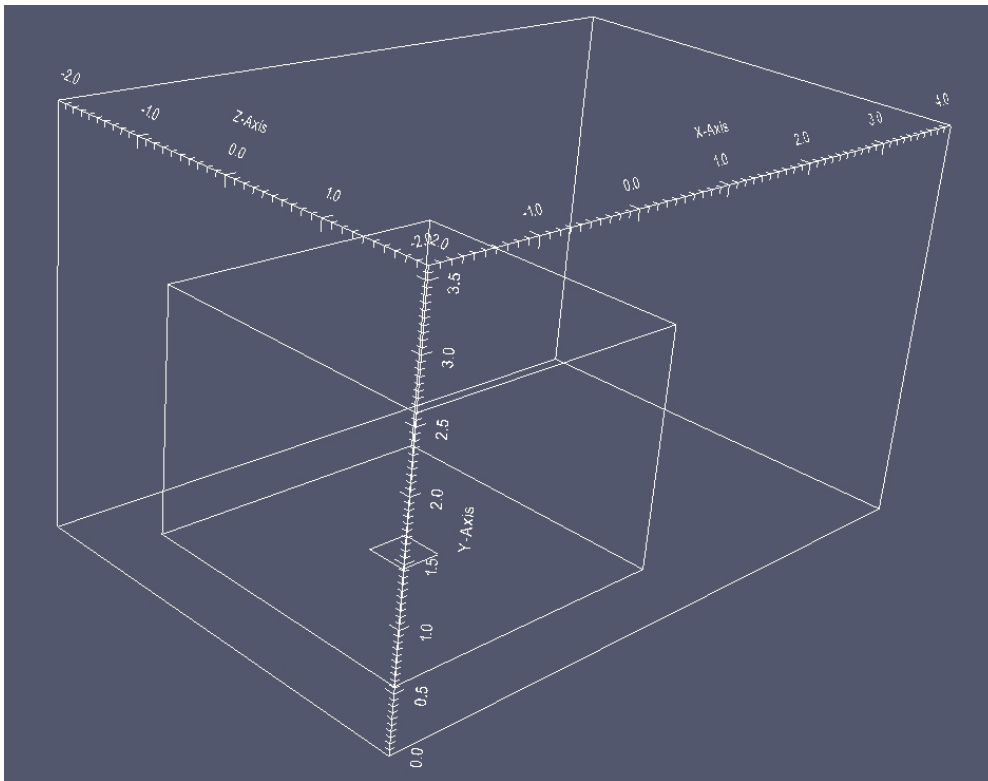


Figure 3. The Steckler room model. Door is at the plane  $x=1.4$  m. (Dimensions in m).

### Fire source

A surface (patch) is needed for the fire source. In this case, a patch called burner is created using the createPatches utility. The geometry of the burner is defined by the topoSet utility, see the file “mesh.sh”.

The rectangular burner with a side length of 0.1524 m is located at the center of the floor in the room. Propane is used by default as the fuel.

### Boundary conditions

#### Fire source

The heat release rate is inputted in terms of mass flow rate in the velocity boundary file in the file “0”. Time dependent inputs are possible. The velocity boundary for the burner is listed here:

```
burner
{
  type      flowRateInletVelocity;
  massFlowRate  table

3
(
(0 0.03)
```

```
(60 0.03)
(100 0.03)
)
;
```

The heat release rate can be estimated based on the flow rate given that the fuel is known as propane.

### **Wall**

As mentioned, all the walls in this tutorial case are simulated by 1D thermal baffles. In the boundary files, boundary conditions for this thermal baffle wall need to be inputted.

The thermal properties of the 1D thermal baffle can be found in `\0\include\1DBaffle`. The content is listed in the following:

```
specie
{
  nMoles      1;
  molWeight   20;
}
transport
{
  kappa       1; //conductivity
}
thermodynamics
{
  Hf          0; //heat of fusion, be default it should be zero.
  Cp          10; //heat capacity
}
equationOfState
{
  rho         10; //density
}
```

### **External boundaries**

The boundaries of the domain are treated as pressure boundary that allows inflows and outflows. The pressure boundary for the top surface is set to be zero gradient while others are fixed ambient pressure.

### **Running**

The case can be executed by the command line:

```
./run.sh
```

By default the simulation time is 2 seconds which can be revised in the System folder. Parallel is also possible by use of the file `decompose.sh`.

### **Postprocessing**

To invoke `paraView`, insert the following command line:

```
paraFoam
```

Slice or vector can be plotted. At first we click the “Mesh Parts” and “Volume Fields” to load the geometrical data and simulation results and apply. Then click the slice in Filters - Alphabetical and choose a plan, and apply. Choose one parameter we want to show in the screen, for example temperature  $T$ .

Figure 4 and Figure 5 show the temperature slices across the fire source and the door at 2 seconds and 30 seconds respectively. To obtain smooth results a slightly finer mesh was used, that is, 60 grid points in x axis, 30 in y axis and 40 in z axis. The simulation time was changed to 30 seconds. The puffing phenomenon can be clearly observed in the first figure. The second figure shows that the predicted temperatures are as high as 1890.5 K, that is, 1617 °C.

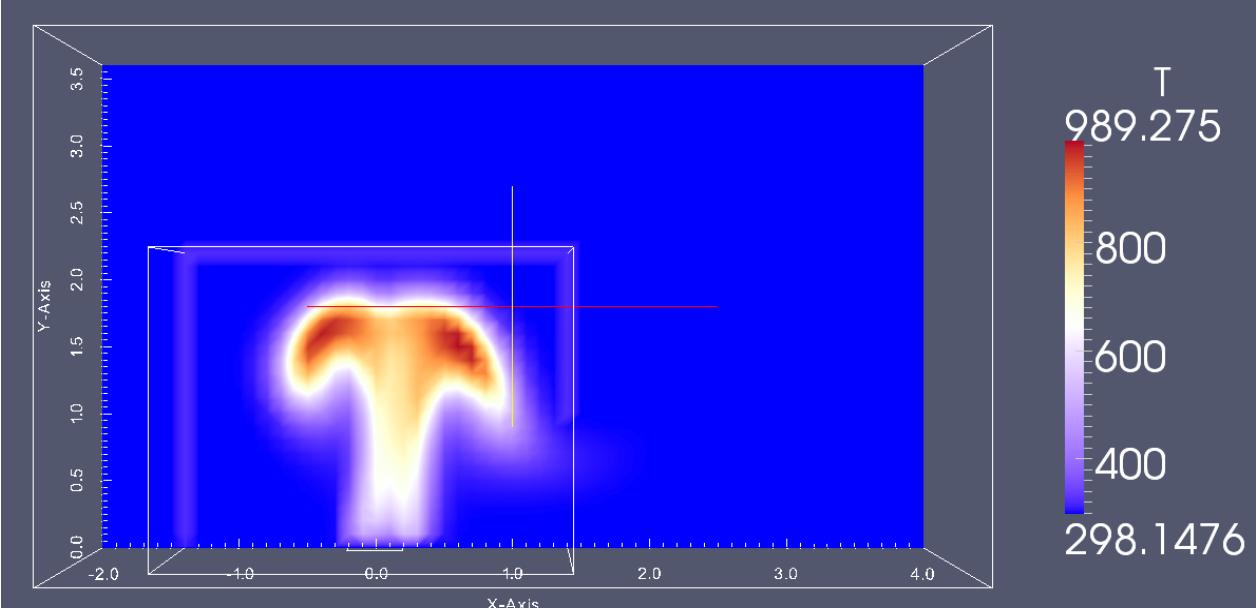


Figure 4. Temperature slice across the fire source and door at  $t=2$  s.

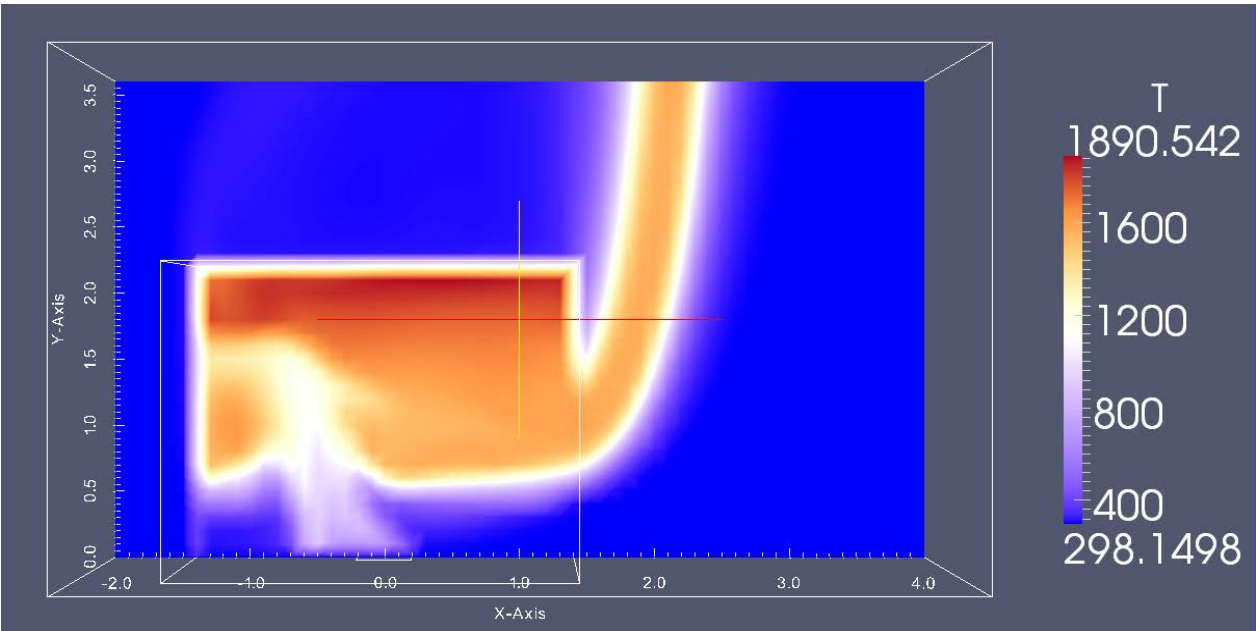


Figure 5. Temperature slice across the fire source and door at  $t=30$  s (Temperature unit: K).

### Parallel running of the case

The above case has been run for 300 seconds (10 minutes). This is a realistic time frame for a typical fire simulation. Three different grid sizes have been used and it can be seen in Table 2 that speed-up is roughly about a factor of 2 by using 4 cores instead of a single core. Further, the speed-up decreases when increasing the number of cells.

Table 2 Parallel speed-up on the Steckler room using FireFOAM-dev (Dec 2016)

Number of cores	Coarse grid 9000 cells [s]	Coarse grid Relative to 1 core	Medium grid 72000 cells [s]	Medium grid Relative to 1 core	Fine grid 243000 cells [s]	Fine grid Relative to 1 core
1	2845	1	52162	1	303230	1
2	1685	1.69	31169	1.67	190990	1.59
3	1334	2.13	25652	2.03	164520	1.84
4	1144	2.49	22530	2.31	149070	2.03

Comparing with a similar two similar setups in FDS and OpenFOAM it can be seen in Table 3 that FDS is much more efficient than FireFOAM. FDS is about 2.5 faster to do the same task, - even that not the most efficient parallelization method was used for FDS. (MPI is more efficient than OpenMP in FDS).

Table 3 Comparison using FDS 6.5.2 with 4 cores (OpenMP) and FireFOAM-dev (Dec 2016) with 4 cores (MPI)

Version	parallelization method	Number of nodes	Computational time [hour]	Relative to FDS
FDS 6.5.2	OpenMP	294912	15.6	1
FireFOAM-dev (Dec. 2016)	MPI	243000	41.4	2.6

### Short summary

In case that only fire in the open or fire in an enclosure with thermally-thin walls (e.g. a steel container) is interested, this tutorial case can be directly used after revising the meshes and the relevant parameters such as fire size. This method is not recommended to be used to simulate the heat loss through the walls in the cases with thermally-thick walls.

Further, it was found that FireFOAM is up to 2.5 slower than the Fire Dynamic Simulator to do a similar computation.

## 4 Verification of heat transfer in FireFOAM

“Verification is a process to check the correctness of the solution of the governing equations” according to the definition from the FDS Verification Guide [28]. A complete check of all parts of FireFOAM was not done and would be a tremendous task, but it was chosen to verify the three modes of heat transfer. Heat transfer is important in all fire application. So to verify FireFOAM, - checking that the program solves the equations correctly, FireFOAM was verified against analytical solutions for radiative, convective and conductive heat transfer.

### 4.1 Radiative heat transfer

FireFOAM has two different radiation models currently implemented. One is called the finite volume discrete ordinates model (fvDOM) and the other is called P1. The fvDOM-model is the most common for fire applications and is similar to the FVM-method implemented in FDS.

A list of advantages and limitations of the different models can be found bellow and is adopted from Vdovin [29].

**Table 4 Advantages and limitations of the two radiation models available in fireFoam**

	<b>fvDOM</b>	<b>P1</b>
<b>Advantages</b>	<p>It is a conservative method that leads to a heat balance for a coarse discretization. The accuracy can be increased by using a finer discretization.</p> <p>It is the most comprehensive radiation model: Accounts for scattering, semi-transparent media, specular surfaces, and wavelength-dependent transmission using banded-gray option.</p>	<p>The radiative heat transfer equation is easy to solve with little CPU demand.</p> <p>It includes effects of scattering. Effects of particles, droplets, and soot can be included.</p> <p>It works reasonably well for applications where the optical thickness is large</p>
<b>Limitations</b>	<p>Solving a problem with a large number of ordinates is CPU-intensive.</p>	<p>It assumes that all surfaces are diffuse.</p> <p>It may result in loss of accuracy (depending on the complexity of the geometry) if the optical thickness is small.</p> <p>It tends to overpredict radiative fluxes from localized heat sources or sinks.</p>

Comparison of the two radiation models for different practical applications is beyond the scope of this report. The verification in this chapter is performed using the fvDOM-method.

The case used in this verification is adopted from the verification guide for FDS (McGrattan et al, [28]) and is called `radiation_in_a_box`. The case consists of a box with 1 meter sides and with one warm and five cold patches. The influx in the diagonal of the opposite side is measured and compared to the analytical solution. The setup is presented in the figure bellow.

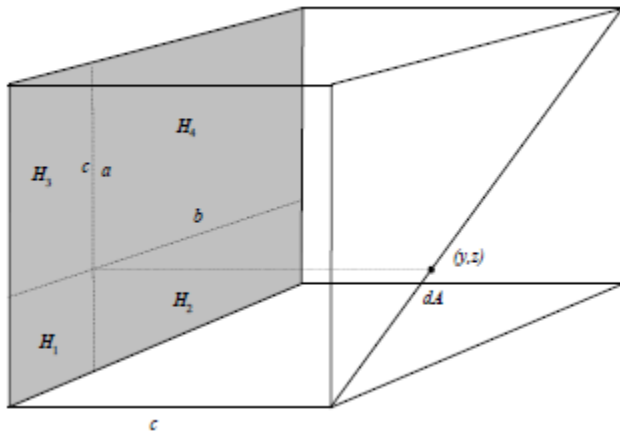


Figure 6 Radiation in a box geometry (adopted from, McGrattan et al, [28])

Ideally the cold patches would have a fixed temperature of 0 K so that they emit no radiation. However, the fluid solver employed in fireFoam is only valid for temperatures above 200 K. Therefore the cold patches were set to a temperature of 200 K and the hot patch was set to 1000 K. The net influx of the opposite wall was measured with a patchprobe and therefore to calculate the influx from the hot wall the outgoing radiation (at 200 K) of the opposite patch had to be added. This correction can be done with perfect accuracy since it only involves correcting the source term.

Further, the influx from the sidewalls had to be removed by using the analytical solution for this case from the SFPE Handbook [30]. This correction is approximate since the correction is based on the analytical solution whereas the modelled influx was based on the numerical scheme. However, the correction needed was small compared to the influx from the hot wall (about 0.5-0.9 %) and therefore the numerical accuracy of the modelled influx will not affect the comparison.

The distribution of integration angles is different between FDS and FireFOAM and therefore an exact comparison with the same number of angles and the same number of cells was not possible. FDS uses an algorithm that varies the numbers of angles in the azimuthal direction ( $\phi$ ) depending on the polar direction ( $\theta$ ) so that the solid angles are of similar sizes. In FireFOAM, however, the polar and azimuthal angles are independent and therefore the density of angles close to the “poles” will be much higher than closer to the “equator”. This comparison is conducted in such way that the maximum size of the solid angle is the same in FDS and FireFOAM. This leads to that the numbers of angles in FireFOAM is slightly higher than in FDS. Simulation is conducted for 300, 1000 and 3000 angles in FDS, which compares to 448, 1536 and 4640 angles in FireFOAM.

The simulations are conducted for the volume divided into 20x20x20 cells (i.e. 5 cm-cells). The results can be found in the Figure 7 below where results from both FireFOAM and FDS are plotted against the analytical solution.

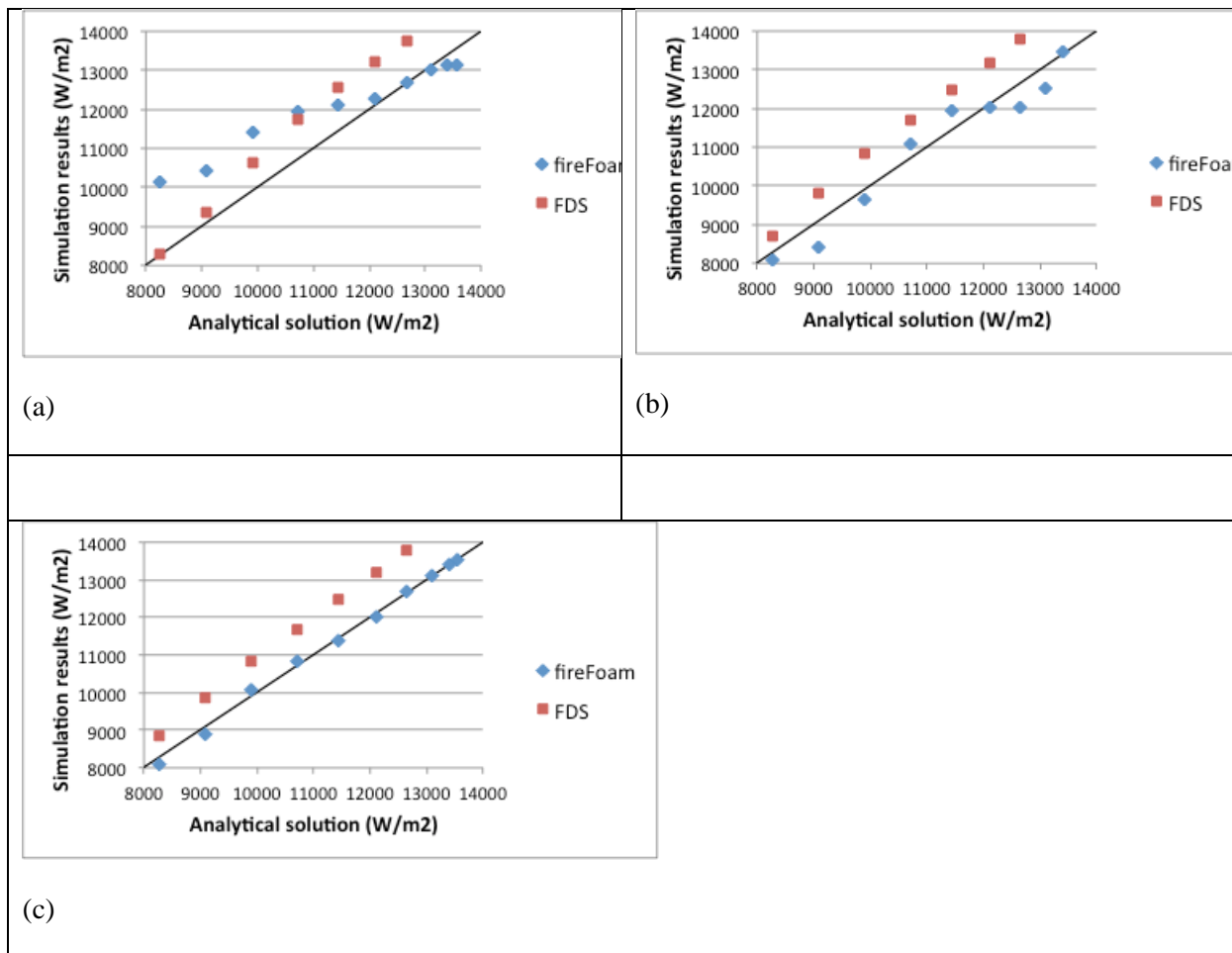


Figure 7 Comparison between FireFOAM, FDS and the analytical solution for 20x20x20 cells. The simulations were performed with 300 (a), 1000 (b) and 3000 (c) solid angles

As can be seen from the simulations FireFOAM overestimates the incident heat flux on low view angles while FDS overestimates it on high view angles. The average error for the current vase was 604 W/m<sup>2</sup> for FireFOAM and 877 W/m<sup>2</sup> for FDS.

More interestingly, the solution converges towards the analytical solution for FireFOAM with increasing number of angles while FDS systematically overestimates the influx about 9 % over the entire range of view angles. This is surprising given that both FireFOAM and FDS uses similar models. The difference is likely to be due to differences in the numerical implementations of the models. A closer comparison should be performed to investigate if changes in the implementation in FDS can be performed without to much penalty on the computational time.

## 4.2 Convective heat transfer

Validation of convective heat transfer were done by simulating example 19-9 from the book by Çengel & Turner [31] where air at  $80^{\circ}\text{C}$  where blown into a 8 meter long tube with a quadratic cross section with 0.2 meter sides. The air is blown with a velocity of 3.5 m/s. The walls are kept at a constant temperature of  $60^{\circ}\text{C}$  and the temperature of the air leaving the tube are calculated. See Figure 8 for additional information.

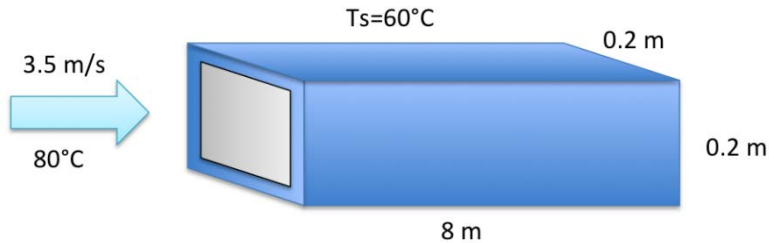


Figure 8 Case used for verification of the models of convective heat transfer

The simulation was performed using the same input as the analytical solution, but additionally a discretization of the domain was needed. This was preformed using a mesh with  $10 \times 10 \times 400$  cells.

The analytical solution yields an exit temperature of  $71.3^{\circ}\text{C}$  and the steady state temperature in the simulation was  $70.7^{\circ}\text{C}$ . The slight difference of  $0.6^{\circ}\text{C}$  can be due to either the discretization of the domain or inaccuracies in the equations for either the analytical solution or the equations implemented in FireFOAM. The difference is however so small that the validation has been successful.

### 4.3 Conductive heat transfer

The verification of the simulation of conductive heat transfer is made by constructing a domain of 1x1x1 meters (divided into 20x20x20 cells) and dividing it by a 0.3 m thick wall. The wall is defined using the thermal baffle algorithm in FireFOAM. This boundary condition assumes a thermally thin material (i.e. steady state conduction). This is an unreasonable assumption in many scenarios, but since this is the most common thermal boundary condition used, it was chosen for validation.

On one side of the wall a hot stream of 1000 K at 1 m/s where blown in the z-direction and on the other side a cool stream of 400 K at 1 m/s were blown also in the z-direction as shown in Figure 9. Temperature were measured along a line parallel to the x-axis going through the center of the slab.

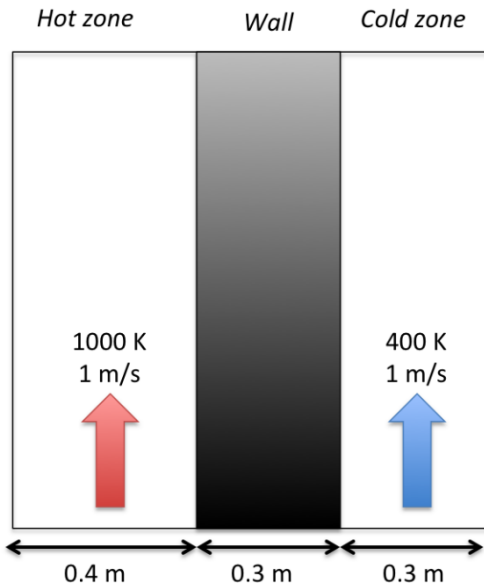


Figure 9 Case used for verification of heat conduction through walls

Since the validation is of a steady state conduction only the thermal conductivity and thickness of the slab is needed to validate against the simulation results. The thermal conductivity was set to 1 W/mK and the thickness was 0.3 meters.

The heat transfer coefficient,  $h$ , was measured in the simulation and was determined to be 41,8 W/mK on the warm side and 11,0 W/mK on the cold side. Using the equations for conductive and convective, steady state, heat transfer and eliminating the transferred energy per second and unit area the following equation is found.

$$\dot{q}'' = h(T_{\text{warm}} - T_1) = \frac{k}{L}(T_1 - T_2)$$

Where  $T_{\text{warm}}$  is the temperature of the air at the warm side (1000 K),  $T_1$  is the surface temperature on the warm side and  $T_2$  is the surface temperature on the cold side. Solving for the thermal conductivity and implementing numbers from simulations yield the results bellow.

$$k = \frac{h(T_{\text{warm}} - T_1)L}{(T_1 - T_2)} = \frac{41,82 \cdot (1000 - 965,4) \cdot 0,3}{(965,4 - 531,3)} = 1,0 \text{ W/mK}$$

This is equal to the thermal conductivity prescribed to the model.

#### **4.4 Short summary**

It was verified that FireFOAM handles the three modes of heat transfer appropriately in the code.

## 5 Case studies – validation of FireFOAM

In order to get confidence in the results from CFD simulation the tools used need to be validated. Validation is comparing simulation results with full scale experiment and check that the simulation results are similar to the experimental. “Validation is a process to determine the appropriateness of the governing equations as a mathematical model of the physical phenomena of interest” as stated in the FDS Fire Dynamics Simulator, Technical Reference Guide, Volume 3: Validation.[9]

A tunnel fire, a room fire and smoke ventilation in a large room has been chosen to validate FireFOAM.

The tunnel fire is an interest due to the difficulties in obtaining a solution for the pressure equation as the pressure can only be relieved at the openings of the tunnel. This is a general issue related to tunnels and has for example been covered in the FDS User Guide [32]. This subject has also be investigated by Kilian and Münch [33].

The room fire is relevant when doing enclosure fire simulations, where it is important to predict temperatures and radiation. Lastly fire ventilation is of great interest in industrial application, e.g. the performance of fire ventilation in large warehouses.

### 5.1 Small scale

#### 5.1.2 Inclined tunnel

##### *Experimental setup*

Long tunnels with a height difference between the tunnel portals, for the distribution of energy and communication, can in case of fire obtain thermal pressure differences that suddenly can overturn the normal direction of the air movement in the tunnel. This phenomenon could represent a risk for the fire and rescue operation and thereby influence the outcome of the fire. To understand the risks in such cases and to define indicators that could be used by the fire and rescue services, model scale tests have been performed.

Model scale tests were performed at SP – the Technical Research Institute of Sweden in autumn 2010. A tunnel model was built in the scale 1:20 with the total length of 7.5 meters and a square cross-section of 0.3\*0.3 meters. The tunnel walls were made of calcium silicate aluminate boards (promatect) on three sides with thickness of around 0.01 meters, and the fourth side consisting of shutters was made of fire retardant glass with thickness of around 0.01 meters. The thermal properties of tunnel wall materials are shown in Table 5. The model tunnel was placed on a rack which could be altered regarding inclination. The counteracting wind was simulated by an axial fan, with variable adjustment, placed at the top end of the tunnel. The fan was placed around 2 meters in front of the tunnel upper entrance and was redirected between the different inclinations so the axis of the fan at all times was in line with the length axis of the tunnel. The test set up is shown in Figure 10. A propane burner was used to simulate the fire, and it was located in the middle of the tunnel with an estimated size of 0.18\*0.18 m<sup>2</sup>. Seven thermocouples and four velocity measurement points were located inside the tunnel. Thermocouples T1, T2, T6 and T7 were located 0.15 m below the tunnel ceiling, and thermocouples T3, T4, T5 were located 0.1 m, 0.05m, 0.1 m from the tunnel ceiling, respectively; see Figure 10 for detailed positions. Velocity measuring points u1, u2, u3 and u4 were located in the central line in the tunnel.

**Table 5 Thermal properties of tunnel walls**

Material	Thermal conductivity, $k$ [W/(m <sup>2</sup> ·K)]	Density, $\rho$ [kg/m <sup>3</sup> ]	Specific heat, $c_p$ [J/(kg·K)]
Promatect	0.19	870	1130
Glass	0.78	840	2700

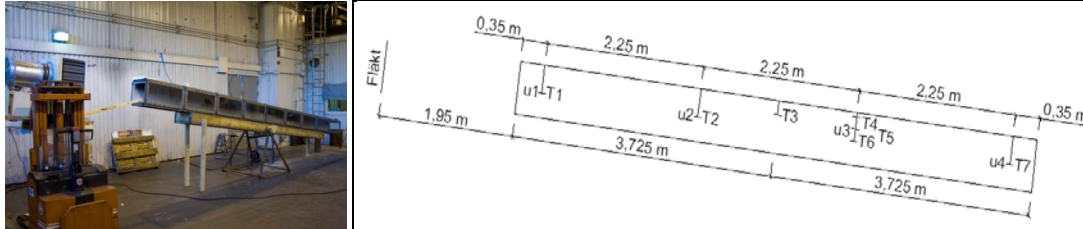


**Figure 10. Test set up and location of measuring equipment.**

**Numerical setup**

FireFOAM code was applied to simulate the fire and heat transport in the inclined tunnel. It solves numerically a form of the Navier-Stokes equations appropriate for low-speed, thermal-driven flow with an emphasis on smoke and heat transport from fires. FireFOAM code is based within the framework of LES (Large Eddy Simulation). The sub-models and model constants used in the simulations are listed in Table 2.

**Table 6. Summary of sub-models used in FireFOAM simulations and their constants**

Sub-models	Name	Constants
Turbulence	compressible LES Smagorinsky	$C_e = 1.048, C_k = 0.02, Pr_t = 1.0$
combustion	Eddy Dissipation Model	$C_{EDM} = 4.0, C_{diff} = 0, C_{stiff} = 1.0$
radiation	fvDOM, grey mean absorption emission	
thermo-physical	Idea gas, JANAF coefficients	
Soot	Off	

The heat conduction through the tunnel walls is highly transient and it depends on many parameters, e.g. thermos physical properties of wall material, fire effect, fire dynamics inside tunnel, surrounding gas temperature and so on. All the walls including promatect and glass walls are assumed to have a fixed value of room temperature, i.e. 293.15 K. The computational domain covers only the inside of the tunnel, and the computational mesh consists of 84 375 cells with a cell size of 2 cm in each direction of the Cartesian coordinates. The geometry and boundaries of inclined tunnel is shown in Figure 11. The rest of the initial and boundary conditions are shown in Table 7. Since this work focuses on the fire dynamics inside the inclined tunnel, the simple temperature wall boundary condition is adopted for model validation.

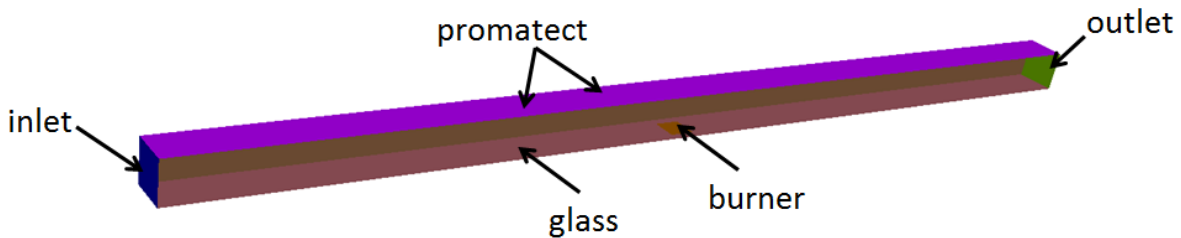


**Figure 11. Geometry and boundaries of inclined tunnel.**

**Table 7. Initial and boundary conditions**

Parameter	Initial value	Boundary type
$k$ [m <sup>2</sup> /s <sup>2</sup> ]	1.0e-4	inlet/outlet: inletOutlet promatect/glass: zeroGradient burner: fixedValue
$p$ [Pa]	101325	calculated
$T$ [K]	293.15	inlet/outlet: inletOutlet promatect/glass/burner: fixedValue
$ \mathbf{u} $ [m/s]	0	inlet: fixedValue 1.0 outlet: pressureInletOutletVelocity promatect/glass: fixedValue 0 burner: flowRateInletVelocity massFlowRate 3.7e-4 [kg/s] (propane)

It is assumed that the fire source has an area of 0.0324 m<sup>2</sup>(0.18\*0.18 m). A constant value of mass flow rate of propane 0.00037 [kg/s] was specified in the middle of the tunnel in order to simulate a gas burner with a power of 17 kW. The heat of combustion of propane is 46.45 MJ/kg [34]. In order to simulate the effect of inclination, the gravity vector  $\mathbf{g}$  was adjusted depending on the inclined angle  $\theta$  as follows

$$\mathbf{g} = (-|\mathbf{g}| \sin \theta, 0, -|\mathbf{g}| \cos \theta)$$

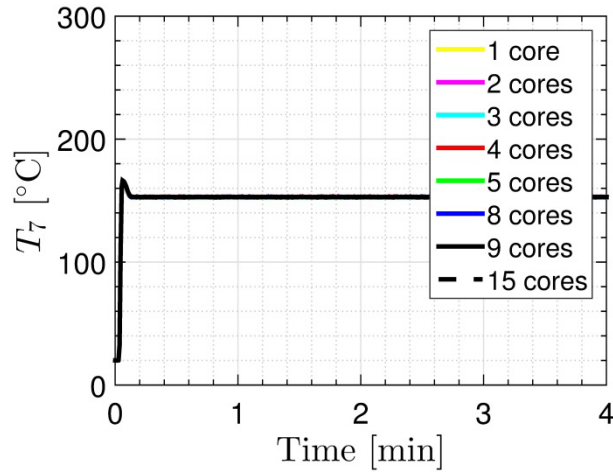
### *Results and discussions*

In this section, the comparison of results obtained using FireFOAM and FDS are reported regarding parallelization, computational speed and grid. Then the sensitivity study was performed for FireFOAM model regarding several important model parameters, i.e. grid size, EDM model constant  $C_{EDC}$ , and turbulent Prandtl number. Finally, validation of computed gas temperature and velocities are compared to the measured data.

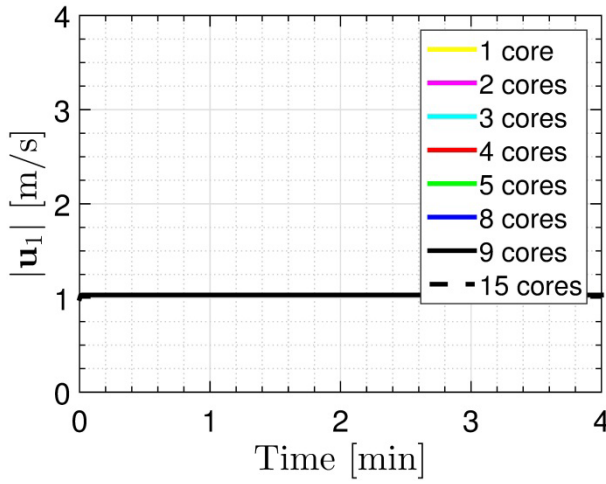
#### Parallelization

##### *Result consistency in parallelization*

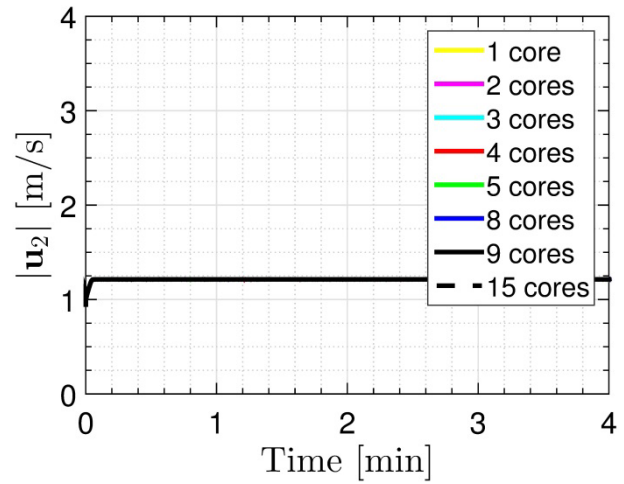
The parallel computation is more and more frequently used in CFD simulations due to the associated huge number of computational cell and more and more detailed modelling of physical and chemical phenomena. In this part, the capability of FireFOAM solver in parallel computation is tested. The inclined tunnel domain was decomposed in to 1, 2, 3, 4, 5, 8, 9 and 15 sub-domains evenly along the horizontal line, and subsequently these cases were run on 1, 2, 3, 4, 5, 8, 9 and 15 processors on a Linux cluster called Calculon (a SP's cluster located in Södertälje) with 256 cores and 1 TB RAM. The cell size is 5 cm and the total number of computational cell is 5 400. The inlet velocity at the tunnel portal is 1.0 m/s. The computed gas temperature at location for thermocouple 7 and gas velocities at four locations along the tunnel using different number of processors are shown in Figure 12. It can be seen that the parallel computation of FireFOAM is very consistent as far as different number of processors are concerned regarding to the computed gas temperature and velocities along the tunnel. It is also worth noting that the fire source is located in the middle of the tunnel. In the cases of parallel computations performed by even number of processors, e.g. 2, 4 and 8, the fire source, which is crucial in determining temperature distribution, is distributed on at least two different processors. Even in such cases, the computed temperature curves are overlapping; see Figure 12(a). Such results prove the results consistency when using FireFOAM in parallel computation.



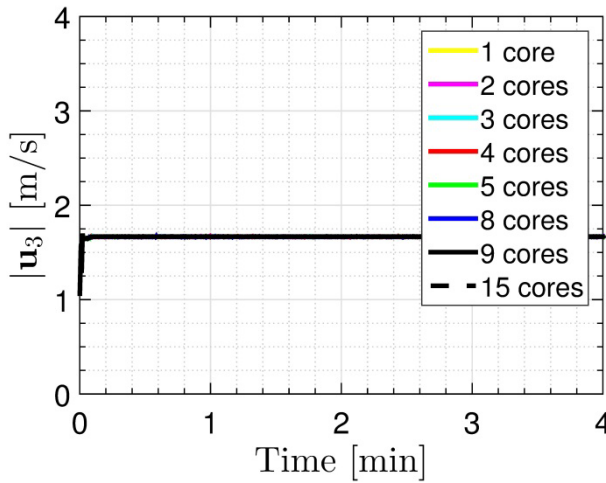
(a) Temperature at thermocouple T7



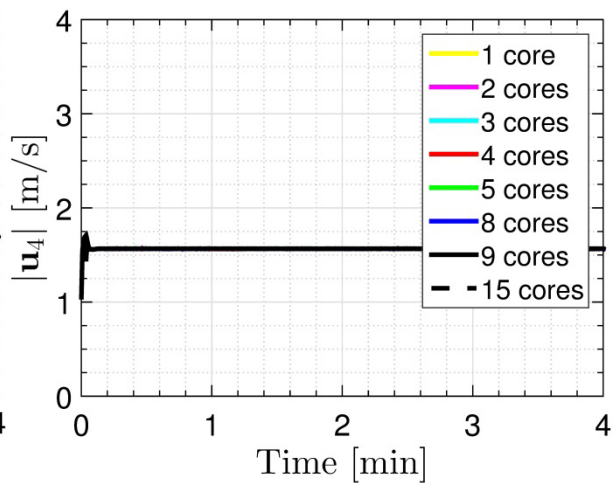
(b) Velocity magnitude at u1



(c) Velocity magnitude at u2



(d) Velocity magnitude at u3



(e) Velocity magnitude at u4

Figure 12. The effect of number of processors in parallel computation using FireFOAM on the calculated temperature and velocity at different locations in the tunnel.  $|u_{fan}|=1.0$  m/s.

### Speed in parallelization

It is interesting to investigate the speedup factor or relative clock time using FireFOAM. Seven simulations were performed to investigate the speedup factor of parallel computation using FireFOAM. The simulation duration is 4 minutes. The number of computational mesh is the same for all the cases, i.e. 5 400 cells, with a grid size of 5 cm. The computer resource is the same as mentioned above. It can be seen in Figure 13 the relative clock time decrease as the number of cores increases, especially when using 2 cores, the computational time is shortened by almost 50%. The speedup effect is negligible if more than 3 cores are used according to Figure 13. If many cores are used, e.g. 8 cores, there is a slight increase in relative clock time. This might be due to the fact that too much time is consumed in data communication among the cores instead of solving the partial differential equations. It is worth noting that if another type of computational mesh is used, the speedup trend is very likely to be the same, but the optimum number of cores for computation might differ.

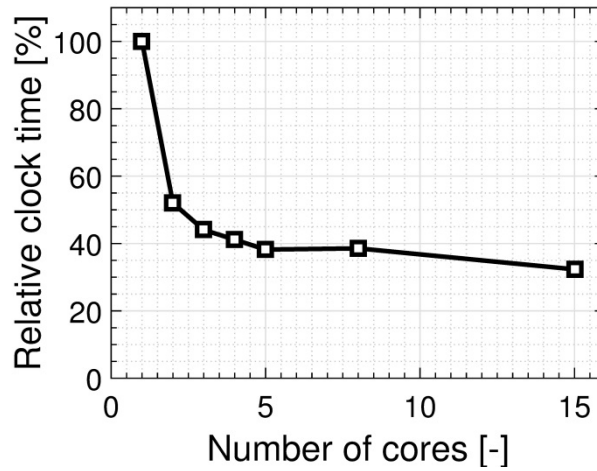


Figure 13. Comparison of relative clock time using different number of cores using FireFOAM.

### Sensitivity study

#### Grid size

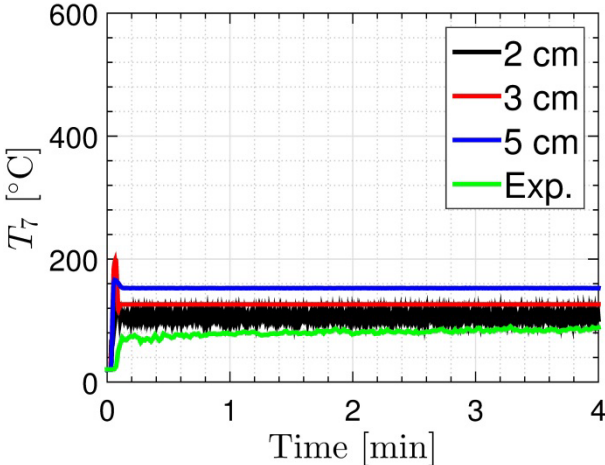
Grid size dependency is a commonly discussed problem in fire dynamics simulations. According to the FDS user's guide [35], a non-dimensional parameter  $D^*/\delta x$ , is recommended to measure how well the flow field is resolved, where  $D^*$  is a characteristic fire diameter and it is defined as follows,

$$D^* = \left( \frac{\dot{Q}}{\rho_\infty c_p T_\infty \sqrt{g}} \right)^{2/5}$$

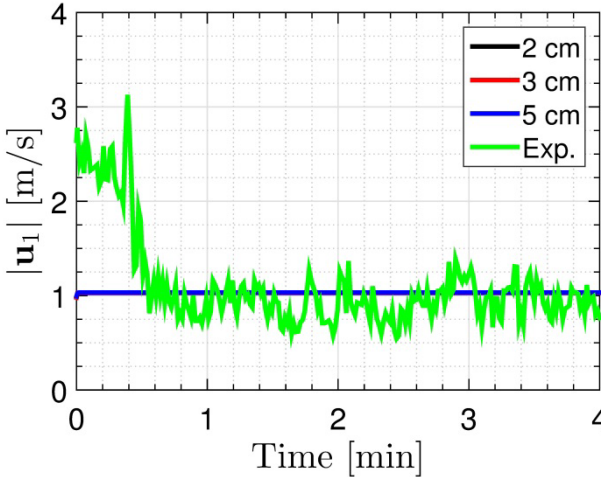
where,  $\delta x$  [m] is the mesh size around fire source;  $\dot{Q}$  [W] is the heat release rate of the fire;  $\rho_\infty$  [ $\text{kg}/\text{m}^3$ ] is the air density in the surrounding, value 1.2 for standard condition;  $c_p$  [J/kg/K] is the specific heat capacity of air, value 1000 for standard condition;  $T_\infty$  [K] is the air temperature in the surrounding, value 293 for standard condition;  $g$  [ $\text{m}/\text{s}^2$ ] is the standard gravity, value 9.81.  $D^*/\delta x$  can be considered as the number of cells spanning the fire source. Therefore, the more cells the better resolution it will be. Nevertheless, it is recommended to have  $D^*/\delta x$  value in the range of 4 and 16.

The effect of grid size on calculated temperature and velocity at four locations is shown in Figure 14. Three sets of mesh are used in the simulations, with a mesh size being 2, 3 and 5 cm, respectively. According to the above equation,  $D^*/\delta x$  value of the three mesh (from fine to coarse) are 3.8, 6.3 and

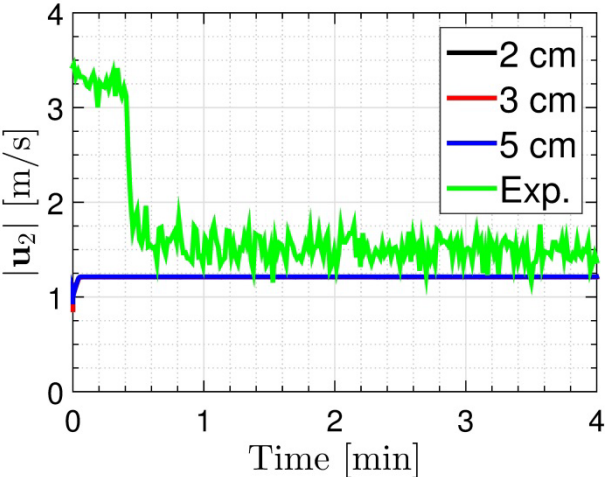
9.4, respectively. The inlet velocity was set as 1 m/s with the rest of sub-models and initial/boundary conditions listed in Table 7. The calculated temperature at measuring point 7 (downstream in the tunnel in Figure 10) is slightly affected by the mesh size; see Figure 14(a). A larger grid size yields a higher temperature at measuring point 7. More fluctuations in temperature are observed for a smaller mesh size as compared to a coarser mesh size. This is explained by the fact of better resolution of turbulence associated with a smaller mesh size. As far as velocity in the four measuring locations are concerned, there is negligible effect of mesh size on calculated velocity; see Figure 14(b)-(e). In the subsequent simulations, a mesh size of 2 cm is adopted since the computed temperature at measuring point 7 using 2cm grid agrees better with experimental results; see Figure 14(a).



(a) temperature at T7



(b) Velocity magnitude at u1



(c) Velocity magnitude at u2

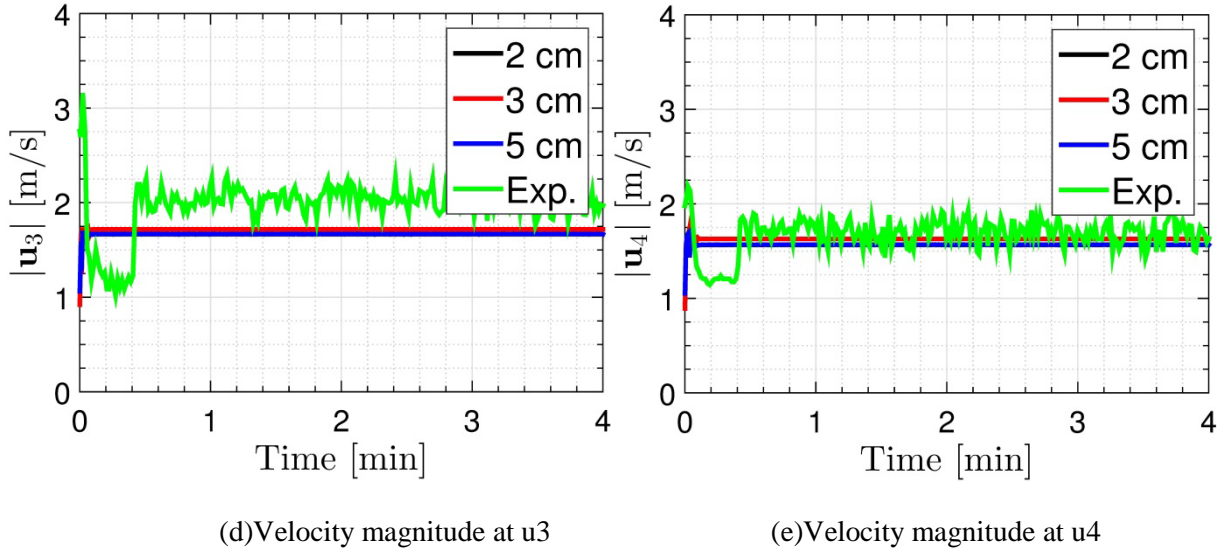


Figure 14. The effect of mesh size on the calculated temperature and velocity at different locations in the tunnel using FireFOAM model.  $|u_{fan}|=1.0$  m/s.

#### Combustion model constant $C_{EDC}$

According to the implementation of EDC model in FireFOAM code, the model constant  $C_{EDC}$  is a critical parameter in determining the characteristic turbulent time scale, thus the mean fuel reaction rate, and thus combustion rate in a diffusion flame.  $C_{EDC}$  is a constant which depends on the flame structure and reaction rate between fuel and oxidant, and its value varied substantially in literatures. For instance, Magnussen and Hjertager [18] applied  $C_{EDC}=4.0$  for city gas turbulent diffusion flames within the flame work of RANS. Panjwani et al. [36] recommended that  $C_{EDC}=0.25$  yielded reasonable results for Sandia Flame D. The effect of adjusting  $C_{EDC}$  on the computed results (temperature, velocities and Heat release rate) are shown in Figure 15 based on three simulations with  $C_{EDC}$  being 2.0, 4.0 and 8.0, respectively. The constant  $C_{EDC}$  has little effect on temperature to the left of the fire source, i.e. T1 - T3, since the temperatures, i.e. T1 - T3, are almost room temperature. However, it has noticeable effect on the temperature to the right of the fire source, i.e., T4 - T7; see Figure 15. This is mainly due to the strong convection from the fan located at upstream of the tunnel. Accordingly, in the downstream of the tunnel, the constant  $C_{EDC}$  plays important role in consuming fuel, thus heat release rate and temperature. It can be seen in Figure 15 that the higher  $C_{EDC}$  value the higher the calculated temperature, i.e. T4 - T7, but the effect of  $C_{EDC}$  is less pronounced especially at the end of the tunnel, i.e. T7. The calculated gas velocities along the tunnel is weakly affected by the constant  $C_{EDC}$ , and the results are not shown here.

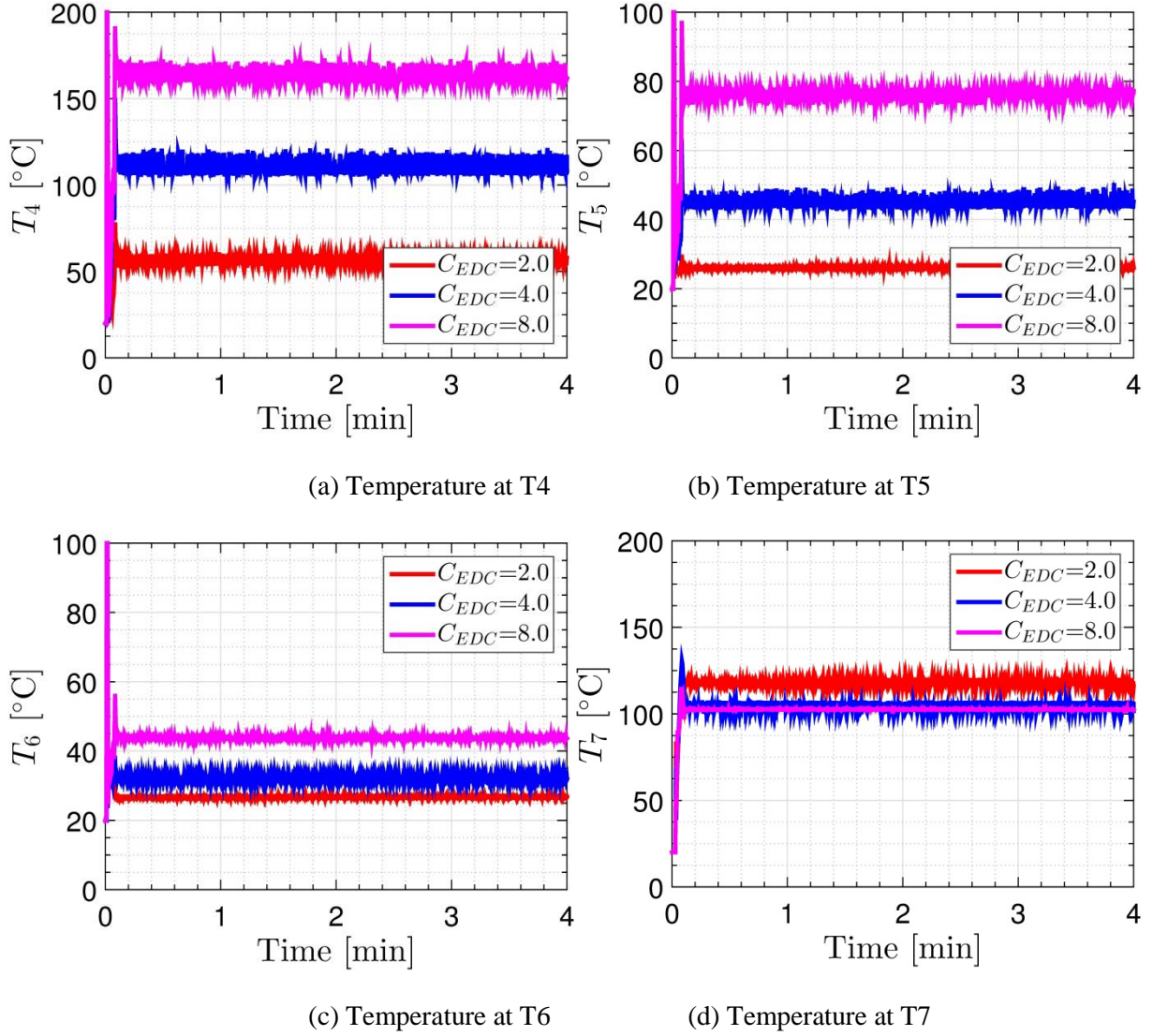


Figure 15. The effect of  $C_{EDC}$  on the calculated temperature at different locations in the tunnel.  $|u_{fan}|=1.0$  m/s.

#### Turbulent Prandtl number

Turbulent Prandtl number  $Pr_t$  is defined as the ratio of the turbulent/eddy viscosity  $\mu_t$  and the turbulent heat diffusivity  $\alpha_t$  as follows

$$Pr_t = \frac{\mu_t}{\alpha_t}$$

The default value of  $Pr_t$  in FDS is 0.5 whereas that in FireFOAM is 1.0. Moreover, the values of  $Pr_t$  reported in the CFD literature range typically from 0.7 to 0.9 depending on the type of flow being considered, but can be much lower e.g. 0.35 in some cases [37]. The effect of the turbulent Prandtl number on the turbulent combustion was investigated by conducting simulations in which  $Pr_t$  was varied from 0.25 to 1.0. As shown in Figure 16(a), variation within this range had noticeable effect on the calculated temperature at T7. A higher turbulent Prandtl number yielded higher temperature in the end of the tunnel. As far as the velocities are concerned, turbulent Prandtl number has little effect on the calculated velocity in the upstream of the tunnel (results are not shown here), but it has a weak effect on the calculated velocity in the end of the tunnel; see Figure 16(b).

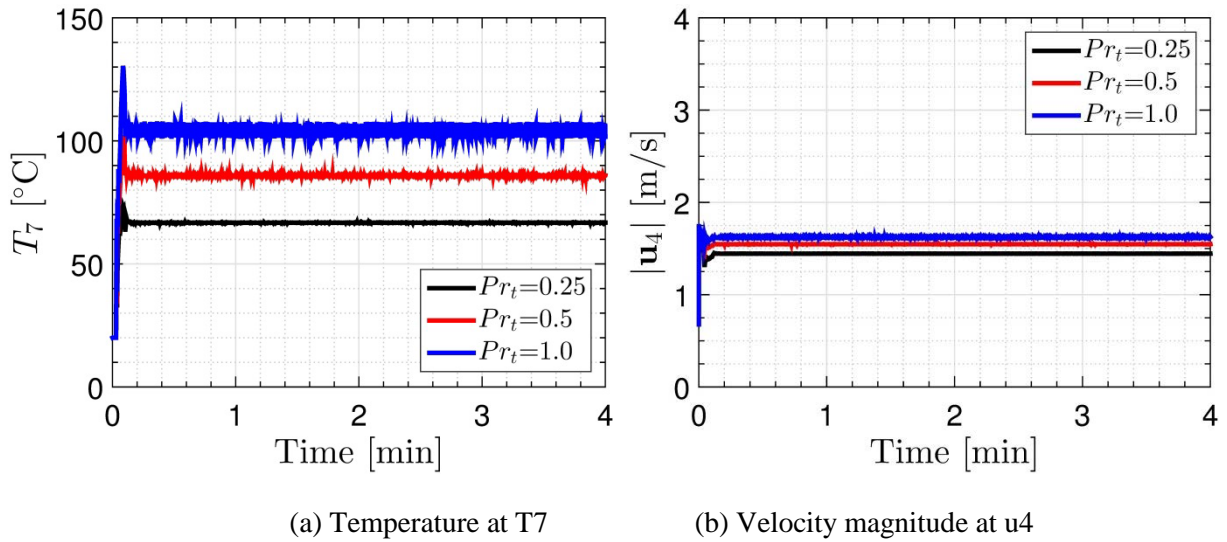
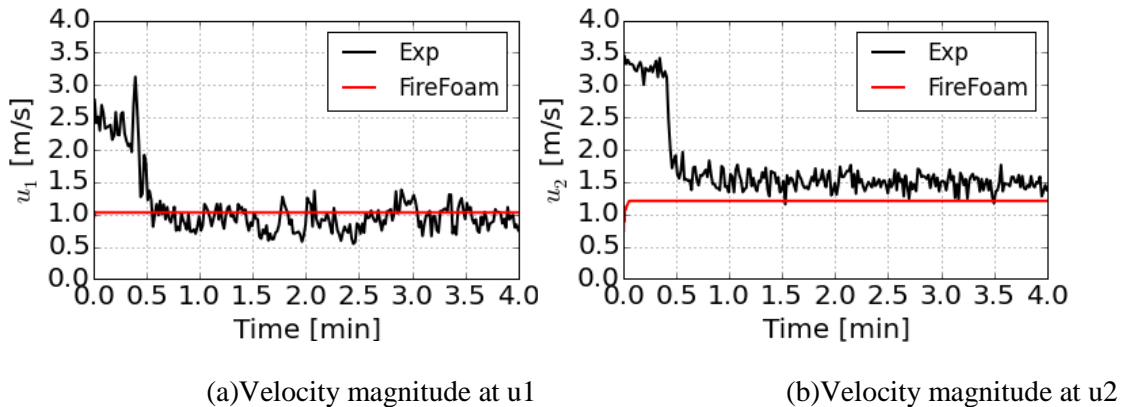


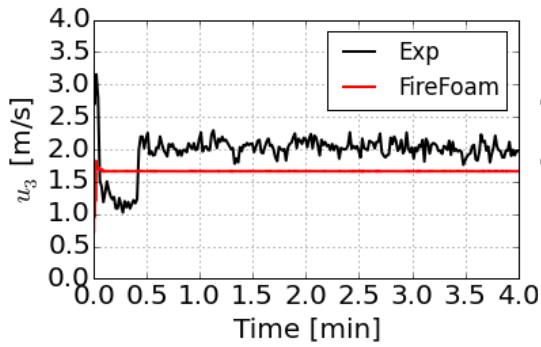
Figure 16. The effect of  $Pr_t$  on the calculated temperature and velocity at different locations in the tunnel.  $|u_{fan}|=1.0$  m/s.

### Validation

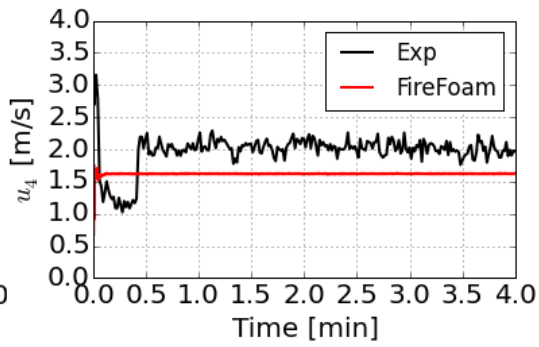
In this section the comparison between measured quantities (velocities and temperatures) and calculated ones using FireFOAM are discussed. Even though a FDS model of the inclined tunnel was built in parallel to the FireFOAM model, the calculated results using FDS are not shown here. This is due to the fact that FireFOAM and FDS code are sustainably different in terms of code structure and implementation of sub-models, and turbulence models. There is no point to judge which code is better when comparing with experimental data.

The comparison of measured velocity and calculated ones using FireFOAM are shown in Figure 17. In these simulations, the computational domain covers only the inside of the tunnel, and an initial fan velocity of 1.0 m/s was assumed at the inlet port of inclined tunnel. In order to simulate heat losses through the wall, a fixed temperature of 298.15 K at the tunnels walls was set for walls of promatect and glass. Important model constants and boundary conditions are shown in Table 2 and Table 7. In the beginning of the measurements, i.e. 0-0.4 minute, due to the transient effect from fan blowing air into the tunnel, there is some instability in the measured velocities, and we can focus on the stabilized values from 0.4- 1 minute. The calculated gas velocities agree well with the measured value, and simulation shows a slight increase of gas velocity along the tunnel which is in line with measured data. In current simulations, the outer loop called PIMPLE for velocity, momentum and energy equations are re-calculated for 6 loops whereas the inner loop called PISO for pressure equation was recalculated for 4 times.





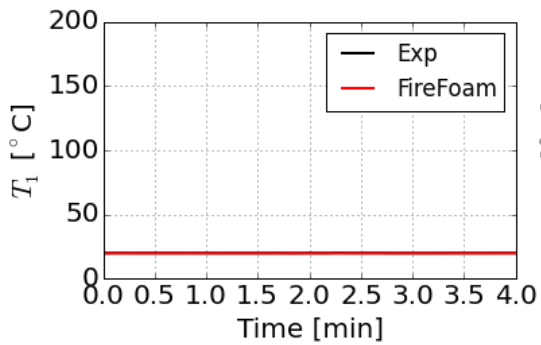
(c) Velocity magnitude at u3



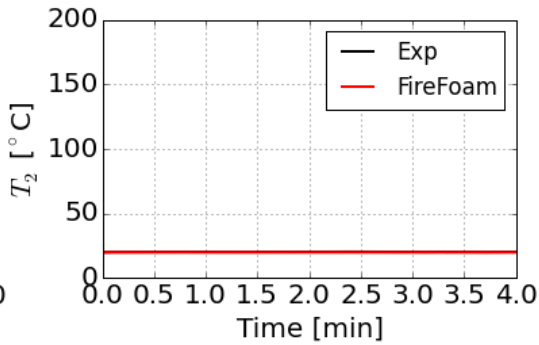
(d) Velocity magnitude at u4

Figure 17. Comparison of measured (black) and calculated velocities using FireFOAM (red) at different locations in the tunnel.  $|u_{fan}|=1$  m/s.

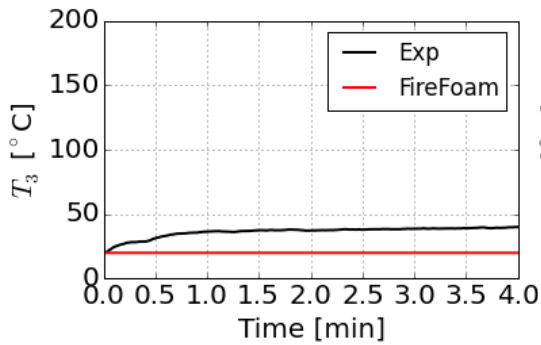
The comparison of measured and calculated temperatures using FireFOAM along the tunnel is shown in Figure 18. We should focus us on the stabilized temperature after around 0.4 minutes. It can be seen that the calculated temperature agree generally well with the measured data.



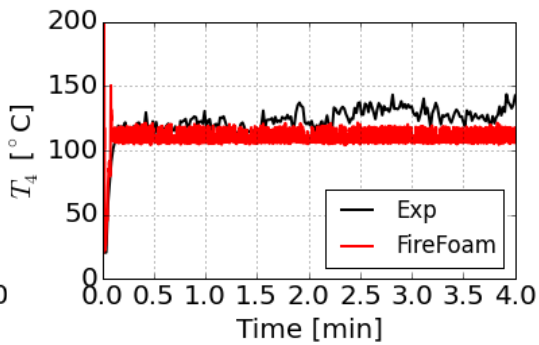
(a) gas temperature at T1



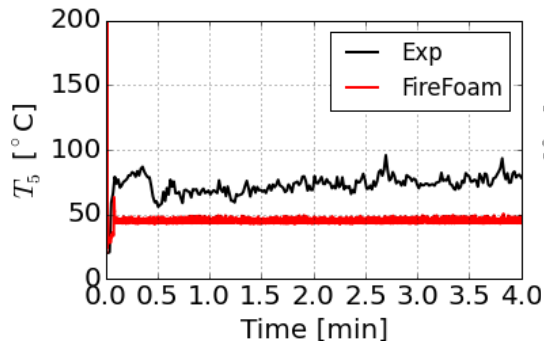
(b) gas temperature at T2



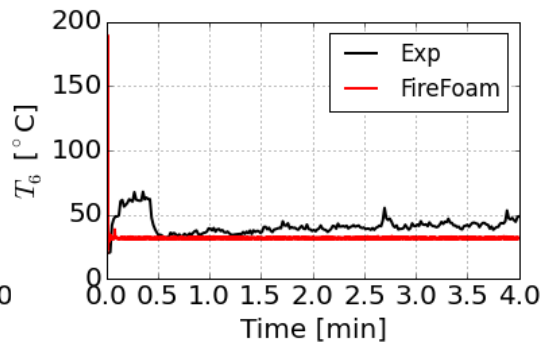
(c) gas temperature at T3



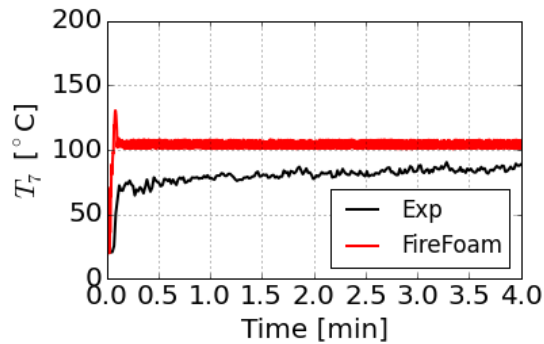
(d) gas temperature at T4



(e) gas temperature at T5



(f) gas temperature at T6



(g) gas temperature at T7

**Figure 18.** Comparison of measured (black), calculated gas temperature for around 5 seconds using FireFOAM (red).  $|\mathbf{u}_{fan}|=1.0$  m/s.

### Summary

The heat spread in an inclined tunnel was simulated using FireFOAM solver in OpenFOAM software package. The capability of this program was evaluated in terms of parallelization. It was found that FireFOAM code yielded excellent result consistency in parallelization regardless of the domain decomposition positions. The relative clock time is reduced to 50% if 2 cores are used for the current case.

Sensitivity study was performed for FireFOAM code in terms of important modelling parameters (grid size, combustion model constant and turbulent Prandtl number). It was found that grid size, combustion model constant, and turbulent Prandtl number had noticeable effect on the calculated temperature, whereas minor effect on the calculated velocities.

Comparison of calculated velocities and temperatures using FireFOAM and experimental results were performed. It showed that FireFOAM yielded reasonable results.

## 5.2 Large scale

### 5.2.1 Room fire

#### *Test set-up*

Two series of room fires were tested in three different scales were carried out by Li and Hertzberg [38] to investigate the scaling of enclosure fires, including internal wall temperatures and heat fluxes, based on an advanced scaling method proposed. The full scale test 1 is simulated using FireFOAM in this section to make a comparison with the test results.

The geometry of the room in full scale is 3.6 m (L) × 2.4 m (W) × 2.4 m (H) and the door is 2 m high and 0.8 m wide, see Figure 19. In other words, the full scale room has the same geometry as in room corner test. In test 1, the rectangular propane burner with side length of 30 cm was placed at the center and its surface was 30 cm above the floor.

The interior walls and floor were covered with 6 cm thick mineral wool (stone wool). The thermal conductivity is 0.038 W/m·K, density 170 kg/m<sup>3</sup> and heat capacity 750 J/kg·K .



*Figure 19. Photo of the room fire test 4. The heat release rate was 1.2 MW.*

Various measurements were conducted during each test. Figure 20 shows the layout and identification of instruments in the full scale room.

One thermocouple tree was placed at the center of the room, i.e. T1 to T6. Another thermocouple tree was positioned at the centerline of the door, i.e. T7 to T11. Four thermocouples, i.e. T12 to T15 were placed 0.2 m below the ceiling, see Figure 20. All the thermocouples have a diameter of 0.25 mm.

Five plate thermometers[39, 40], i.e. PT1 to PT5, were either placed on the walls or on the floor of the room center.

Hot gas flow velocity through the door, i.e. BP1, was measured using a bi-directional tube [41] placed beside the centreline of the door and 0.2 m below the upper edge of the door in full scale. The pressure difference was measured with a pressure transducer with a measuring range of +/- 30 Pa.

Gas concentrations through the door, including CO<sub>2</sub>, CO and O<sub>2</sub>, i.e. G1 to G3, were sampled by one probe consisting of open copper tube beside the bi-directional probe, i.e. 0.2 m below the upper edge of the door.

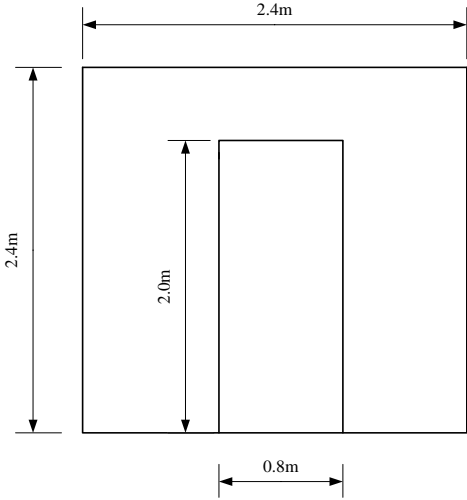


Figure 19 Front view of the room.

The thermocouple series inside the walls were placed at 5 positions in the room, i.e. TS1 to TS5. At each position, a thermocouple series consisting of 5 thermocouples was placed in different depths below the interior wall surface, see Figure 5. The five depths from the interior wall surfaces are 10%, 20%, 40%, 60% and 80% of the thickness (6 cm).

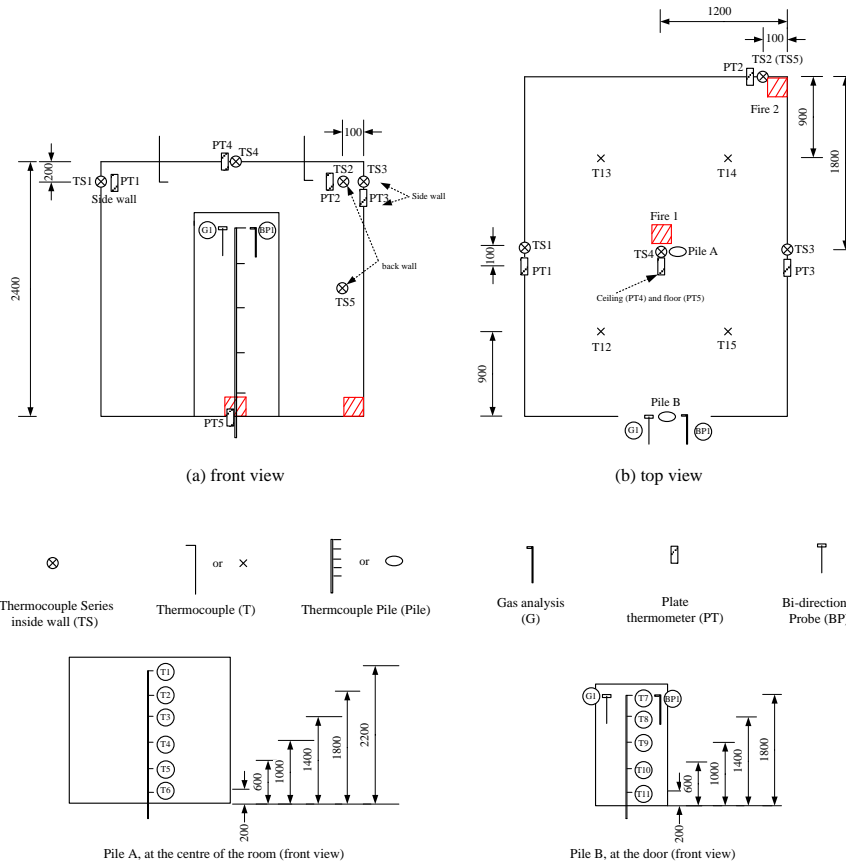


Figure 20 Layout of instrumentation in the full scale tests (Dimensions in: mm).

A rectangular burner with a side length of 0.3 m is located at the centre of the floor in the room. Propane is used as the fuel.

The heat release rate is a two step-wise fire curve. At the early 10 min the heat release rate is 100 kW and then 20 kW for another 10 min.

### Simulation settings

The room model is shown in Figure 21. The computation domain consists of the room and a region outside of the door with dimensions of 1.8 m (L)  $\times$  2.4 m (W)  $\times$  3.6 m (H).

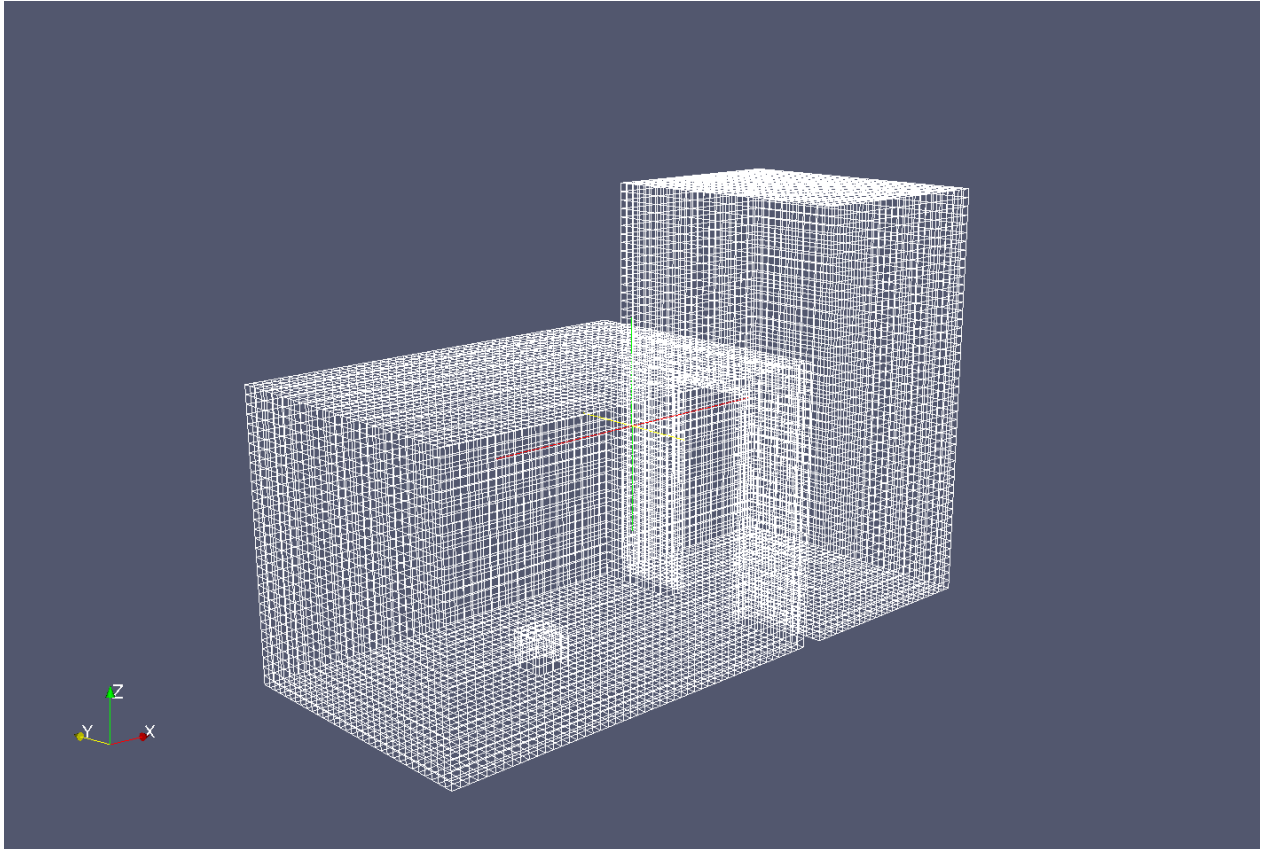


*Figure 21 The room model for fireFoam simulations. The grid size in this model is 75 mm.*

All the walls should be applied as thermally thick boundary conditions and therefore the 1D baffle model cannot be used. Instead, the pyrolysis model in the fireFoam is used for simulating the heat loss through the wall. The pyrolysis process is deactivated and solutions of the relevant parameters are not processed.

The radiation transfer is simulated using the finite volume discrete ordinate method (fvDOM). By default, the radiation source is simulated using the constant radiation fraction model (constRadFractionEmission) with a radiation fraction of 30 % and 60 solid angles were simulated. In one simulation, the grey mean absorption radiation model, accounting for CO<sub>2</sub>, H<sub>2</sub>O, and the fuel was also conducted for comparison.

The simulations were carried out on a work station with 8 cores (Intel Xeon, X5672, 3.2 GHz) and 16GB RAM.

### *Parametrical study*

#### *Stability and accuracy of parallel simulations*

A comparison of single processor simulations and multiprocessors (parallel) simulations are compared here. The heat release rate (HRR) and gas temperature at the ceiling are compared.

A comparison of simulations using single CPU and multiprocessors was carried out to investigate the capability of parallel simulations in FireFoam. The parallel simulations were carried out using 2, 4 and

6 cores respectively. To reduce the computation time, the grid size was chosen to be 15 cm in this comparison.

The results of HRR curves with single processor and parallel simulations are shown in Figure 22. Clearly, the heat release rates follow the designed HRR curve appropriately in all the cases. Note that the input design HRR curve is executed by means of fuel mass flow rate and the outputs shown in the figure are realistic combustion heat released into the domain.

It can also be seen from Figure 22 that the HRR curve at the second stage in the case with 4 CPUs scatters slightly more significant than the others. This indicates that parallel simulations with too many CPUs may result in too much pulsation and instability problem although it did not in this study.

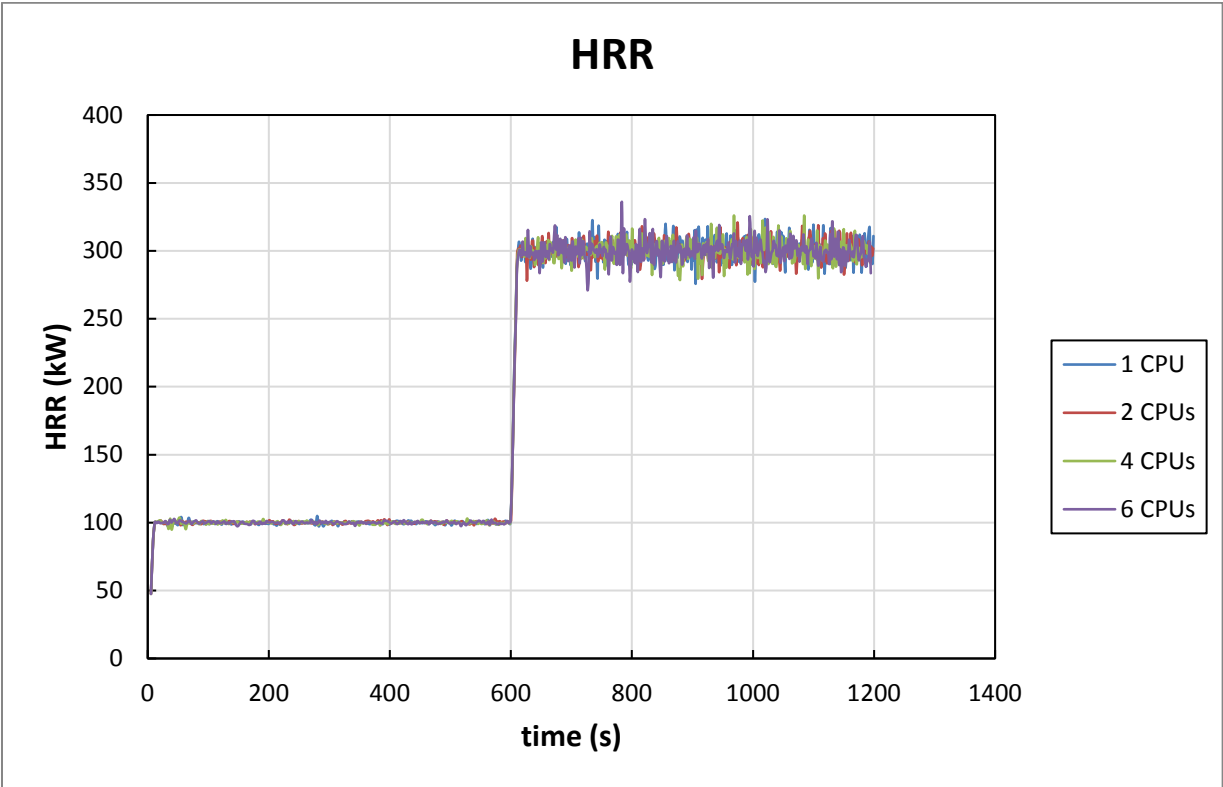


Figure 22 Effect of parallel simulations on the HRR.

The results of ceiling gas temperatures with single processor and parallel simulations are shown in Figure 23.

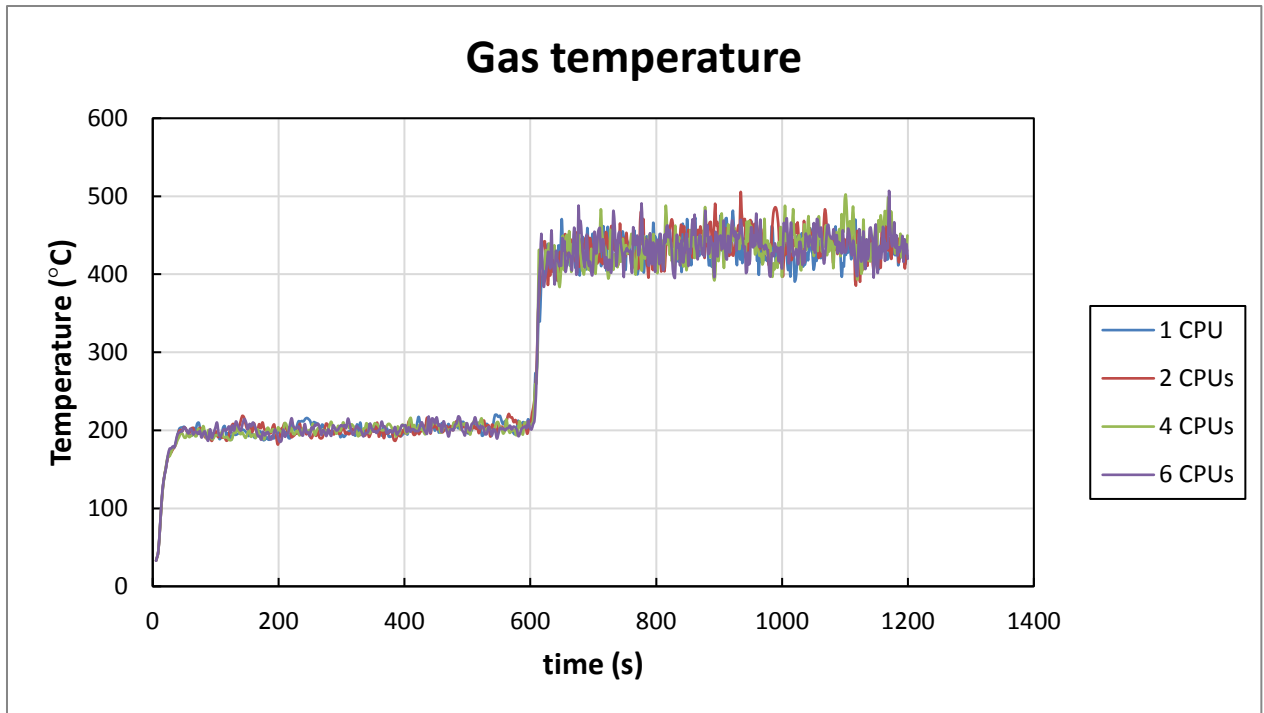


Figure 23 Effect of parallel simulations on the ceiling gas temperatures at T12.

The total computation time cost with the number of CPUs used is shown in Figure 24. The execution time reduces with the number of CPUs used but this time reduction decreases with the increasing number of CPUs. Further, the real time (Clock time) is slightly greater than the execution time for the number of CPUs less than 4 but it is much larger for 6 CPUs. This could be due to the fact that much more time is spent on communication between different CPUs. It should be kept in mind that this phenomenon could be case-sensitive.

The results indicate that use of double CPUs does not mean half computation time. Further, for a specific case, after exceeding a certain number the computation time for the parallel simulations can be much longer than that with less CPUs.

Despite this, the use of parallel simulations in some cases could be the only option when the number of grid size is huge where vast memories are required, as fireFoam divides the computation domain to sub-domains and allocate them to different CPUs and memories in one computer or other computers.

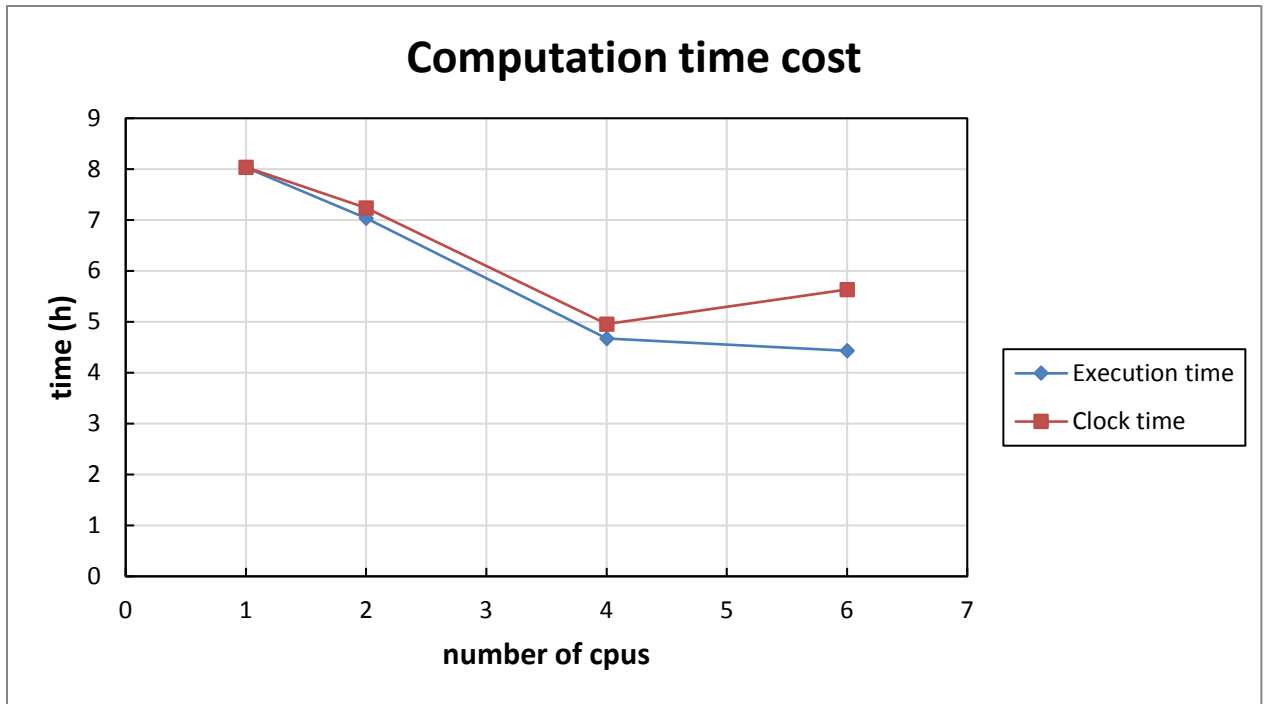


Figure 24 Hours spent vs. number of CPUs.

#### Grid sensitivity

The grid sizes analyzed are approximately 0.15 m, 0.1 m, 0.075 m and 0.05 m. The HRR curves are shown in Figure 25. All the results strictly follow the designed HRR curve although they show some scattering effect especially for fine grids.

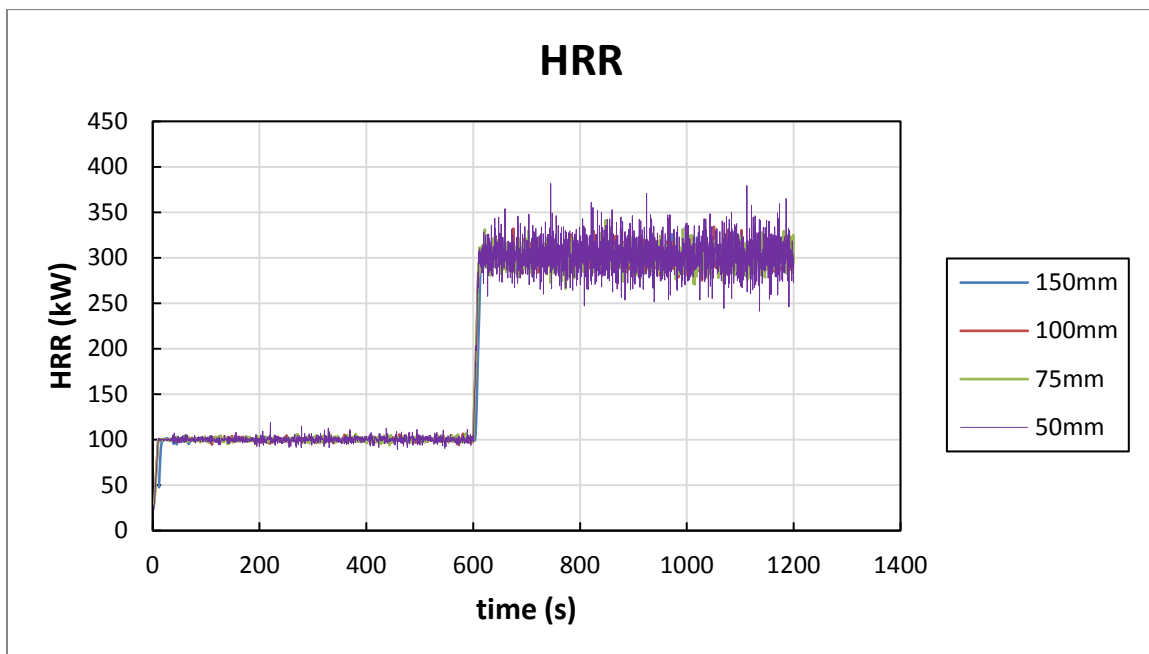


Figure 25 Effect of grid size on the HRR.

A comparison of the ceiling temperature T12 is shown in Figure 26.

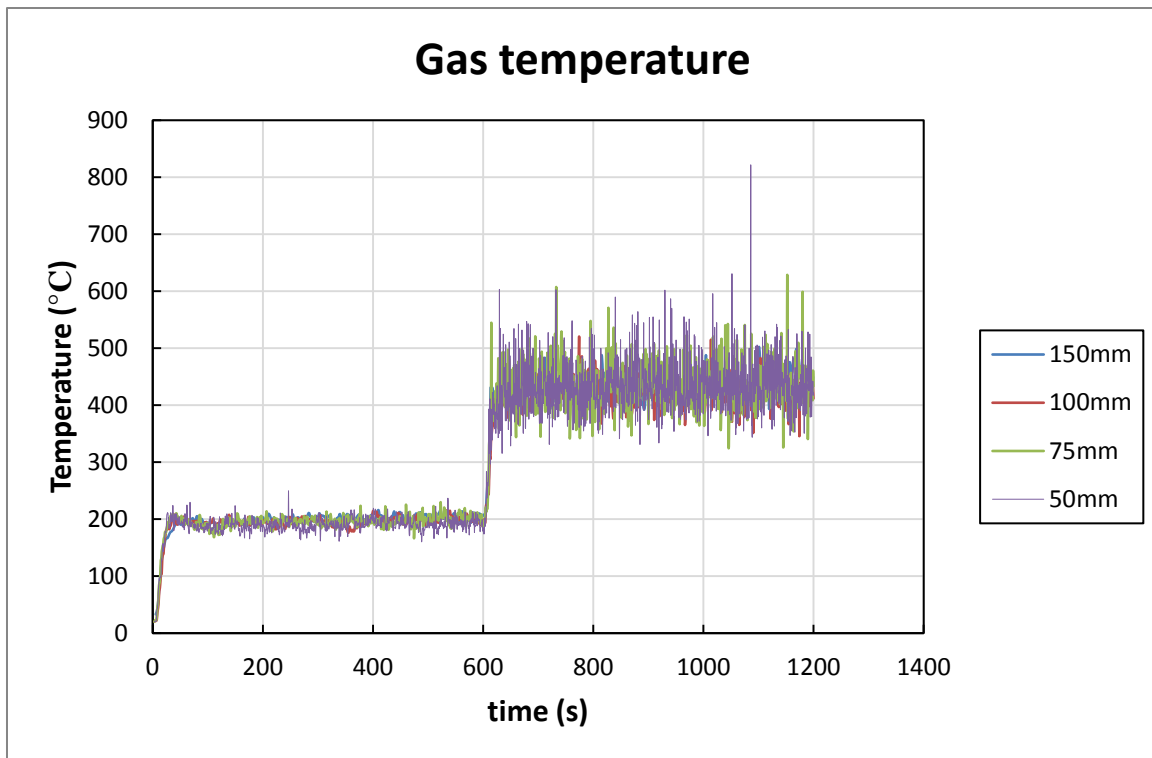


Figure 26 Effect of grid size on the ceiling gas temperature at T12.

A comparison of the gas velocity at the door is shown in Figure 27. The gas velocities for 100 mm, 75 mm and 50 mm correlate very well, while the gas velocities for 150 mm is much lower than the others.

This indicates the grid size should be at least 100 mm in this case.

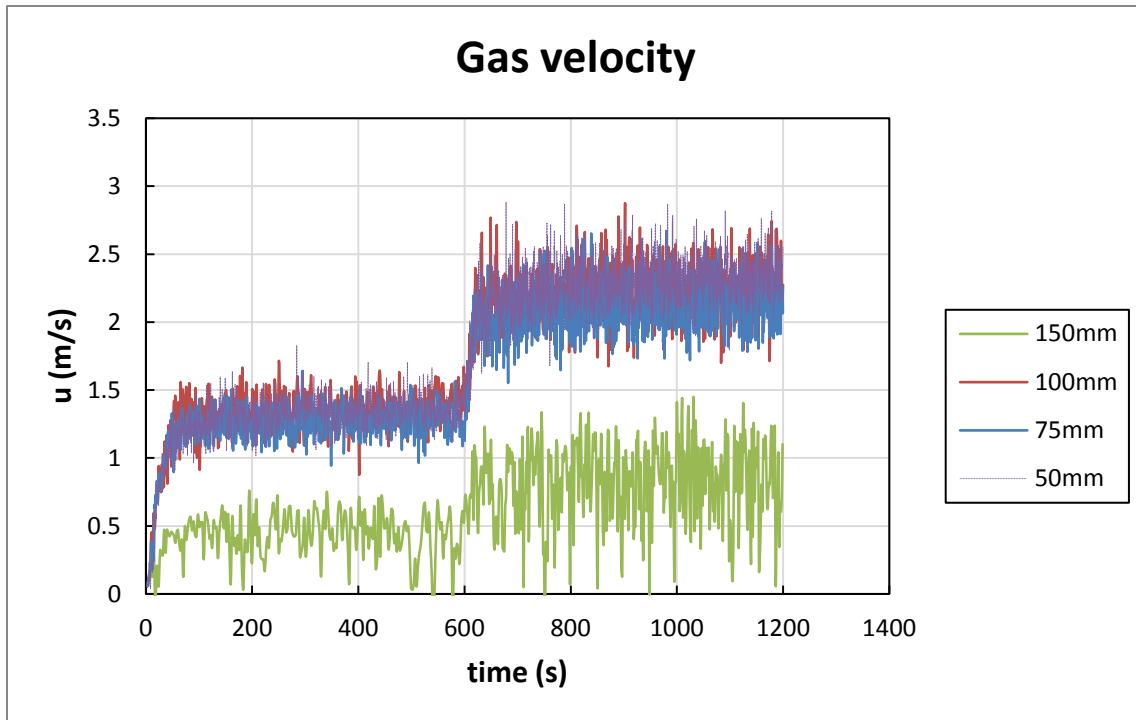


Figure 27 Effect of grid size on the gas velocities.

A general term to quantify the requirement for the grid size used in LES simulations is the non-dimensional fire diameter:

$$D^* = \left( \frac{Q}{\rho_o c_p T_o g^{1/2}} \right)^{2/5}$$

The requirement of at least 100 mm in this case could indicate a minimum grid size of  $0.15 D^*$ . This, however, could be case-sensitive.

The time spent with the number of grids by the 8-core computer used is shown in Figure 28. Clearly, the computation time cost approximately increases linearly with the number of grids in the domain. This indicates the matrix solver is relatively efficient. Despite this, the computation time is of a rather huge value.

This indicates the grid size should be at least 100 mm in this case.

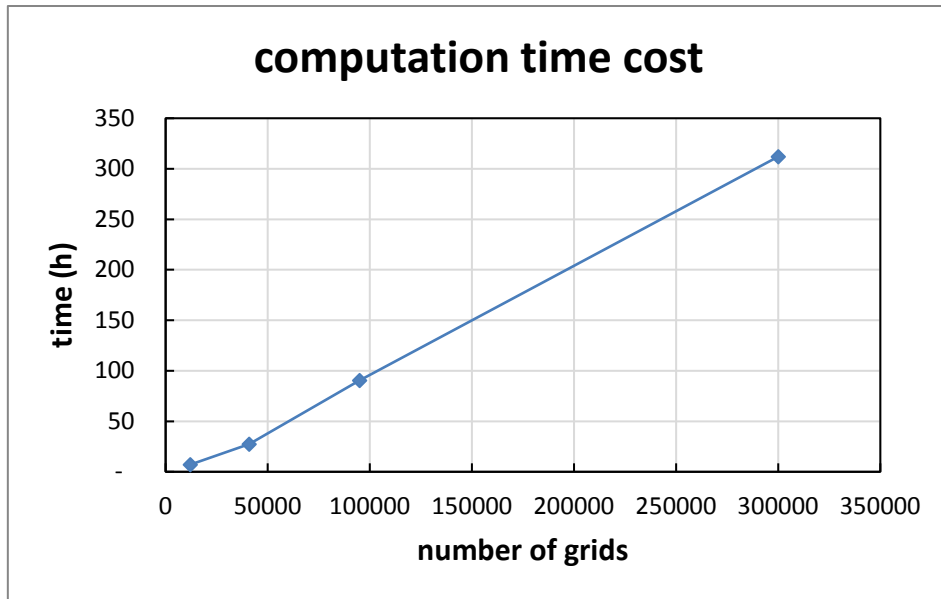


Figure 28 Hours spent vs. number of grid size.

#### Effect of radiation models

There are three radiation models available in fireFoam:

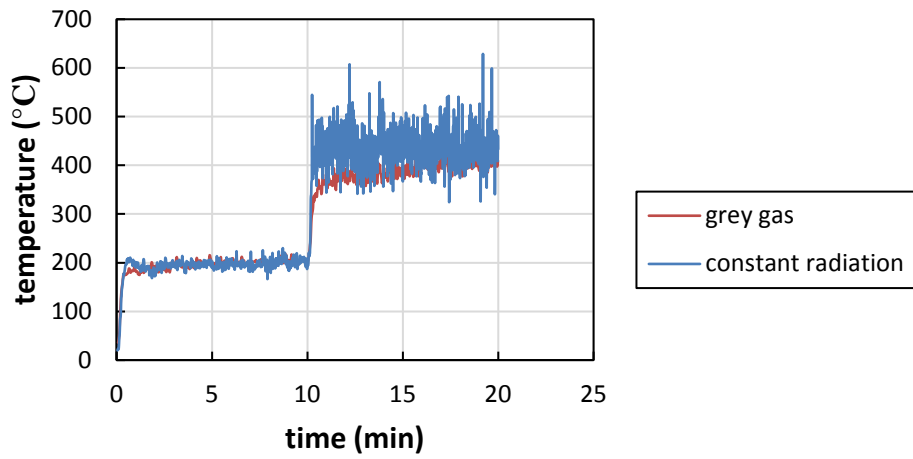
- (1) constant radiation fraction
- (2) constant extinction grey gas model
- (3) grey gas model

The constant radiation fraction model indicates the emissive radiation source is fixed to a certain fraction of the heat release rate. The constant extinction grey gas model means use of a constant extinction coefficient. The grey gas model accounts for the volume fraction of different species and thus could be considered as being most realistic. However, it appears that only fuel, CO<sub>2</sub>, and H<sub>2</sub>O are considered as radiation mediums. Also, it seems that the most important medium – the soot is not considered in the model by default although there is some documentation about the soot model developed based on OpenFOAM [5].

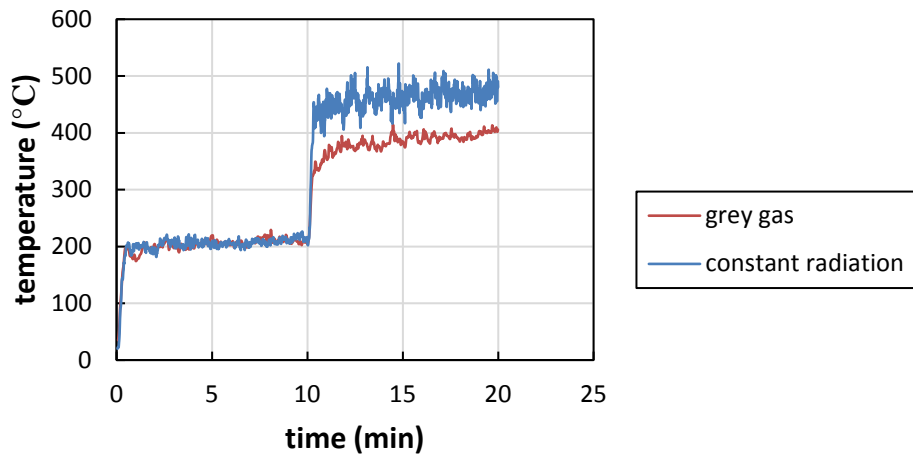
Here a simple comparison of the constant radiation fraction model and the grey gas model is made.

The ceiling temperatures are compared in Figure 29. Clearly, the grey gas model produces lower ceiling gas temperatures and the difference between the two models is mostly in a range of 25 to 75 °C. Further, the gas temperatures using the grey gas model are much more stable than the constant radiation fraction model, especially at the second stage. This could be due to that the constant radiation model is intimately related to the heat release rate that appears to fluctuate significantly, see Figure 22. In contrast, for the grey gas model, the radiation is directly related to the properties of the gas volume, rather than the heat release rate.

### Ceiling gas temperature T12



### Ceiling gas temperature T13



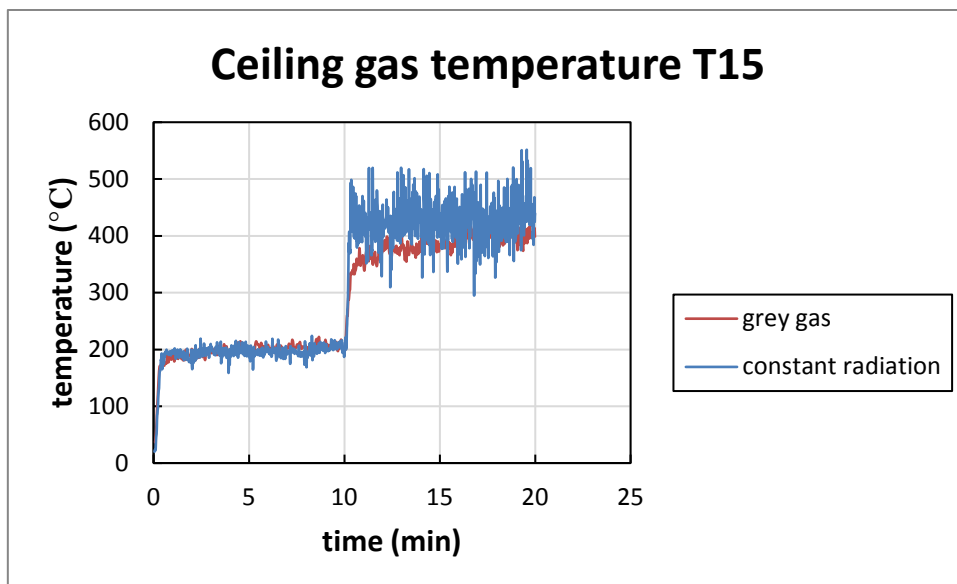
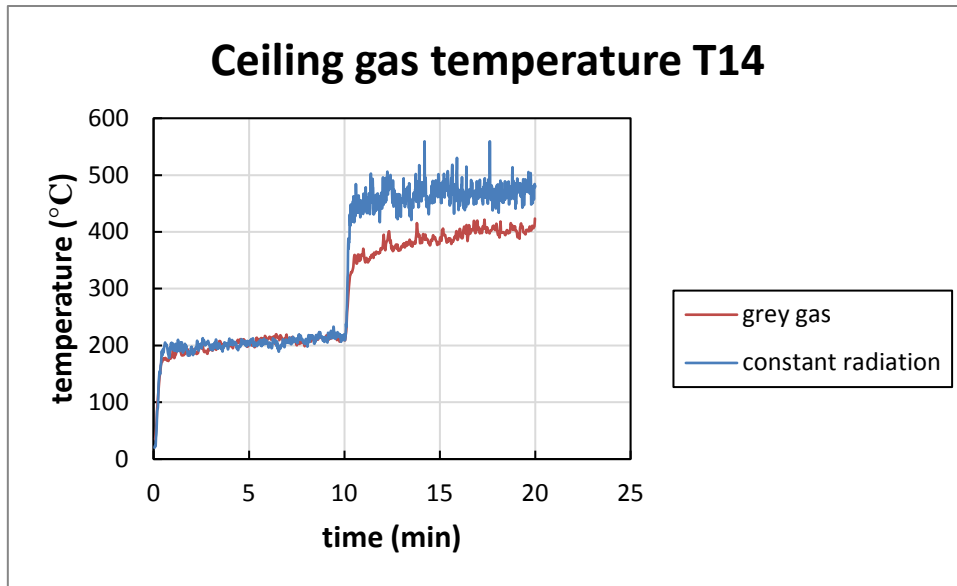


Figure 29 Effect of radiation models on the ceiling gas temperatures.

The gas temperatures at the door are compared in Figure 30. Clearly, the grey gas model produces lower ceiling gas temperatures at 1.8 m height, which is consistent to the results for the ceiling gas temperatures. However, the gas temperatures at 1.4 m height using the grey gas model are much higher than those using the constant radiation model. This could be due to the fact that smoke layer height is lower for the case with grey gas model.

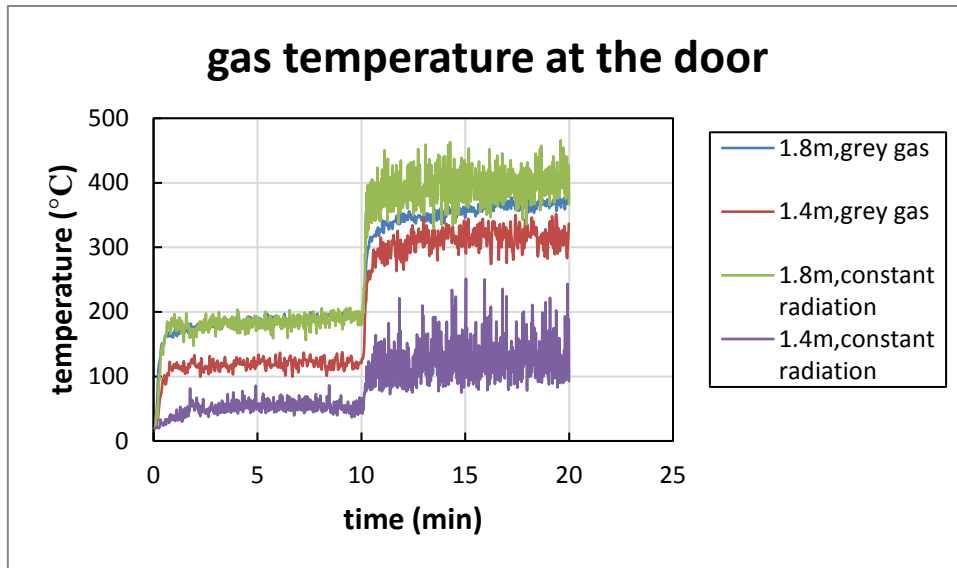


Figure 30 Effect of radiation models on the gas temperatures at the door.

Here a comparison of incident heat fluxes between the constant radiation fraction model and the grey gas model is presented in Figure 31, Figure 32, Figure 33, Figure 34 and Figure 35. For PT1 to PT3 the incident heat fluxes predicted by the two models correlate very well. However, at PT4 (ceiling right above the fire), the grey gas model corresponds to much higher incident heat fluxes. On contrary, at PT5, the grey gas model corresponds to much lower incident heat fluxes. Also, note that all the incident heat fluxes predicted using the constant radiation model are at the same level. This indicates that the incident heat fluxes using the constant radiation model vary insignificantly with the locations, while those using the grey gas model vary significantly with the locations. Comparison of the fireFoam results to the test data will be carried out in next section. There will it be found that the test data lie between those predicted by the constant radiation model and the grey gas model.

As in most of the references related to FireFOAM, the constant radiation model was applied and it is also the default radiation model in FireFOAM. Therefore in the following, the constant radiation model will still be applied.

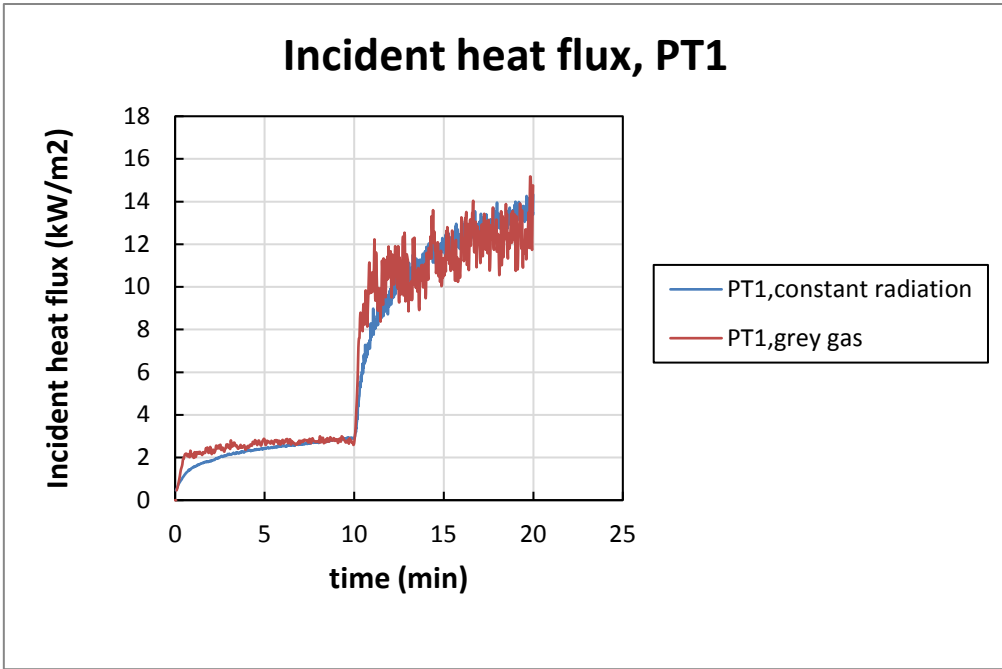


Figure 31 Effect of radiation models on incident heat fluxes at PT1.

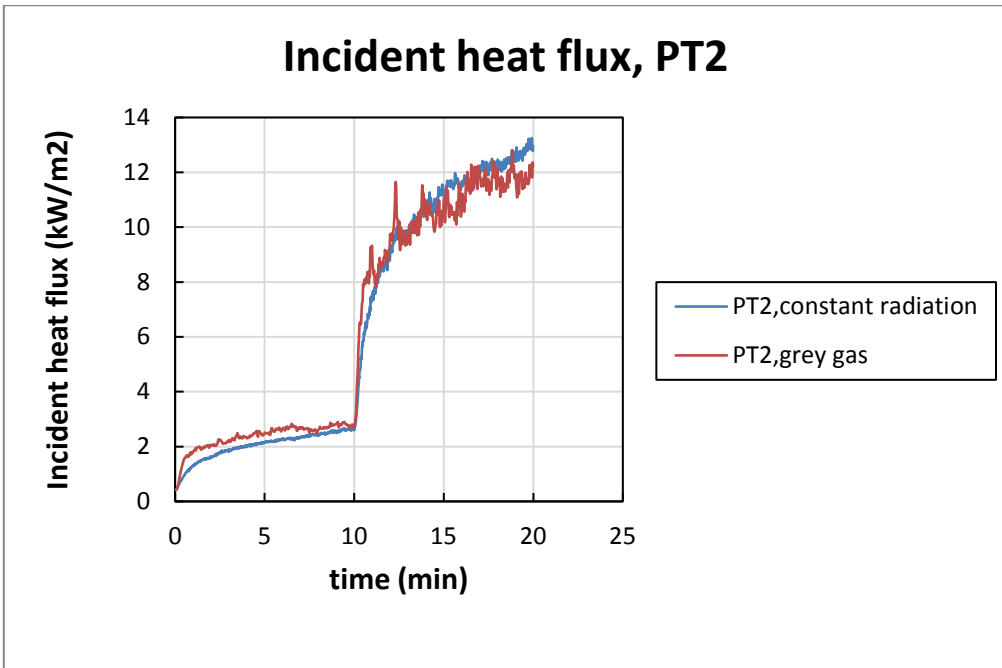


Figure 32 Effect of radiation models on incident heat fluxes at PT2.

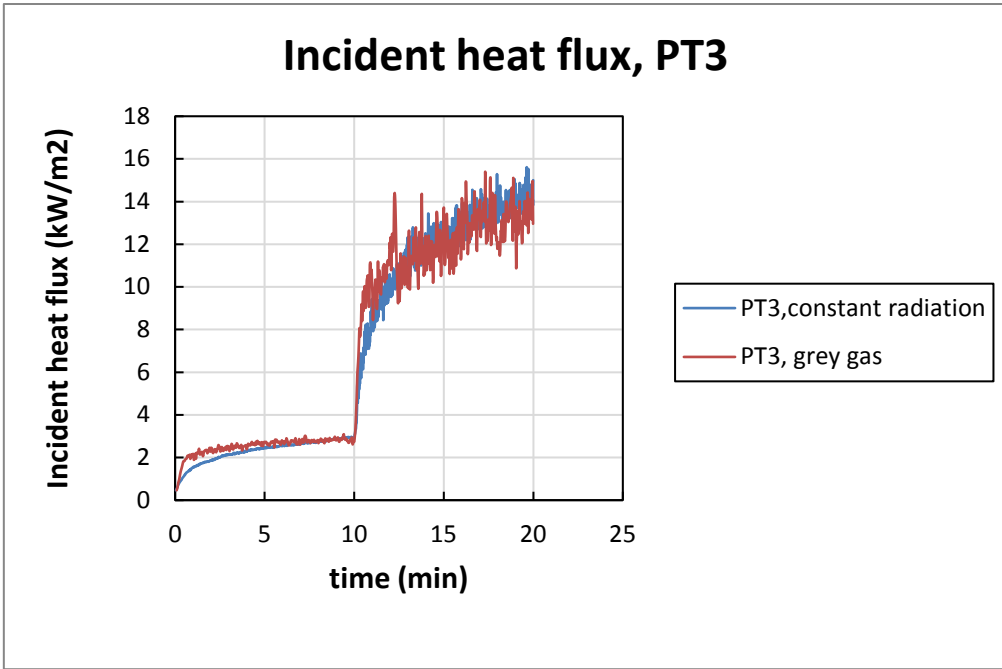


Figure 33 Effect of radiation models on incident heat fluxes at PT3.

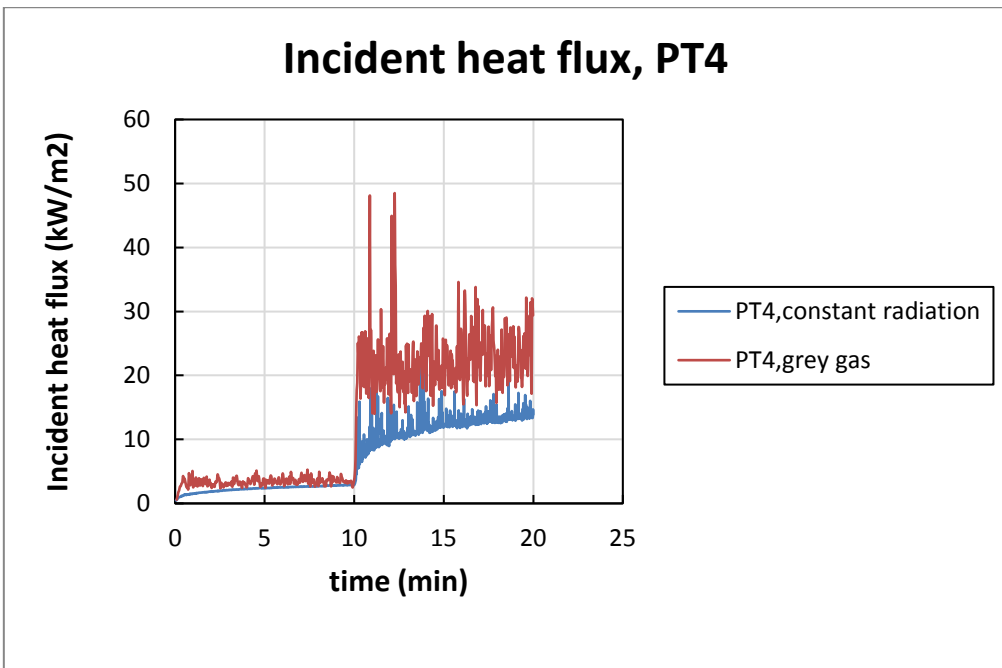


Figure 34 Effect of radiation models on incident heat fluxes at PT4.

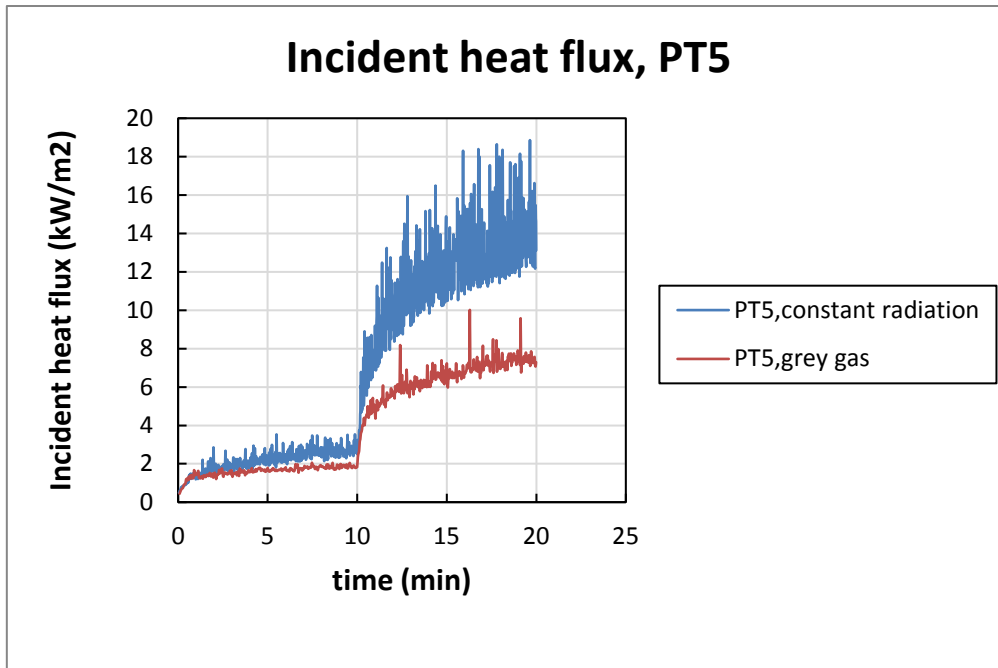


Figure 35 Effect of radiation models on incident heat fluxes at PT5.

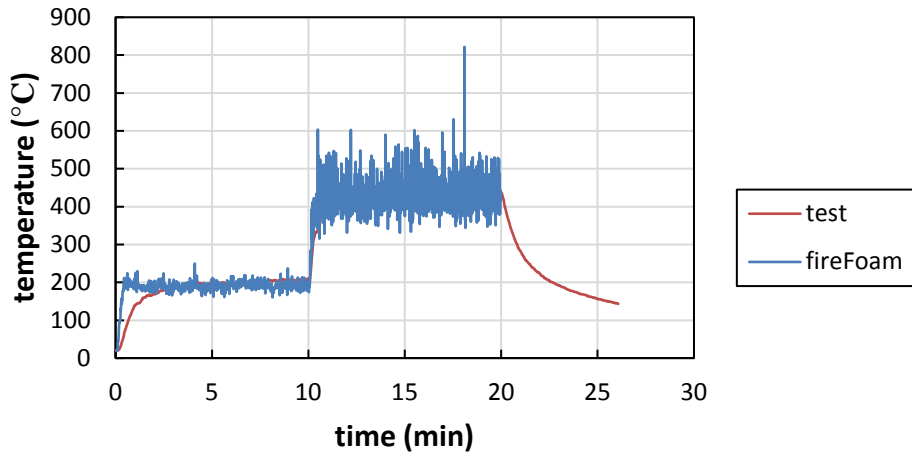
### Comparison of fireFoam and test data

#### Gas temperatures

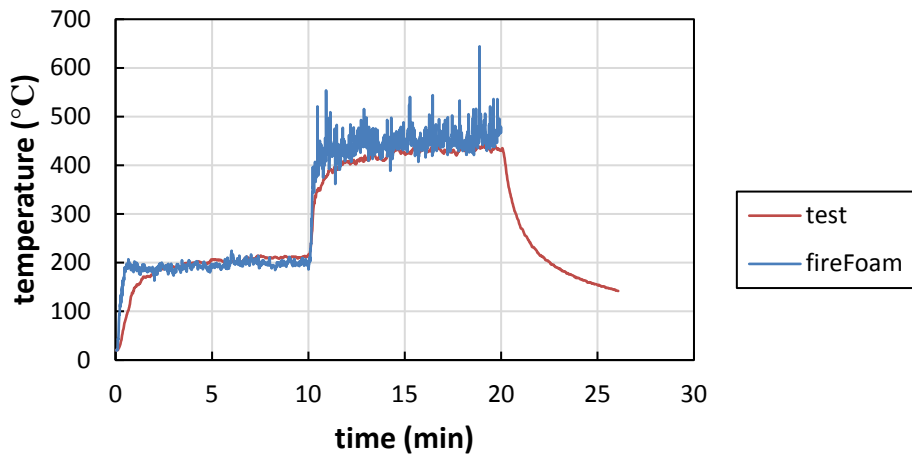
The gas temperatures measured in all the tests are given in Figure 36. T1 to T6 correspond to the thermocouple tree located at the centre of the room, and T7 to T11 correspond to the thermocouple tree located along the centreline of the door. T12 to T15 are the gas temperatures measured 20 cm beneath the ceiling.

Note that in each test, the fire heat release rate can be divided into several stages. In tests 1 to 3, the heat release rate was 100 kW for the early 10 min in full scale (0 min to 10 min), and 300 kW for another 10 min in full scale (10 min to 20 min). In tests 4 to 7, the heat release rate was 1.2 MW for 7 more min in full scale (20 min to 27 min). Note that the gas temperatures increase with time at each stage, therefore, the maximum values generally correspond to the values at the last moment of the corresponding stage.

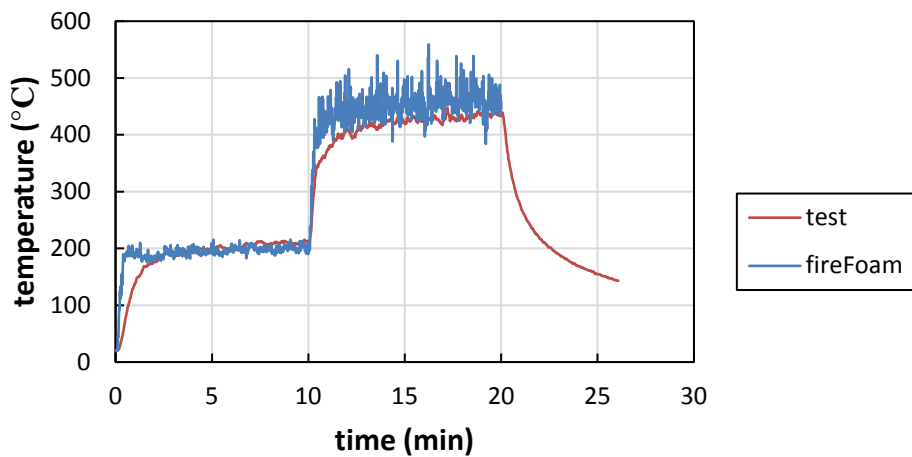
### Ceiling gas temperature T12



### Ceiling gas temperature T13



### Ceiling gas temperature T14



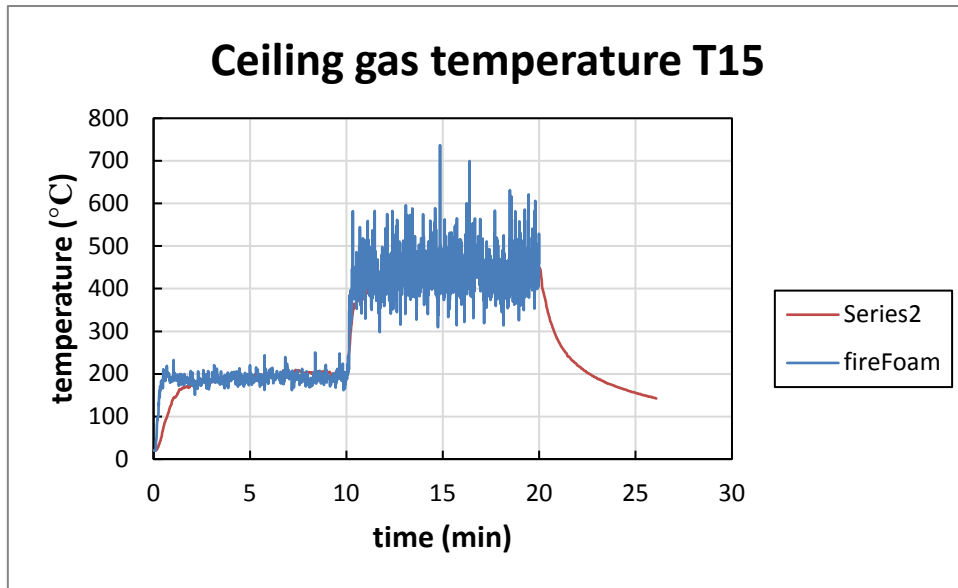
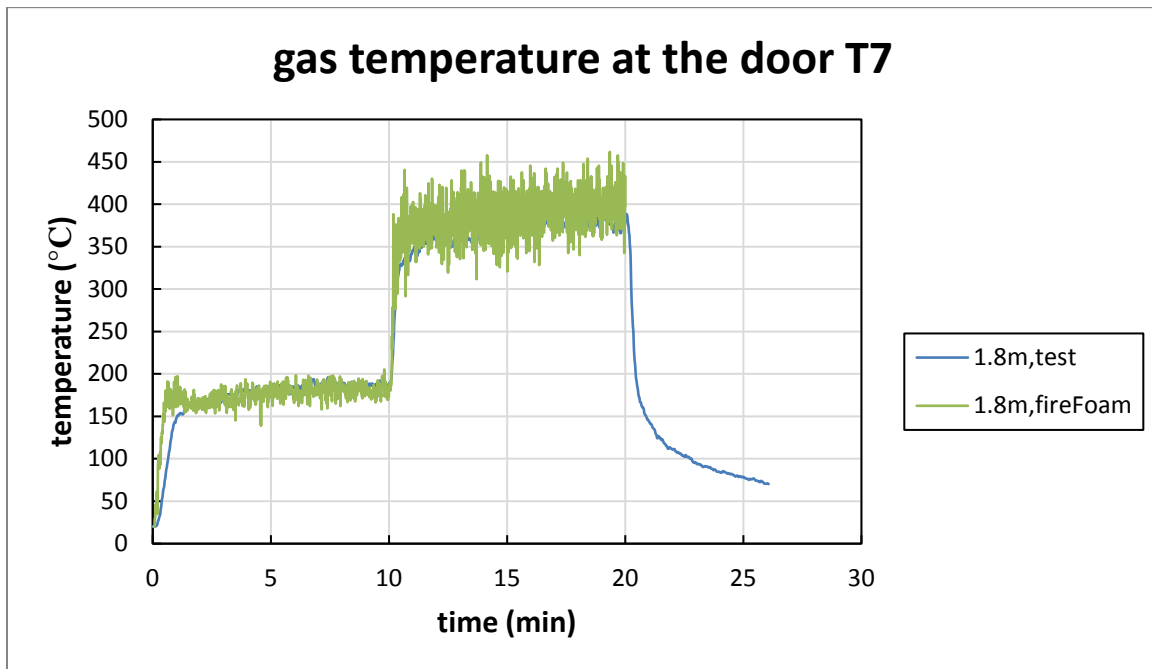


Figure 36 Ceiling gas temperatures.



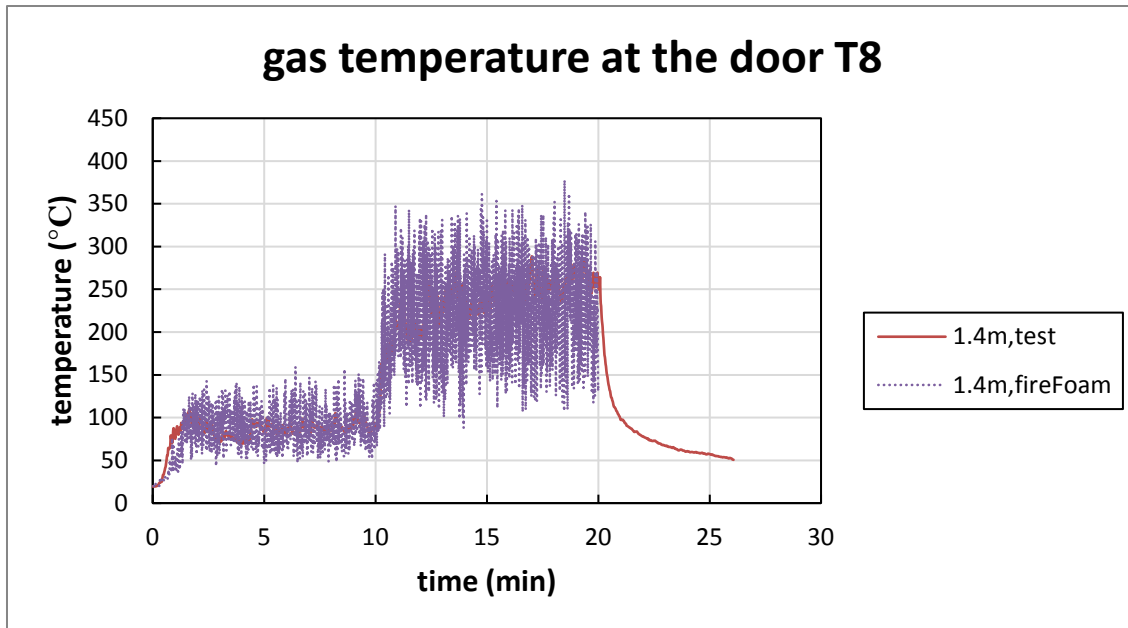


Figure 37 Temperature distributions at the door.

The simulated flame temperatures at the room center show significant variations with time. The temperatures are mostly over 1000 °C for T2 to T6 at the second stage, and therefore are overestimated by FireFOAM.

#### Gas flow at the door

Gas flow velocity measured by bi-directional pressure tubes are presented in Figure 38.

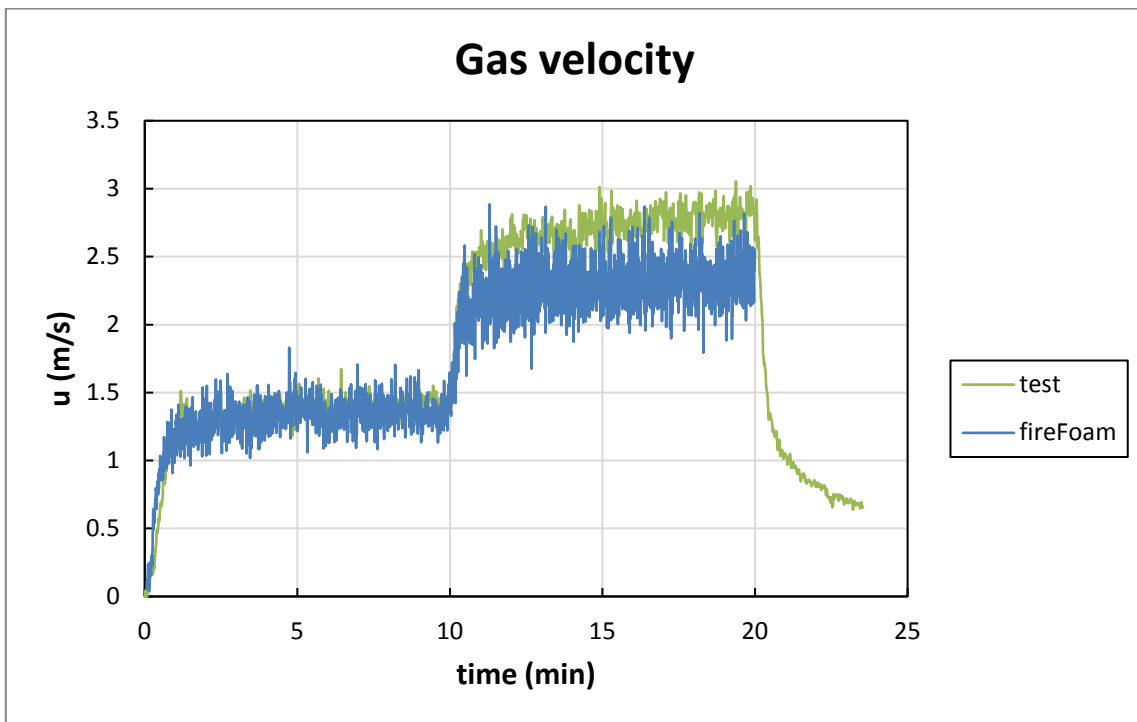
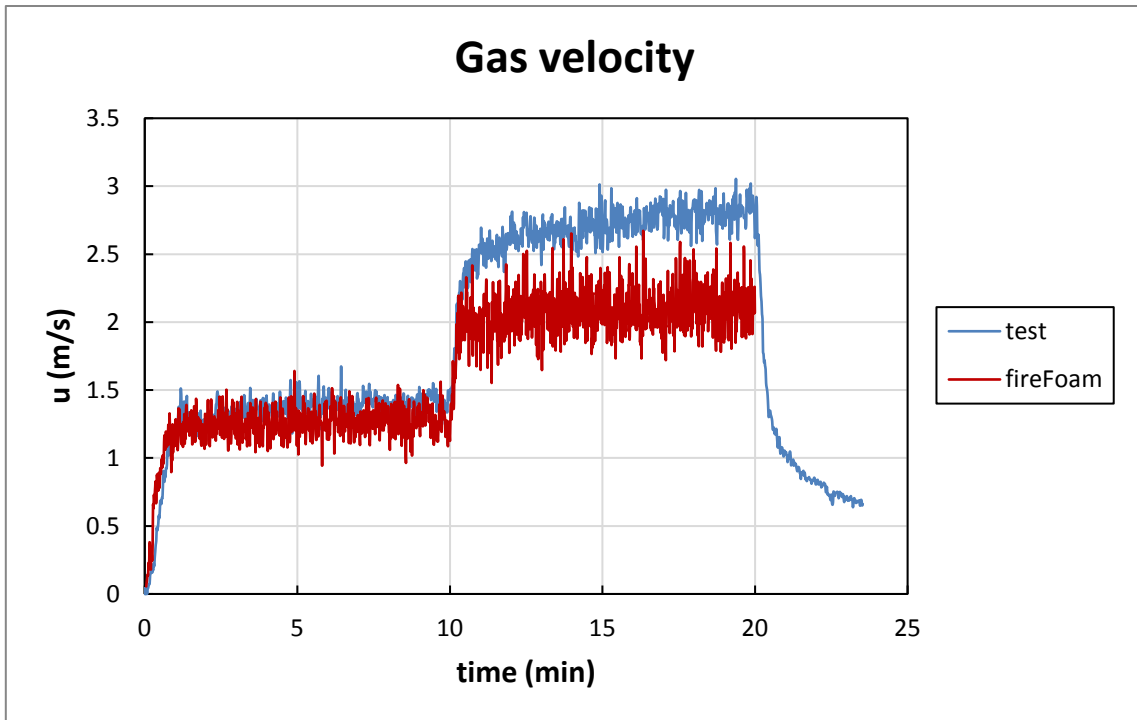


Figure 38 Full-scale gas velocity through the doors for center fires (data scaled up).

Gas concentration at the door

Gas concentrations, including  $O_2$  and  $CO_2$  are compared in Figure 39 and Figure 40.

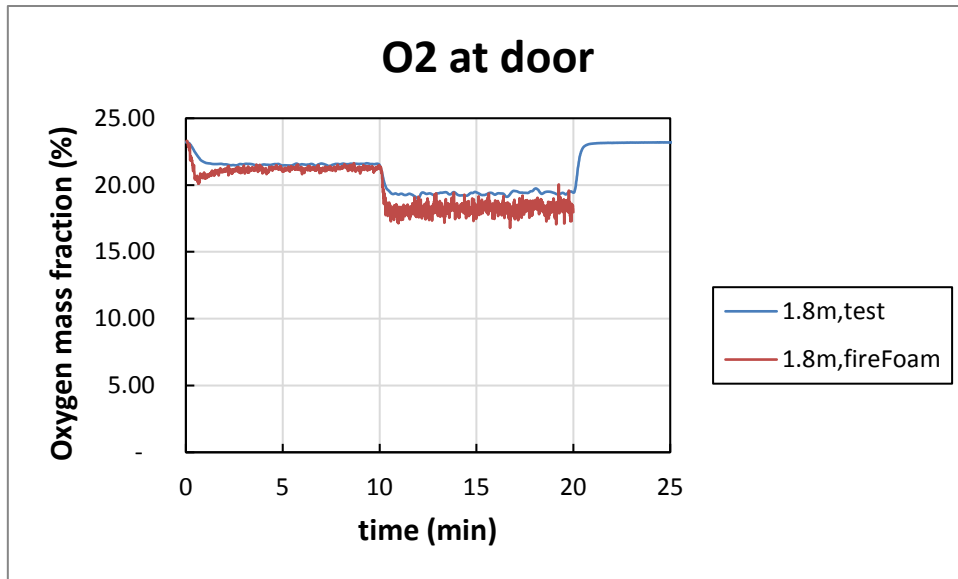


Figure 39  $O_2$  concentration at the doors for center fires.

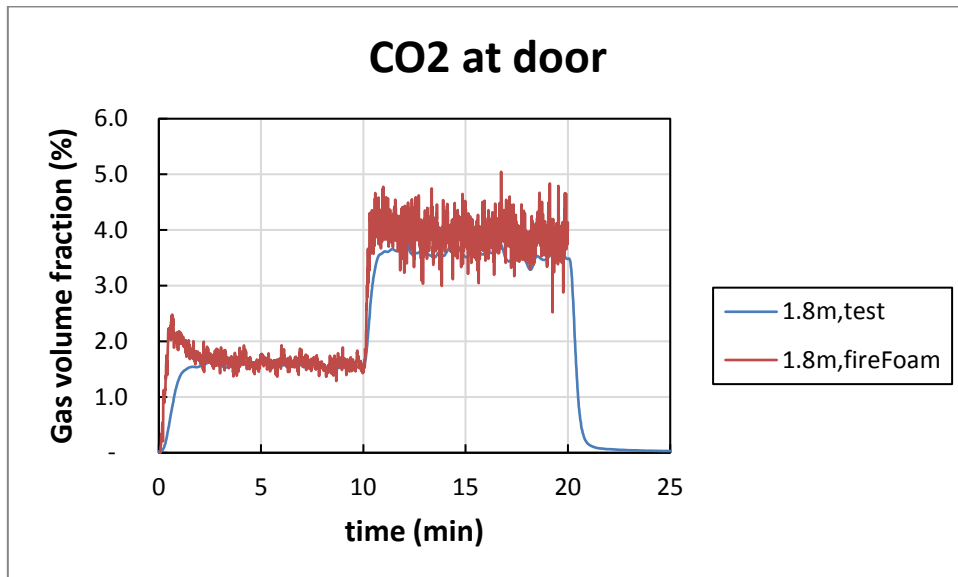


Figure 40.  $CO_2$  concentration at door for center fires.

#### Incident heat flux

Incident heat fluxes measured by the plate thermometers are presented in Figure 41 to Figure 44. The maximum values generally correspond to the value at the last moment of a stage.

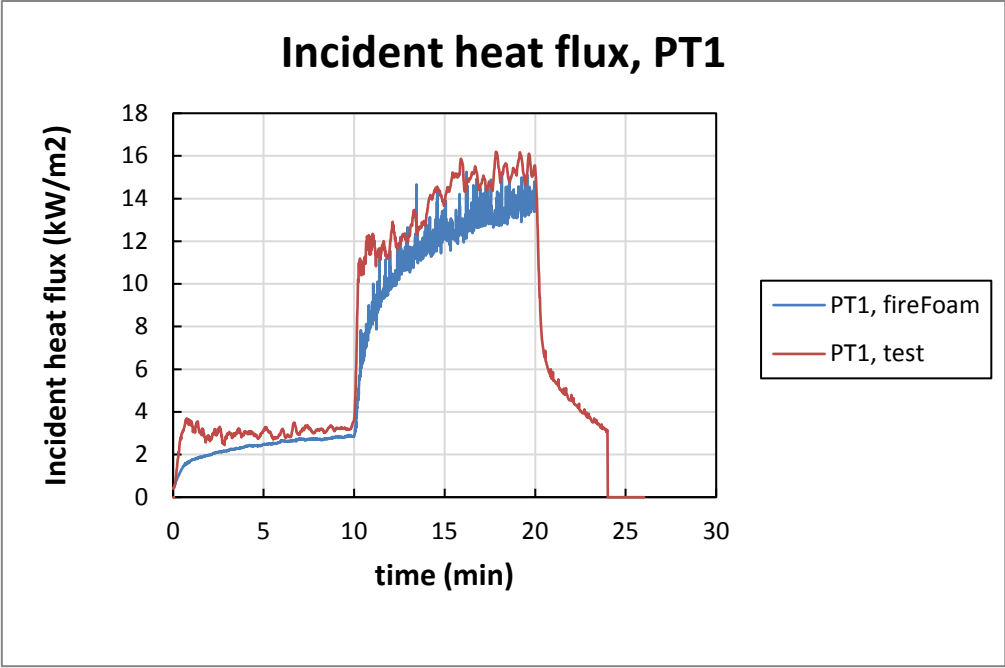


Figure 41 Comparison of measured and predicted incident heat fluxes at PT1.

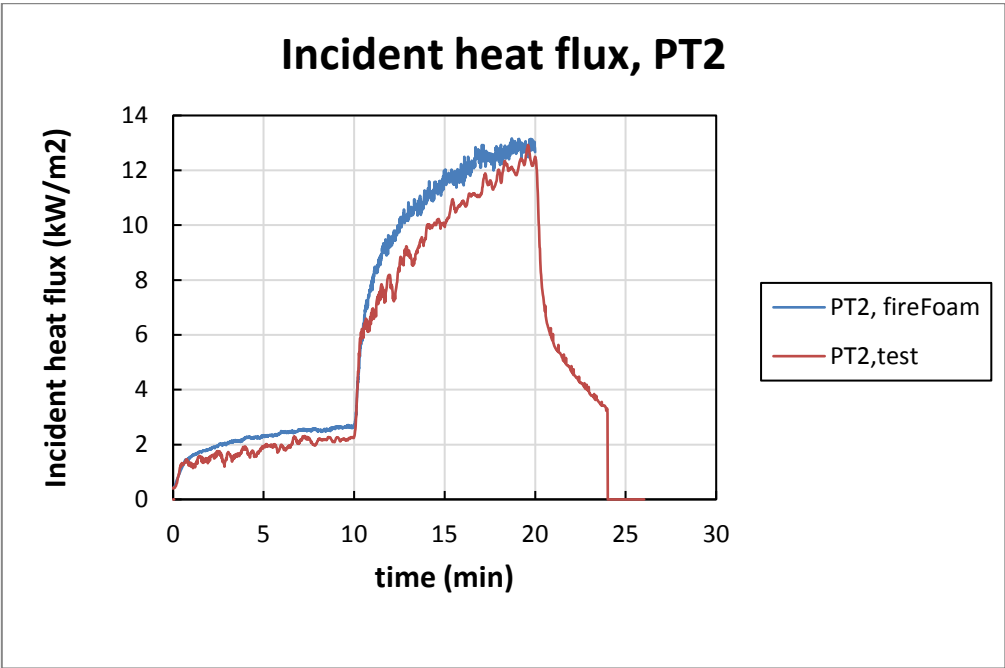


Figure 42 Comparison of measured and predicted incident heat fluxes at PT2.

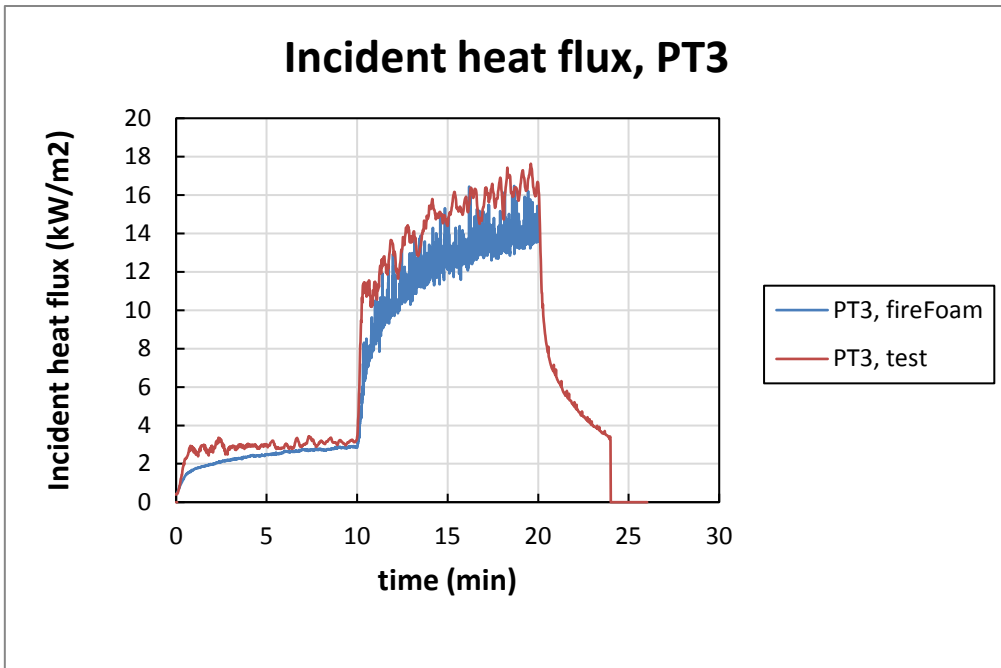


Figure 43 Comparison of measured and predicted incident heat fluxes at PT3.

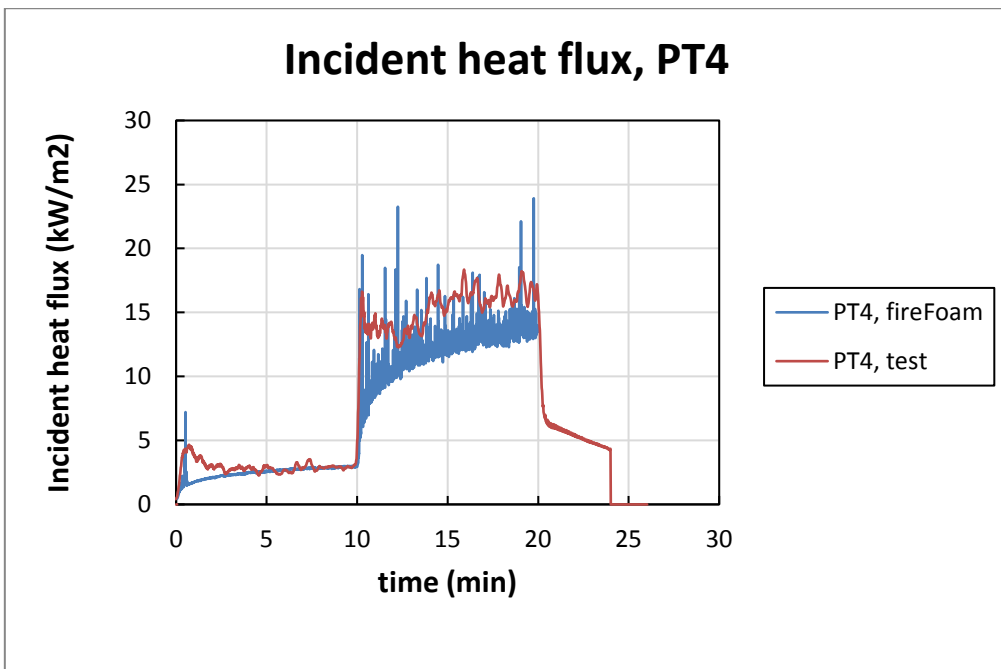


Figure 44 Comparison of measured and predicted incident heat fluxes at PT4.

**Short summary**

The grid size in this case should be at least 100 mm. This parameter depended on the actual case and thus cannot be unified simply to a single value.

The fireFoam parallel simulations are rather efficient and robust. However, parallel simulations could result in some numerical errors although the simulations appear to be robust. Further, for a specific case, the computation time cost could increase with the number of processors after it reaches a certain

value. Therefore, parallel simulations should be conducted with special caution. The number of processors should be as few as possible to maintain the accuracy of the results.

FireFOAM predicts the ceiling gas temperatures well. The incident heat flux is simulated relatively well. It has also been found that FireFOAM slightly underestimates the gas velocity and O<sub>2</sub> concentration at the door, and slightly overestimates the CO<sub>2</sub> concentration at the door. This could be due to the fact that the boundary layer at the door is not well resolved as a result of inappropriate wall functions for coarse grids.

The fluid model and combustion model are appropriate.

The main drawbacks are the wall heat conduction models and the radiation model. There is no wall heat conduction model in fireFoam except the 1D thermal baffle model. By adjusting the pyrolysis model to a heat conduction model, fireFoam now can take heat loss into account, however, the model has not been optimized and the computational cost is huge. The radiation heat flux model lack of appropriate grey gas properties, and the relevant parameters such as soot yield need to be embedded.

Another problem is that FireFOAM (also OpenFoam) uses a lot of computer memory, and the computation speed is not as fast as other fire-specified software, such as FDS.

## 5.2.2 Fire hall

### *Introduction*

Smoke ventilation facilitates fire-fighting and evacuation. Furthermore it reduces smoke spread within the building and decreases the impact on load-bearing and separating elements by emitting heat, smoke and other combustion gases directly to the outside. Moreover, in a fire situation, properly functioning smoke ventilation maintain a smoke-free layer close to the floor. A thermally driven, also known as natural, smoke ventilation system consists of exhaust openings at the top of the building and an inflow of air into the bottom of the building. The natural ventilation is driven by the density difference between the hot gases and the surrounding air that occurs in a fire situation. The hot gases rises and an overpressure compared to the ambient occurs in the upper part of the building due to the column of hot gases above the neutral pressure level has a lower density than air outside the building. Smoke exhaust can be driven by fans and is usually referred to as mechanical or forced smoke ventilation. Unwanted effects such as plugholing can occur if the smoke ventilation system is improperly set-up or dimensioned. Plugholing is the effect of having fresh air from the floor sucked through the smoke gas layer which creates turbulence and smoke transport barriers with reduced efficiency of the ventilation system as a result.

One of the most important considerations when determining the properties of the smoke ventilation system is to take into account that the air and other gases are not ideal therefore are not frictionless, incompressible and isothermal. The flow volume is compressed during the passage through a vent which means that there is a resistance when flowing through the vent that is often described by an effective exhaust area or contraction factor. This phenomenon is called the *vena contracta* and means that the aerodynamic area is not the same as the geometric area. The phenomenon was first described by Evangelista Torricelli in 1643. It is usually described through the quotient of aerodynamic and geometric area called the contraction factor ( $C_v$ ). A low contraction factor means that only a small part of the geometric area can be considered as vent and vice versa.

As an example we note that the recommended values of the contraction factor used in hand calculations of smoke filling in Sweden is  $C_v = 0.7$  for horizontal and  $C_v = 0.6$  for vertical openings. For openings that cannot be opened straight outward, such as windows that opens at an angle e.g.  $45^\circ$ , the recommended factor is  $C_v = 0.5$ . All three of the previous examples are according to the guidance in reference [42]. According to the European standard, significantly lower values of the contraction factor is recommended  $C_v = 0.2-0.5$  for non-tested designs and depending on the wind direction. This suggests that Sweden is less conservative in this aspect compared to the rest of EU.

Both FDS and FireFOAM solve the Navier-Stokes equations adapted for thermally driven flows at low speeds and with a focus on smoke and heat transport (a set of partial differential equations for mass, momentum and energy). In a fire situation the combustion is uncontrolled and no pre-mixing of fuel and oxidizer is present thus most of the fires are considered to be turbulent diffusion flames where mixing limits the combustion rate. The combustion rate is controlled by a turbulent mixing time scale of fuel and oxidant, and the chemical reaction time scale is considered to be very small in comparison to the turbulent time scale. Therefore, in the vast majority of fire applications, the Eddy Dissipation Model (EDM) is used, in which the mean chemical source term for fuel is mainly controlled by turbulence time scale and deficient species (either fuel or air), and the chemical reaction rate is assumed infinitely fast. In this study we will compare the two codes FDS and FireFOAM.

In FDS there are certain limitations where explosions and rapid gas flows out through vents cannot be simulated as such situations are prone to have large Mach numbers. FDS is developed by NIST in cooperation with VTT Technical Research Center and others and is open source software free to download. The FDS software with default settings uses structured, uniform staggered grid in order to utilize the efficiency of the Fast Fourier transforms in the pressure solver. In the default setting radiation is calculated using 100 discrete angles in a finite volume approximation of the radiation transport equation with gray gas. The FDS model is not limited to these simple algorithms however any additional physics included incur increased computational costs.

FireFOAM is yet another available tool for fire simulations. FireFOAM is aimed at modelling problems relevant to thermo- and fluid-dynamics and multiphase flow similar to FDS. However, it should here be mentioned that there are two versions of FireFOAM code. One is released as a solver by Open CFD (an official release) included in the OpenFOAM package. The other is an extended version of the official release, and it is maintained by FM Global consisting of modified libraries, solvers and extra cases for fire research. In this report the FireFOAM version released by FM Global on 24 November 2014 is used.

The FireFOAM solver is built open the versatile OpenFOAM platform and calls the general turbulence library, meaning that it is able to run simulations using both Large Eddy Simulation (LES) and Reynolds-Averaged Navies-Stokes (RANS) turbulence models. Unlike FDS, in which the flow is treated as incompressible, FireFOAM is a compressible flow solver. The current pyrolysis model in FireFOAM as well as that in FDS is considered to be relatively crude and semi-empirical. In FireFOAM, the pyrolysis modelling is based on the assumption of one-dimensional treatment, which is perpendicular to the exposed solid surface, of thermal degradation across a solid based on conservation statement for heat and mass.

One important limitation in ventilation modelling with FDS and FireFOAM is the filtering process called Large Eddy Simulation (LES). The LES filters out the small eddies while describing the large eddies in the turbulence correctly and approximates by a simple model the energy transfer from the smaller eddies (smaller than the cell size) to the large eddies. By default, in FDS5 the Smagorinsky model is used while the Deardorff model in FDS6. Interestingly, in the Smagorinsky model there is a constant  $C_s = 0.2$  (default value) that applies to fully developed turbulence and might be adjusted in some cases to get a credible smoke spreading.

In the BIV guidance [43] it is indicated that FDS has had difficulty in describing the contraction effect correctly except possibly with relatively small cell size however it is often unrealistic to apply such a fine mesh to the large structures that are to be studied in their entirety. They note that it appears that the flow through the vents is strongly cell size dependent but that an infinitely thin roof gives conservative values. In addition, they note that the larger cells may provide an overestimate of the volume flow out and a non-conservative estimate is obtained. Here it is interesting to note that the cell size is rarely less than 10 cm for calculations of smoke filling in large buildings so this negative effect can be significant.

In an early CFD study of smoke ventilation [44], two cases of smoke spreading in a shopping mall with sloped ceilings and an industrial building with horizontal ceiling were studied. It was shown that wind effects could cause the flow rate be halved if the wind speed increases from zero to 20m/s [44]. They also mention that for some particular conditions the flow can go in through the ventilator depending on the wind direction and speed. In Reference [10], results of CFD simulations of ventilators are presented with the conclusion that for detached houses and houses of the same height

the wind effects are small or positive for the mass flow out but however if there are taller buildings nearby or higher building elements they have the opposite impact. Furthermore, they estimated the calculation domain size to be at least 4 times the object's height and 5 times the item's side to give good accuracy in the results.

In other words an easy and fast model to describe the contraction phenomenon correctly or at least conservatively in a CFD tool used for fire sciences is strongly called for. This is to prevent that improper ventilations systems are installed and the required safety levels are met. From the examples and the different results that have been seen previously in CFD tools we find that there is a need for a consistent practice of how a vent should be handled in a smoke filling calculation.

### **Mesh sensitivity and turbulence resolution in FDS**

A vital ingredient in successfully assess the quality of the CFD solution and to achieve a reliable simulation are quantitative numbers on turbulence resolution and grid independence studies. All simulations have been performed using 12 meshes in order to have results in a reasonable amount of time. It should be noted that to avoid any additional uncertainties regarding the pressure accuracy in multi mesh problems where the number of pressure iterations may have to be increased [45]. In McDermott [46] several different methodologies to assess numerical accuracy are presented that we will adopt in this report such as  $D^*/\delta x$  as the minimum of the between the fire height and the characteristic diameter of the fire, the measure of turbulent resolution (MTR). One additional property that may be investigated is the  $y^+$  namely the properties close to the wall and the wall function that could be of importance in the exhaust area but will be omitted.

The fire is a provided by a large propane diffusion burner with prescribed HRR as shown below. A widely used number to assess mesh resolutions is the quotient  $D^*/\delta x$  where  $D^*$  is computed as

$$D^* = \frac{\dot{Q}}{\sqrt{g} \rho_{\infty} T_{\infty} c_p}$$

Here,  $\dot{Q}$  is the total heat release rate of the fire,  $g$  is the gravity,  $\rho_{\infty}$  is the ambient density,  $T_{\infty}$  is the ambient temperature and  $c_p$  is the ambient specific heat. In this study two different HRRs have been used presented in Table 8, with the different  $D^*/\delta x$  for the different mesh resolutions used.

**Table 8. shows the  $D^*/\delta x$  for different mesh resolutions**

$\dot{Q} \backslash \delta x$	$D^*$	$D^*/\delta x$ ( $\delta x=50\text{cm}$ )	$D^*/\delta x$ ( $\delta x=20\text{cm}$ )	$D^*/\delta x$ ( $\delta x=10\text{cm}$ )
1750 kW	1.48	2.96	7.4	14.8
3500kW	2.96	5.92	14.8	29.6

We note that typically this value should be  $D^*/\delta x > 10$  however during the growth phase the required meshing typically much finer. In the case of the 3500kW fire both 20cm and 10cm should yield reasonable results whereas 10cm grid is expected to be needed for the smaller 1750kW fire. In the rest of the report only the lower HRR case will be studied.

In order to evaluate the turbulence resolution close to the vent some other indicator is needed and firstly we look at the turbulence resolution (MTR) with

$$MTR(x, t) = \frac{k_{SGS}}{k_{RES} + k_{SGS}}$$

Here  $k_{SGS}$  is the kinetic energy sub-grid scale and in the denominator is the total kinetic energy where this value should exceed 0.2. This is similar to what is known as the Pope criterion [47].

Using the tools mentioned above the mesh resolution may be assessed were it is noted that for 50cm grid resolution the turbulence is much less resolved and very likely the pressure difference driving the exhaust is not very well represented giving less accuracy in the mass flow rates as indicated by the  $D^*/\delta x$  values in Table 1. It is found that for the 50 cm case large areas under the ceiling describing the buoyant smoke movements are not well resolved. Although the areas with under resolved turbulence is significantly smaller for the 20 cm grid there are some patches just at the exhaust vent with under resolved kinetic energy indicating that the resolution is too low even though the  $D^*/\delta x > 10$  indicating a resolved case. To this end it is obvious that other measures of numerical accuracy rather than  $D^*/\delta x$  are needed to determine the quality of the analysis. It is noted that the turbulence resolution is rather good and reliable results can be expected for 10 cm grid. Onwards the focus will be on the low HRR case used as a comparison between FDS and FireFOAM.

### *Smoke ventilation modelling in FireFOAM*

A corresponding model is set up using the FireFOAM code with similar dimensions, fuel and openings. It should be noted that the buoyancy in FireFOAM code has been verified and validated in one earlier publication with good agreement [48]. Due to the versatility of the FireFOAM solver, using LES (Large Eddy Simulation), there are a number of coefficients and model constants to be set. These sub-models and model constants used in the simulations are listed in Table 9. However, the model is kept as close as possible to the FM Global release version (The same applies to the FDS model). This decision is made to avoid parameter fitting to one singular case. One interesting feature available in the FireFOAM code is using non-structured grids which could make a difference for the flow along the sloped ceiling.

**Table 9. Summary of sub-models used in smoke ventilations simulations in FireFoam and their constants**

<b>Sub-models</b>	<b>Name</b>	<b>Constants</b>
Turbulence	compressible LES Smagorinsky	$C_e = 1.048$ , $C_k = 0.02$ , $Pr_t = 1.0$
Combustion	Eddy Dissipation Model	$C_{EDM} = 4.0$ , $C_{diff} = 0$ , $C_{stiff} = 1.0$
Radiation	fvDOM, grey mean absorption emission	
thermo-physical	Ideal gas with JANAF coefficients	
Soot	Off	

One interesting difference here is that the Smagorinsky LES is used for FireFOAM however in FDS 6 the Deardorff model is implemented. The thermoBaffle1D model in OpenFOAM is implemented. ThermalBaffle1D is a boundary condition by solving steady-state 1D analytical heat transfer model across a solid baffle. The baffle is usually considered as zero thickness in the fluid domain, but non-zero thickness in heat transfer calculation. The total volume in the test case is 22m x 22m x 22m, as shown in Figure 1. Using a cubic 10 cm grid the simulation has almost 10.7 million grid cells. The simulations are performed using cubic 50cm, 20cm and 10cm grids however the 50cm case yielded a numerical instability in FireFOAM.

## Results

In this section we will briefly look at the estimated mass flow rates in the models with a mesh sensitivity study and comparisons between FireFOAM and FDS6 using the geometrical set-up shown in Figure 1. The size of the model is adopted from the size of the large fire hall at SP with a model geometry of 18m x 18m x 18m for the hall, as shown in Figure 45.

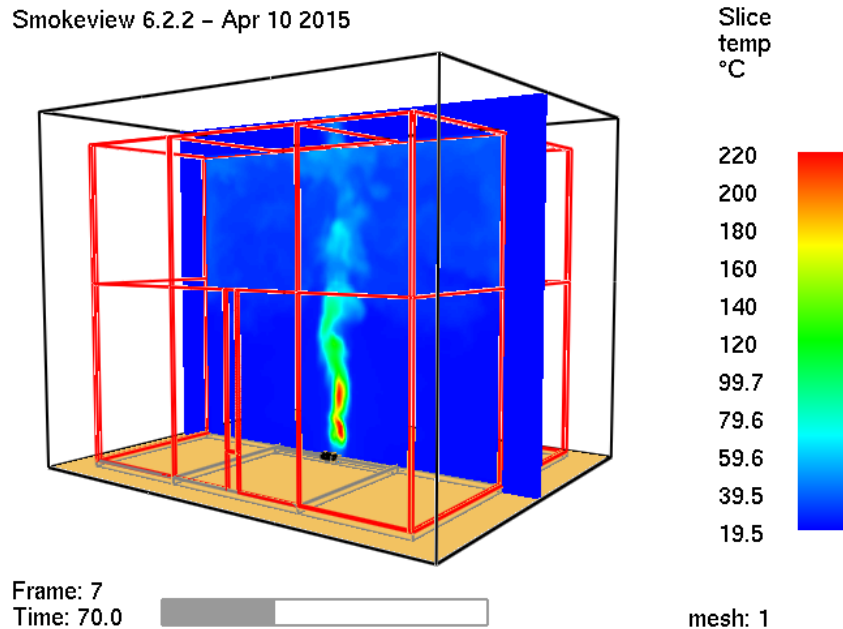


Figure 45 Geometry of smoke ventilation test with cubic volume in FDS.

First a comparison of code performances with varying number of processors is performed, it has been noted earlier that FDS scales rather poorly with increasing the number of processors however in this simple cubic geometry it scales rather well however no in-depth analysis of the scaling for FDS is made at this stage. One point for running the FDS model on 12 processors is added in comparison with FireFOAM, however in general FDS is faster than FireFOAM. In Figure 2 the run time of the simulation divided by actual simulation time (50 s) as a function of the number of processors is displayed. FDS seems to have similar performance in run times compared to fireFOAM, as is displayed in Figure 46. It is found that the run times decrease quite significantly by using a multi-processor simulation however the benefit of using more and more processors soon saturates.

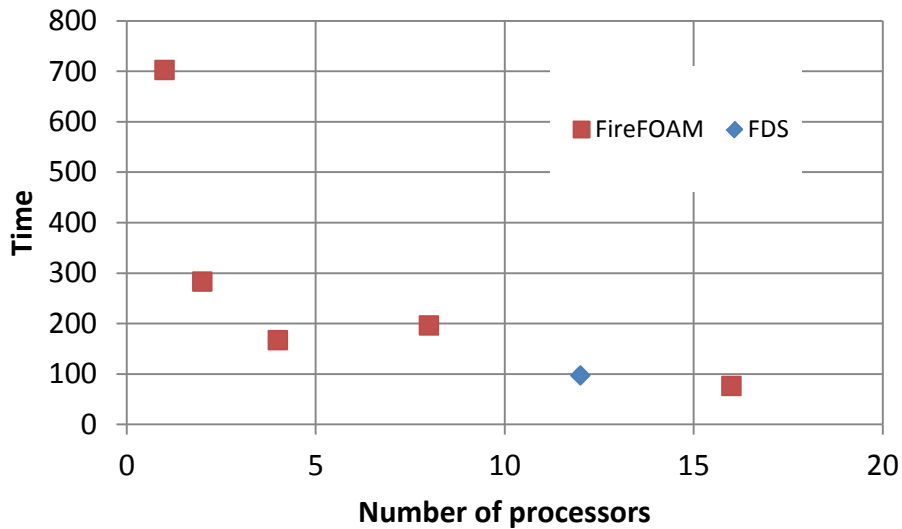


Figure 46 Scaling of run time (normalized by unit of simulation time) by the number of processors for FireFOAM and FDS for the cubic 20cm grid.

The models are set-up using the same type of mesh cubic staggered grid using 50 cm, 20 cm and 10 cm grid spacing. It is noted that the results for 50 cm grid yield a lot of fluctuations in the mass flow time trace for FDS whereas the FireFOAM yields numerical stability. The results of the 50 cm grid will not be discussed further since the corresponding FireFOAM data is lacking.

Next the models using a 20 cm grid will be compared. The heat release rates are approximately the same in both models, although some fluctuations can be seen in the FDS model using a 20 cm grid, see Figure 47.

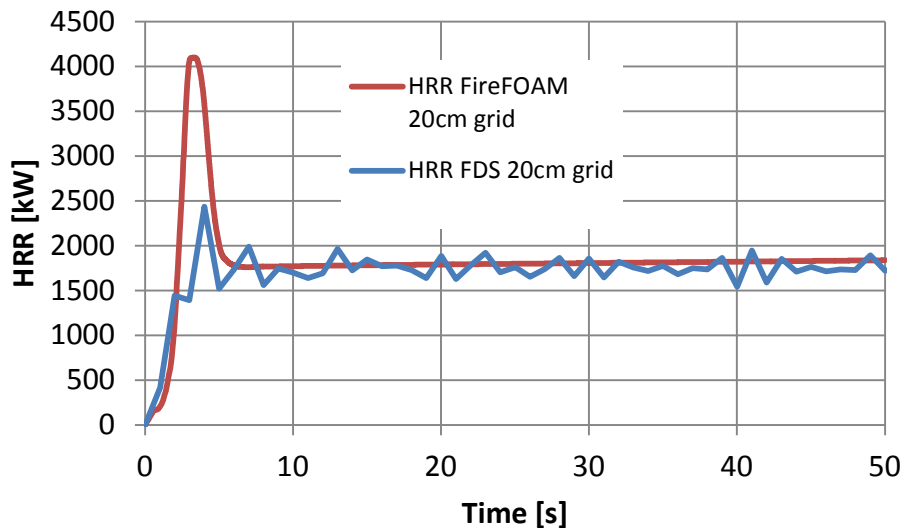


Figure 47 A comparison of the heat release rates implemented in FDS and FireFOAM.

The mass flow out of the vent in the ceiling is estimated by the mass flow command in FDS whereas no such command is implemented in OpenFOAM there is a utility that can perform this action. In this study the mass flow is directly estimated numerically by,

$$\dot{m} = \iint \rho U_z dA \cong \sum_{i=1}^N \rho_i U_{zi} dA_i,$$

where  $\rho$  is the density,  $U_z$  is the velocity upwards in the z-direction and the integral is computed over the vent area. Here the mass flow is sampled at 100 points across the vent area to accommodate for the resolution of the 10 cm grid.

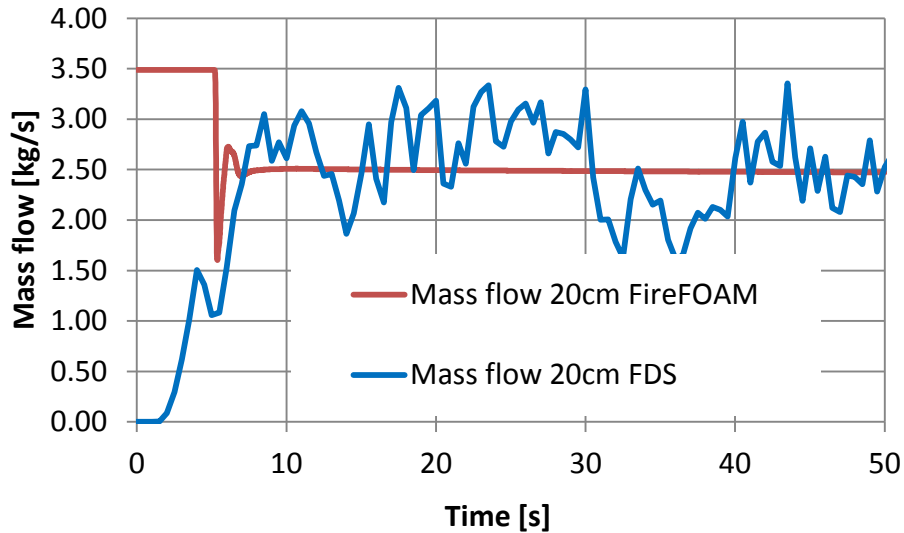


Figure 48 Comparison of mass flux through a vent in the ceiling as computed by FireFOAM and FDS.

Note that good agreement is found in comparing the mass flow rates out of the vent in the ceiling between the simulations in FDS and FireFOAM, see Figure 48. Although, the initial mass flow time trace from FireFOAM looks not very well resolved the solution soon converges to a rather stable level of slightly less than 2.5 kg/s with the FDS values fluctuating around the predicted mass flow rates from FireFOAM.

Next, the mass flow for in the 10 cm grid case will be discussed. First the heat release rates are compared. A peak in the heat release rates are found for both 20 cm and 10 cm grid spacing for FireFOAM however a steady state is soon reached that is comparable to the heat release rate found in FDS, c.f. Figure 49 and Figure 50.

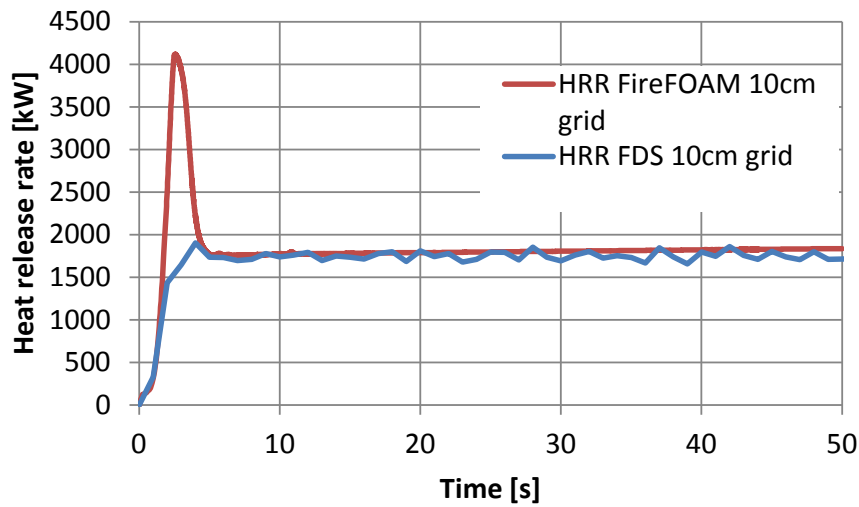


Figure 49 A comparison of the heat release rates implemented in FDS and FireFOAM.

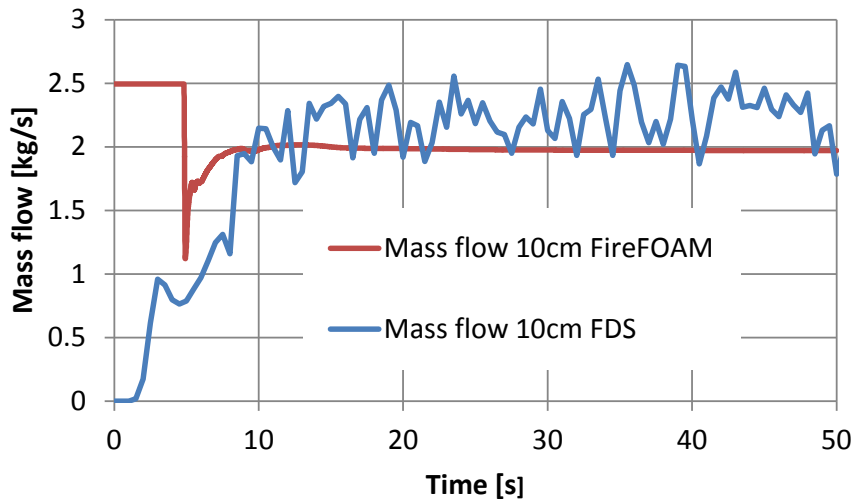


Figure 50 Comparison of mass flux through a vent in the ceiling as computed by FireFOAM and FDS.

Quite good agreement between FireFOAM and FDS is found. The mass flow for FireFOAM saturates to a level around 2 kg/s. However, the mass flow is slightly lower in the FireFOAM case as compared to the FDS result.

Although the total mass flow out of the vent is similar it seems that the dynamics in FDS and FireFOAM is rather different, the volume of high temperature above the diffusion burner seems to be larger yielding larger buoyancy with higher velocities upwards however contributing on a smaller exhaust area of the vent. Note that positive y is upwards in the FireFOAM model, see Figure 51 and Figure 52. Note that the perceived discrepancy in the induced mass flow from the difference in the velocity and temperature figures between FDS and FireFOAM can be understood from the fact that as the temperature increase the density decreases approximately inversely proportional to the temperature and the mass flux can on average be very close to each other.

In general, a quite significant difference in the mass flow as a function of grid size is found. The result obtained with the largest grid size in FDS show a large oscillation and an overall unreliable result (not shown in the present report). Moreover, the 20cm grid shows a nice smooth mass flow however it over predicts the result from the 10 cm grid by around 25%. It should be noted that previously it has been shown that results obtained with FDS5 and FDS6 show a decreased mass flow rate using FDS6 indicating that results using FDS5 may be even less conservative. These cases clearly show the importance of quality control when performing this kind of study. Earlier investigations using FDS6 have shown that that the buoyancy driving the flows is completely changed by having flat ceiling however by introducing tilted ceiling the mass flows are only changed by a small amount. One other factor that may influence the predicted mass flow is the thickness of the ceiling material however here the material is already thin steel plate which means it is deemed to be on the safe side according to the BIV study. The ceiling is considered infinitely thin in the FireFOAM model whereas in the FDS model it is an obstruction with 1 mm thickness. In the heat transfer calculation however both models have the same thickness.

As a rule of thumb, using the FDS model for smoke ventilation, the dependency on the grid used is 10% if there are 10 cells along one edge of the vent and up to 50% if only 2 cells are used. Provided that the area can be well resolved it is possible to achieve very accurate values using FireFOAM since the user has full control over the used wall functions or if the boundary layer could be resolved. However most often the resolution needed is impractical to use.

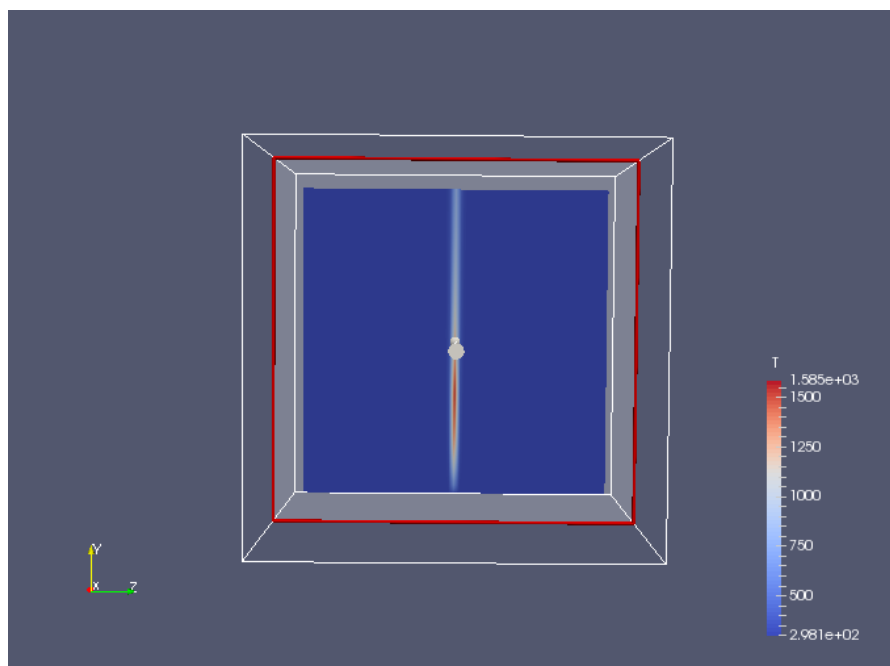


Figure 51 Snapshot of the temperature at steady state in FireFOAM.

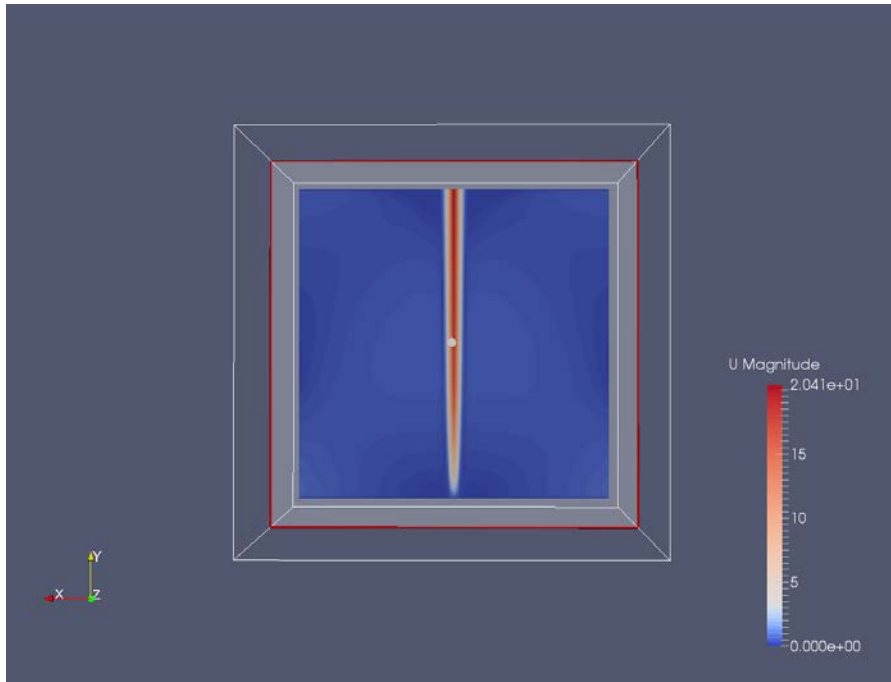


Figure 52 Snapshot displaying the magnitude of the velocity at steady state in FireFOAM.



## 6. Discussion

In order to evaluate FireFOAM five different cases have been simulated in FireFOAM. The tutorial case with the Steckler room, verification of heat transfer, inclined tunnel case, room fire case and the smoke filling and ventilation case.

### 6.1 Tutorial case with Steckler room

For free burning fires or for fires in an enclosure with thermally-thin walls (e.g. a steel container) the tutorial case in chapter 2 can be directly used after revising the meshes and the relevant parameters for such a fire size. The case assumes thermally-thin wall, which is not very realistic for real fire cases, where most wall are thermally-thick. A typical thermally-thick wall is a concrete wall, so the model is less suitable in a building with concrete walls. The Steckler room has thermally-thick walls, so therefore the simulations results cannot be directly compared with the experimental results

### 6.2 Verification of heat transfer

The verification of the heat transfer models in FireFOAM was done in chapter 3. It was verified that FireFOAM handles the three modes of heat transfer correctly in the code. This work has also lead to a publication at Interflam 2016 about the verification of the radiation model. [49]

### 6.3 Inclined tunnel

The heat transfer in an inclined tunnel was simulated using FireFOAM solver in the OpenFOAM software package. Further, the capability of this program was evaluated in terms of parallelization. It was found that FireFOAM code yielded consistently excellent result when using parallelization, regardless of the domain decomposition for this particular case. The relative clock time is reduced to 50% if two cores are used for the inclined tunnel case. However, for the Steckler room case in chapter 2, four cores had to be used to get the same speed-up. Further, the best speed-up in the Steckler case were achieved with the smallest number of cells, where the speed-up makes less sense. Comparing the Steckler case with a similar case using the Fire Dynamic Simulator (FDS) showed that FDS is at least 2.5 times faster than FireFOAM. Therefore, speed up is not consentingly for all cases, when using parallelization in FireFOAM. FireFOAM is in general much slower than the FDS, even when using parallelization.

A sensitivity study was performed for FireFOAM for the inclined tunnel in terms of important modelling parameters (grid size, combustion model constant and turbulent Prandtl number). It was found that grid size, combustion model constant and turbulent Prandtl number had noticeable effect on the calculated temperature, whereas it has minor effect on the calculated velocities.

Comparison of calculated velocities and temperatures using FireFOAM and measurements were also performed. It showed that FireFOAM yielded reasonable results in lieu of the above mentioned sensitivity study.

### 6.4 Room fire case

For the room fire validation case the grid size should be at smaller than 100 mm (10 cm). This parameter depends on the actual case and thus has to be determined on a case-by-case basis. The FireFOAM parallel simulations for the room fire case are rather efficient and robust. FireFOAM predicts the ceiling gas temperatures well. The incident heat flux is simulated relatively well. It has also been found that FireFOAM slightly underestimates the gas velocity and the O<sub>2</sub> concentration at the door, and slightly overestimates the CO<sub>2</sub> concentration at the door. This could be due to the fact

that the boundary layer at the door is not well resolved as a result of inappropriate wall functions for coarse grids. The fluid model and combustion model are appropriate. The main drawbacks are the wall heat conduction models and the radiation model for gas properties. There is no wall heat conduction model in fireFoam except the 1D thermal baffle model. By adjusting the pyrolysis model to a heat conduction model, fireFoam now can take heat loss into account, however, the model has not been optimized and the computational cost is huge. The radiation heat flux model lack appropriate grey gas properties and relevant parameters such as soot yield need to be embedded.

Another problem is that FireFOAM (including OpenFoam) uses a lot of computer memory, and the computation speed is not as fast as other fire-specified software, such as FDS.

## 6.5 Smoke filling and ventilation

Lastly smoke filling and ventilation was compared between the Fire Dynamics Simulator (FDS) and FireFOAM. An important factor in smoke ventilation is that the effective smoke exhaust area is smaller than the geometrical area by some factor due to differences in dynamical pressure, wind, temperature etc. This factor is the so-called contraction factor. The contraction factor is strongly dependent on the mesh resolution of the model and how well the turbulence is resolved in the vicinity of the vent. In this project, we have investigated the venting condition in a large hall, where the fire was a propane diffusion burner. There are quite a few parameters influencing the venting conditions in this model such as the geometry of the hall, size of the air inlet, size of the outlet, the HRR of the fire. However, the focus has been on the grid resolution and the fact that different results are obtained with FireFOAM and FDS6. In general we find a good agreement of the mass flow predicted in FDS compared to that of FireFOAM. However, it should be noted that somewhat different temperature distributions and velocities were found. A larger volume with higher temperature was found in the FireFOAM solution as well as higher velocities. The mass flows in the vent decreased as the resolution was decreased for both models by approximately the same amount. This indicates that a large grid resolution may be quite non-conservative in this respect.

It should be noted that several good tools for quality control has been added to FDS 6. However, no such easy-to-use tools are present in FireFOAM and thus it is up to the users to perform quality control of the obtained solution!

## 7. Conclusion

The aim of the project is to verify and validate the open source code FireFOAM by comparing with analytical solutions, experiments and another software - FDS6. The focuses are the basic fluid models, heat transfer models and combustion models, which are mostly related to practical use of CFD tools in a performance-based fire safety design. The other models such as pyrolysis models and fire suppression models are not evaluated which are deemed less significant in this study.

In general, predictions of gas temperatures, gas velocities, gas concentrations and heat fluxes by FireFOAM correlate with test results reasonably well for all the cases, although the flame temperatures were generally overestimated.

FireFOAM gave excellent agreement with analytical solution of the three modes of heat transfer: radiative, convective and conductive. But FireFOAM lacks a model for transient heat transfer in walls and can only calculate heat transfer for thin walls.

The FireFOAM code yielded excellent consistency in the results when using parallelization, regardless of the domain decomposition positions. The relative clock time is reduced to 50% when using two cores. FDS is about at least 2.5 times faster to do similar computations than FireFOAM.

However, it should be noted that heat loss to thick walls and smoke radiation are not well accounted for in the present version of FireFOAM. Caution needs to be taken when using FireFOAM to simulate scenarios relevant to these two phenomena.

It should also be noted that in FDS6 several good tools for quality control have been added. However, none of such easy-to-use tools are present in FireFOAM, and thus it is up to the users to perform good quality control of the obtained solution.

Therefore, at present, FireFOAM is more a tool for researchers wishing to exploit some of the special capabilities of the code, than for the consultants wanting to use it for doing standard fire safety engineering analysis.

### 7.1 Suggestion for future work

Incorporate into FireFOAM an easy 1D-heat transfer model for surfaces (walls, ceiling and floors) for modelling room fires. That would make the program more usable when using it for performance-based design. Improve the radiation model for grey gasses in FireFOAM and implement an algorithm to achieve a more even size of solid angles in FireFOAM as suggested in reference [49].



## 8 References

1. Wang, Y., P. Chatterjee, and J.L. de Ris, *Large eddy simulation of fire plumes*. Proceedings of the Combustion Institute, 2011. **33**(2): p. 2473-2480.
2. Meredith, K., et al., *A comprehensive model for simulating the interaction of water with solid surfaces in fire suppression environments*. Proceedings of the Combustion Institute, 2013. **34**(2): p. 2719-2726.
3. Ren, N., et al., *Large-scale fire suppression modeling of corrugated cardboard boxes on wood pallets in rack-storage configurations*. Fire Safety Journal, 2017. **91**(Supplement C): p. 695-704.
4. Chatterjee, P., et al., *Application of a subgrid soot-radiation model in the numerical simulation of a heptane pool fire*. Proceedings of the Combustion Institute, 2015. **35**(3): p. 2573-2580.
5. Chatterjee, P., et al., *A model for soot radiation in buoyant diffusion flames*. Proceedings of the Combustion Institute, 2011. **33**: p. 2665–2671.
6. Chatterjee, P., K.V. Meredith, and Y. Wang, *Temperature and velocity distributions from numerical simulations of ceiling jets under unconfined, inclined ceilings*. Fire Safety Journal, 2017. **91**(Supplement C): p. 461-470.
7. van Hees, P., *Validation and Verification of Fire Models for Fire Safety Engineering*. Procedia Engineering, 2013. **62**(Supplement C): p. 154-168.
8. Borg, A., B.P. Husted, and O. Njå, *The concept of validation of numerical models for consequence analysis*. Reliability Engineering and System Safety, 2014. **125**: p. 36-45.
9. McGrattan, K., et al., *Fire Dynamics Simulator Technical Reference Guide Volume 3: Validation, NIST Special Publication 1018-3, Revision: FDS6.5.3-564-g0eba564*,. January, 2017, National Institute of Standards and Technology, : Gaithersburg, MD USA.
10. Holmstedt, G., et al., *Kvalitetssäkring av olycks- och skadeförebyggande arbete med brandskydd i byggnader*. 2008, Lund University: Lund.
11. Ahmed, S., *Brandgasfyllnadsförlopp av en affärslokal - En valideringsstudie med Fire Dynamics Simulator*, in *Department of Fire Safety Engineering*. 2016, Lund University: Lund, Sweden.
12. Husted, B.B., *Turbulent mixing in the lower part of the smoke layer using the fire dynamic simulator*, in *1st International Symposium K-FORCE 2017*, M. Laban, et al., Editors. 2017, Department of civil engineering and geodesy, Faculty of technical sciences, University of Novi Sad: Novi Sad, Serbia.
13. McGrattan, K., et al., *Fire Dynamics Simulator User's Guide (Version 6)* 2015, National Institute of Standards and Technology: USA.
14. OpenCFD. [cited 2015 June]; Available from: <http://www.openfoam.org/download/git.php>.
15. FireFoam. Available from: <https://github.com/fireFoam-dev/fireFoam-2.2.x>.
16. Huang, C., *Numerical Modelling of Fuel Injection and Stratified Turbulent Combustion in a Direct-Injection Spark-Ignition Engine Using an Open Source Code*, in *Applied Mechanics*. 2014, Chalmers University of Technology: Gothenburg.
17. SPALDING, D.B., *MIXING AND CHEMICAL REACTION IN STEADY CONFINED TURBULENT FLAMES*. Symposium (International) on Combustion, 1971. **13**(1): p. 649–657.
18. Magnussen, B.F. and B.H. Hjertager, *On mathematical modeling of turbulent combustion with special emphasis on soot formation and combustion*. Symposium (International) on Combustion, 1977. **16**(1): p. 719-729.
19. Haworth, D., *A Review of Turbulent Combustion Modeling for Multidimensional In-Cylinder CFD*, in *SAE Technical Paper 2005-01-0993*. 2005.
20. Floyd, R.J.M.K.B.M.J.E., *A Simple Reaction Time Scale for Under-Resolved Fire Dynamics*, in *Tenth International Symposium on Fire Safety Science*. 2011: College Park, MD.

21. Kevin McGrattan, S.H., Randall McDermott, Jason Floyd, Craig Weinschenk, Kristopher Overholt, *Fire Dynamics Simulator Technical Reference Guide Volume 1: Mathematical Model*. NIST Special Publication 1018, Sixth Edition. p. 45-47.
22. Golovitchev, V., Nordin, N., Jarnicki, R., and Chomiak, J., *3-D Diesel Spray Simulations Using a New Detailed Chemistry Turbulent Combustion Model*. SAE Technical Paper 2000-01-1891, 2000.
23. Lipatnikov, A.N. and J. Chomiak, *Turbulent flame speed and thickness: phenomenology, evaluation, and application in multi-dimensional simulations*. Progress in Energy and Combustion Science, 2002. **28**(1): p. 1-74.
24. Almeida, Y.P., P.L.C. Lage, and L.F.L.R. Silva, *Large eddy simulation of a turbulent diffusion flame including thermal radiation heat transfer*. Applied Thermal Engineering, 2015. **81**: p. 412-425.
25. Trouvé, A. and Y. Wang, *Large eddy simulation of compartment fires*. International Journal of Computational Fluid Dynamics, 2010. **24**(10): p. 449-466.
26. Ding, Y.-m., C.-j. Wang, and S.-x. Lu, *Large Eddy Simulation of Fire Spread*. Procedia Engineering, 2014. **71**(0): p. 537-543.
27. Liu, Z., A.K. Kim, and D. Carpenter, *A study of portable water mist fire extinguishers used for extinguishment of multiple fire types*. Fire Safety Journal, 2007. **42**(1): p. 25-42.
28. McGrattan, K., et al., *Fire Dynamics Simulator Technical Reference Guide Volume 2: Verification, NIST Special Publication 1018-2*. 2014, National Institute of Standards and Technology, : Gaithersburg, MD USA.
29. Vdovin, A., *Radiation heat transfer in OpenFOAM, Final assignment in the course "CFD with OpenSource Software"*. 2009, Chalmers University of Technology.
30. DiNenno, P.J., *SFPE handbook of fire protection engineering*. 2002, Quincy, Mass.: National Fire Protection Association.
31. Çengel, Y.A. and R.H. Turner, *Fundamentals of thermal-fluid sciences*. Second ed. McGraw-Hill series in mechanical engineering. 2005: Boston : McGraw-Hill, 2005.
32. McGrattan, K., et al., *Fire Dynamics Simulator User's Guide, FDS Version 6.5.3, Revision: FDS6.5.3-569-ge3d0d6c, NIST Special Publication 1019*. January 2017, National Institute of Standards and Technology, : Gaithersburg, MD USA.
33. Kilian, S. and M. Münch, *A new generalized domain decomposition strategy for the efficient parallel solution of the FDS-pressure equation, Part I and Part 2: Theory, Concept and Implementation*. 2009, Konrad-Zuse-Zentrum für Informationstechnik: Berlin.
34. Drysdale, D., *An Introduction to Fire Dynamics*. 1985.
35. Kevin McGrattan, S.H., Randall McDermott, Jason Floyd, Craig Weinschenk, Kristopher Overholt, *Fire Dynamics Simulator User's Guide*. NIST Special Publication 1019.
36. Balram Panjwani, I.S.E., Kjell Erik Rian, Andrea Gruber, *SUBGRID COMBUSTION MODELING FOR LARGE EDDY SIMULATION (LES) OF TURBULENT COMBUSTION USING EDDY DISSIPATION CONCEPT*, in *V European Conference on Computational Fluid Dynamics*. 2010: Lisbon, Portugal.
37. Spalding, D.B., *Concentration fluctuations in a round turbulent free jet*. Chemical Engineering Science, 1971. **26**(1): p. 95-107.
38. Li, Y.Z. and T. Hertzberg, *Scaling of internal wall temperatures in enclosure fires*. Journal of Fire Science, 2015. **33**(2): p. 113-141.
39. Ingason, H. and U. Wickström, *Measuring incident radiant heat flux using the plate thermometer* Fire Safety Journal, 2007. **Vol. 42**(2): p. 161-166.
40. Häggkvist, A., *The plate thermometer as a mean of calculating incident heat radiation - a practical and theoretical study*, in *NR 2009:183*. 2009, Luleå University of Technology: Luleå.
41. McCaffrey, B.J. and G. Heskestad, *Brief Communications: A Robust Bidirectional Low-Velocity Probe for Flame and Fire Application*. Combustion and Flame, 1976. **26**: p. 125-127.
42. *Vägledning Brandgasfyllnad – Extern Version*. 2012, Briab Brand och Riskingenjörerna AB.

43. Back, A., et al., *CFD-beräkningar med FDS, BIV:s tillämpningsdokument 2/2013 – Utgåva 1*. 2013, SFPE-BIV, Sweden.
44. Ingason, H. and B. Persson, *Effects of Wind on Natural Fire Vents*. 1995, SP Report 1995:04, SP Swedish National Testing and Research Institute: Borås.
45. McDermott, R., et al., *Fire Dynamics Simulator (Version 5), Technical Reference Guide: Volume 2: Verification*. 2010, National Institute of Standards and Technology.
46. McDermott, R.J., *Quality assessment in the fire dynamics simulator (FDS): A bridge to reliable simulations*, in *Fire and Evacuation Modeling Technical Conference*. 2011: Baltimore, Maryland.
47. Pope, S.B., *Ten questions concerning the large-eddy simulation of turbulent flows*. *New Journal of Physics*, 2004. **6**(1): p. 35.
48. Maragos, G., P. Rauwoens, and B. Marci, *Application of FDS and FireFOAM in LES of turbulent buoyant helium plume*. *Cumbustion Science and Technology*, 2012. **184**(7-8): p. 1108-1120.
49. Runefors, M., et al., *A comparison of radiative transfer models in FireFoam and FDS*, in *Interflam 2016 : 14th International Conference*. 2016, Interscience Communications: Royal Holloway College. p. 59-69.



**LUNDS**  
UNIVERSITET

Department of Fire Safety Engineering

Lund University

P.O. Box 118

SE-221 00 Lund, Sweden

brand@brand.lth.se

<http://www.brand.lth.se/english>

Telephone: +46 46 222 73 60

Fax: +46 46 222 46 12

OUR SPONSORS:



**Brandforsk**

OUR PARTNERS:

**RI**  
**SE**

## RAPPORTER UTGIVNA AV BRANDFORSK 2017:

- 2017:1 Fire stops in buildings
- 2017:2 Verification, validation and evaluation of FireFoam as a tool of performance based design
- 2017:3 Fire Safety of Facades
- 2017:4 Framgångsfaktorer vid bo stadsbränder - sammanfattningsrapport
- 2017:5 Gröna Tak - Ur brandtekniskt synvinkel

**1979 bildades Brandforsk som svar på behovet av ett gemensamt organ för att initiera och finansiera forskning och utveckling inom brandsäkerhetsområdet.**

Brandforsk är statens, försäkringsbranschens och industrins gemensamma organ för att initiera, bekosta och följa upp olika slag av brandforskning.

Huvudman för Brandforsk är Brandskyddsföreningen och verksamheten leds av en styrelse och bedrivs i form av projekt vid universitet och högskolor, forskningsinstitut, myndigheter och företag.



**Brandforsk**

Årstaängsvägen 21 c  
Box 472 44, 100 74 Stockholm  
Tel: 08-588 474 14  
[brandforsk@brandskyddsforeningen.se](mailto:brandforsk@brandskyddsforeningen.se)